T.C.
REPUBLIC OF TURKEY
HACETTEPE UNIVERSITY
INSTITUTE OF HEALTH SCIENCES

COMPARATIVE ANALYSIS OF MYELOID-DERIVED SUPPRESSOR CELLS FROM BLOOD AND SPLEEN IN GASTRIC AND PANCREATIC CANCER

Ph.D. Ece TAVUKÇUOĞLU

Tumor Biology and Immunology Program
DOCTOR OF PHILOSOPHY (Ph.D.) THESIS

ANKARA
2022

T.C.
REPUBLIC OF TURKEY
HACETTEPE UNIVERSITY
INSTITUTE OF HEALTH SCIENCES

COMPARATIVE ANALYSIS OF MYELOID-DERIVED SUPPRESSOR CELLS FROM BLOOD AND SPLEEN IN GASTRIC AND PANCREATIC CANCER

Ph.D. Ece TAVUKÇUOĞLU

Tumor Biology and Immunology Program
DOCTOR OF PHILOSOPHY (Ph.D.) THESIS

ADVISOR OF THE THESIS
Prof. Dr. Güneş Esendağlı

ANKARA
2022

APPROVAL PAGE

HACETTEPE UNIVERSITY

GRADUATE SCHOOL OF HEALTH SCIENCES

COMPARATIVE ANALYSIS OF MYELOID-DERIVED SUPPRESSOR CELLS FROM BLOOD AND SPLEEN IN GASTRIC AND PANCREATIC CANCER

Ece Tavukçuoğlu

Supervisor: Prof. Dr. Güneş Esendağlı

This thesis study has been approved and accepted as a PhD dissertation in "Tumor Biology and Immunology Program " by the assesment committee, whose members are listed below, on 20.07.2022.

Chairman of the Committee :	*Prof. Dr. Ayşegül Üner* *Hacettepe University*
Member :	*Prof. Dr. Kerim Bora Yılmaz* *University of Health Sciences*
Member :	*Assoc. Prof. Dr. Füsun Özmen* *Hacettepe University*
Member :	*Assoc. Prof. Dr. Esra Birben* *Hacettepe University*
Member :	*Assist. Prof. Dr. Serkan İsmail Göktuna* *İhsan Doğramacı Bilkent University*

This dissertation has been approved by the above committee in conformity to the related issues of Hacettepe University Graduate Education and Examination Regulation.

25 Temmuz 2022

Prof. Müge YEMİŞCİ ÖZKAN, MD, PhD

Director

YAYIMLAMA VE FİKRİ MÜLKİYET HAKLARI BEYANI

Enstitü tarafından onaylanan lisansüstü tezimin/raporumun tamamını veya herhangi bir kısmını, basılı (kağıt) ve elektronik formatta arşivleme ve aşağıda verilen koşullarla kullanıma açma iznini Hacettepe Üniversitesine verdiğimi bildiririm. Bu izinle Üniversiteye verilen kullanım hakları dışındaki tüm fikri mülkiyet haklarım bende kalacak, tezimin tamamının ya da bir bölümünün gelecekteki çalışmalarda (makale, kitap, lisans ve patent vb.) kullanım hakları bana ait olacaktır.

Tezin kendi orijinal çalışmam olduğunu, başkalarının haklarını ihlal etmediğimi ve tezimin tek yetkili sahibi olduğumu beyan ve taahhüt ederim. Tezimde yer alan telif hakkı bulunan ve sahiplerinden yazılı izin alınarak kullanılması zorunlu metinlerin yazılı izin alınarak kullandığımı ve istenildiğinde suretlerini Üniversiteye teslim etmeyi taahhüt ederim.

Yükseköğretim Kurulu tarafından yayınlanan **"Lisansüstü Tezlerin Elektronik Ortamda Toplanması, Düzenlenmesi ve Erişime Açılmasına İlişkin Yönerge"** kapsamında tezim aşağıda belirtilen koşullar haricince YÖK Ulusal Tez Merkezi / H.Ü. Kütüphaneleri Açık Erişim Sisteminde erişime açılır.

- Enstitü / Fakülte yönetim kurulu kararı ile tezimin erişime açılması mezuniyet tarihimden itibaren 2 yıl ertelenmiştir. (1)
- Enstitü / Fakülte yönetim kurulunun gerekçeli kararı ile tezimin erişime açılması mezuniyet tarihimden itibaren .. ay ertelenmiştir.(2)
- Tezimle ilgili gizlilik kararı verilmiştir.

……./……/…….

……

1"Lisansüstü Tezlerin Elektronik Ortamda Toplanması, Düzenlenmesi ve Erişime Açılmasına İlişkin Yönerge"

(1) Madde 6. 1. Lisansüstü tezle ilgili patent başvurusu yapılması veya patent alma sürecinin devam etmesi durumunda, tez danışmanının önerisi ve enstitü anabilim dalının uygun görüşü üzerine enstitü veya fakülte yönetim kurulu iki yıl süre ile tezin erişime açılmasının ertelenmesine karar verebilir.

(2) Madde 6. 2. Yeni teknik, materyal ve metotların kullanıldığı, henüz makaleye dönüşmemiş veya patent gibi yöntemlerle korunmamış ve internetten paylaşılması durumunda 3. şahıslara veya kurumlara haksız kazanç imkanı oluşturabilecek bilgi ve bulguları içeren tezler hakkında tez danışmanının önerisi ve enstitü anabilim dalının uygun görüşü üzerine enstitü veya fakülte yönetim kurulunun gerekçeli kararı ile altı ayı aşmamak üzere tezin erişime açılması engellenebilir.

*(3) Madde 7. 1. Ulusal çıkarları veya güvenliği ilgilendiren, emniyet, istihbarat, savunma ve güvenlik, sağlık vb. konulara ilişkin lisansüstü tezlerle ilgili gizlilik kararı, tezin yapıldığı kurum tarafından verilir *. Kurum ve kuruluşlarla yapılan işbirliği protokolü çerçevesinde hazırlanan lisansüstü tezlere ilişkin gizlilik kararı ise, ilgili kurum ve kuruluşun önerisi ile enstitü veya fakültenin uygun görüşü üzerine üniversite yönetim kurulu tarafından verilir. Gizlilik kararı verilen tezler Yükseköğretim Kuruluna bildirilir. Madde 7.2. Gizlilik kararı verilen tezler gizlilik süresince enstitü veya fakülte tarafından gizlilik kuralları çerçevesinde muhafaza edilir, gizlilik kararının kaldırılması halinde Tez Otomasyon Sistemine yüklenir*

** Tez danışmanının önerisi ve enstitü anabilim dalının uygun görüşü üzerine enstitü veya fakülte yönetim kurulu tarafından karar verilir.*

ETHICAL DECLARATION

In this thesis study, I declare that all the information and documents have been obtainted in the base of the academic rules and all audio-visual and written information and results have been presented according to the rules of scientific ethics. I did not do any distortion in data set. In case of using other works, reletad studies have been fully cited in accordance with the scientific standards. I also declare that my thesis study is original except cited references. It was produced by myself in consultation with supervisor (Prof. Dr. Güneş ESENDAĞLI) and written according to the rules of thesis writing of Hacettepe University Institute of Health Sciences.

Ece TAVUKÇUOĞLU

ACKNOWLEGEMENT

I would like to express my sincere and deep gratitude to my advisor Prof. Dr. Güneş Esendağlı for his endless patience, advice, support, and motivation all through my graduate studies. His dedication and guidance shaped my perspective and scientific career.

I would also like to thank Assoc. Prof. Dr. Füsun Özmen, Assoc. Prof. Dr. Hande Canpınar, and Assist. Prof. Dr. Güneş Dinç-Akbulut for their scientific support and advice. I would like to say a special thank you to Assist. Prof. Dr. Neşe Ünver for her continuous encouragement and sharing her valuable scientific experiences.

I would sincerely thank Prof. Dr. Ayşegül Üner, Prof. Dr. Erhan Hamaloğlu, and Prof. Dr. Derya Karakoç for their great support to this thesis. I owe a debt of gratitude to Prof. Dr. Kerim Bora Yılmaz for his precious scientific support and contribution. I would also like to thank Prof. Dr. Can Akçalı and Zeynep Büşra Aksoy-Özer for their valuable contribution.

I would also like to thank Turkish Higher Education Council to support me in the context of 100/2000 PhD Scholarship.

I greatly appreciate Feyza Gül Özbay-Kurt for her invaluable friendship and the scientific support. I also owe a special thanks to my precious friends and colleagues, Dr. Diğdem Yöyen-Ermiş, Dr. Utku Horzum, and Hamdullah Yanık for their dedicated contribution to this study. I would also like to thank all Esendağlı Lab members, especially Dr. Süleyman Can Öztürk, Dr. Nazire Pınar Acar-Özen, Sıla Ulutürk, Mubaida Parveen, Sakine Ulusoy, and Gözde Bilir.

I would like to express my gratefulness to Çağrı Ata Demir for his empathy, respect, and everlasting support. I would also like to thank Elçin and Zafer Ziya Demir for their kindness and precious support.

Last but not the least, words are not sufficient to express my gratitude to my parents Büşra and Hakan Tavukçuoğlu and our cats Bulut and Pascal. This thesis would not have been possible without your support. I will always be grateful for your endless love and patience.

ABSTRACT

Tavukçuoğlu E. Comparative analysis of myeloid-derived suppressor cells from blood and spleen in gastric and pancreatic cancer. Hacettepe University Graduate School of Health Sciences, Tumor Biology and Immunology Doctor of Philosophy Program, Ankara, 2022. Under physiological conditions, development and maturation of the myeloid cells take place in the bone marrow. In case of chronic inflammatory disorders such as cancer, production of chemokines, growth factors, and cytokines are augmented, and myelopoiesis is boosted. However, the myeloid cells enter circulation without full maturation and may interfere with immune responses. These immature immunosuppressive cells are called "myeloid-derived suppressor cells (MDSCs)". MDSCs employ different mechanisms such as reactive oxygen species, nitric oxide, arginase 1, indoleamine 2,3-dioxygenase to suppress immune responses. MDSCs are accumulated in the peripheral blood, bone marrow, liver, and especially in the spleen and support tumor formation and metastasis in tumor-bearing mice. On the other hand, since obtaining spleen samples is very challenging, peripheral blood is generally used in human studies. Increased amounts of MDSCs were found in the peripheral blood of cancer patients and were associated with bad prognosis. However, there is more room for research about MDSCs in the human spleen. In this study, from peripheral blood and spleen samples of gastric and pancreatic cancer patients who underwent splenectomy, the subtypes of MDSCs were determined. Particularly, polymorphonuclear MDSCs (PMN-MDSCs) were accumulated in the spleen, and they were in close proximity with T cells. Increased percentages of PMN-MDSCs both in peripheral blood and spleen were associated with bad prognosis regardless of clinical stage. Furthermore, the spleen specimens which were obtained from the patients with traumatic injury served as non-malignant controls. PMN-MDSCs were accumulated in injured spleen similar to that of observed in the cancer patients. Increased percentages of PMN-MDSCs in the spleen were positively correlated with injury severity scores. Furthermore, the splenic PMN-MDSCs as well as the circulating PMN-MDSCs, displayed similar distribution, morphological properties, capacities to produce reactive oxygen species, nitric oxide, and suppressed T cells. Both in cancer and traumatic injury the expression of human MDSC-associated immune regulatory molecules were increased. In conclusion, our results demonstrated the immune modulatory function of the human spleen through MDSCs in inflammatory disorders such as cancer and trauma.

Keywords: spleen, myeloid-derived suppressor cells, polymorphonuclear cells, T cells

This study was supported by The Scientific and Technological Research Council of Turkey (TUBITAK) (Project No:216S264 and Project No:220S701).

ÖZET

Tavukçuoğlu E. Mide ve pankreas kanserinde dalak ve periferik kan miyeloid-kökenli baskılayıcı hücrelerin karşılaştırmalı analizi. Hacettepe Üniversitesi Sağlık Bilimleri Enstitüsü, Tümör Biyolojisi ve İmmünolojisi Doktora Programı, Ankara, 2022. Fizyolojik koşullarda, miyeloid hücrelerin gelişimi ve olgunlaşması kemik iliğinde gerçekleşir. Kanser gibi kronik inflamasyon süreçlerinde, kemokinlerin, büyüme faktörlerinin ve sitokinlerin üretimi artar, miyelopoiez uyarılır. Ancak, olgunlaşmalarını tamamlamadan dolaşıma çıkan miyeloid hücreler immün yanıtları sekteye uğratırlar. İmmün yanıtları baskılama kapasitesine sahip, miyelopoiezin farklı olgunlaşma basamaklarındaki immatür miyeloid hücreler "miyeloid-kökenli baskılayıcı hücreler (MKBH)" olarak bilinmektedir. MKBH'ler reaktif oksijen türleri, nitrik oksit, arjinaz 1, indoleamin 2,3-dioksijenaz gibi farklı mekanizmaları kullanarak immün yanıtları baskılamaktadır. Tümörlü farelerde MKBH'ler periferik kan, kemik iliği, karaciğer ve özellikle dalakta birikerek tümör gelişimine ve metastazına destek sağlamaktadır. İnsanda ise dalak dokusuna erişim çok zor olduğu için çalışmalar genellikle periferik kan ile yapılmıştır. Önceki çalışmalarda, kanser hastalarının periferik kanında MKBH'lerin yüksek düzeyde bulunduğu ve bu durumun kötü prognozla ilişkili olduğu gösterilmiştir. Ancak, insanda dalak dokusunda bulunan MKBH'lerin fonksiyon ve karakteri hakkında çalışmalara ihtiyaç duyulmaktadır. Bu çalışmada, splenektomi olmuş mide ve pankreas kanserli hastaların periferik kan ve dalak örneklerindeki MKBH alt-tiplerinin dağılımı belirlenmiştir. Özellikle, polimorfonükleer MKBH'lerin (PMN-MKBH) dalakta yığıldığı ve T hücreler ile yakın konumda bulunduğu gösterilmiştir. Dalak ve periferik kanda artan PMN-MKBH yüzdesinin, klinik evreden bağımsız şekilde kötü sağkalımla ilişkilendirilmiştir. Ayrıca, bu çalışmada kanser ile ilişkisi olmayan, travma sonucu splenektomi olmuş hastaların dalak örnekleri ile çalışılmıştır. Benzer şekilde, PMN-MKBH'lerin travmatik dalak dokusunda da biriktiği bulunmuştur. Artan PMN-MKBH yüzdesinin, yaralanma şiddet skorları ile pozitif korelasyon içinde olduğu gösterilmiştir. Ayrıca, dalaktaki ve periferik kandaki PMN-MKBH'lerin benzer dağılım gösterdiği, morfolojilerinin, reaktif oksijen türleri, nitrik oksit üretim ve T hücre baskılama kapasitelerinin de benzer olduğu bulunmuştur. Hem kanserde hem travmada, insan MKBH-ilişkili immün regülatör moleküllerinin ekspresyonu artmıştır. Sonuç olarak, çalışmamız, kanser ve travma gibi inflamatuvar hastalıklarda insan dalağının MKBH'ler sayesinde immün modülatör fonksiyonu olduğunu göstermektedir.

Anahtar kelimeler: dalak, miyeloid-kökenli baskılayıcı hücreler, polimorfonükleer hücreler, T hücreler

Bu çalışma TÜBİTAK tarafından desteklenmiştir (Proje No: 216S264 ve Proje No:220S701).

CONTENTS

LIST OF ABBREVIATIONS

ARG	Arginase
BSA	Bovine serum albumin
CD	Cluster of differentiation
CMP	Common myeloid precursors
COX-2	Cyclooxygenase 2
e-MDSC	Early myeloid-derived suppressor cells
EMH	Extramedullary hematopoiesis
FACS	Fluorescence-activated cell sorting
FBS	Fetal bovine serum
GAL	Galectin
G-CSF	Granulocyte colony-stimulating factor
GM-CSF	Granulocyte-macrophage colony-stimulating factor
GMP	Granulocyte/macrophage progenitors
HSC	Hematopoietic stem cells
HSPC	Hematopoietic stem and progenitor cells
IDO1	Indolamine 2,3-dioxygenase1
IFN	Interferon
IL	Interleukin
ITP	Idiopathic thrombocytopenic purpura
iNOS	Inducible nitric oxide synthase
mAb	Monoclonal antibody
M-CSF	Macrophage colony-stimulating factor
MDSC	Myeloid-derived suppressor cells
M-MDSC	Monocytic myeloid-derived suppressor cells
MPP	Mature multipotent progenitors
NO	Nitric oxide
NOX	NADPH oxidase
PALS	Periarteriolar lymphoid sheath
PBMC	Peripheral blood mononuclear cells
PCR	Polymerase chain reaction
PD-1	Programmed death protein 1

PD-L1	Programmed cell death ligand 1
PGE	Prostaglandin E
PMN	Polymorphonuclear
PMN-MDSC	Polymorphonuclear myeloid-derived suppressor cells
RBC	Red blood cells
ROS	Reactive oxygen species
STAT	Signal transducer and activator of transcription
TCR	T cell receptor
TGF-β	Transforming growth factor β
TIM-3	T cell immunoglobulin and mucin domain-containing protein-3
Treg	Regulatory T cell
VEGF	Vascular endothelial growth factor

FIGURES

TABLES

1. INTRODUCTION

Under physiological conditions, immature myeloid cells differentiate into macrophages, dendritic cells, and granulocytes. In case of tissue damage or the existence of a pathogen, the myeloid cells are activated and expanded. This process is called “myelopoiesis” and aims to boost immune elements to protect the organism from pathological conditions (1). However, in the case of chronic inflammation such as cancer, prolonged inflammatory signals and over expression of growth factors stimulate the bone marrow to meet the increased demand for myeloid cells. This results in an emergency myelopoiesis in which the immature myeloid cells fail to differentiate into mature cells before their egress from the bone marrow (2, 3). In recent years, it has become evident that the abnormal accumulation and function of the immature myeloid cells are important facets of the cancer (4).

The term “myeloid-derived suppressor cells (MDSCs)” were first defined in 2007 to identify the immature and suppressive myeloid cells (5). They originated from common myeloid progenitors and growth factors such as granulocyte-macrophage colony-stimulating factor (GM-CSF), granulocyte colony-stimulating factor (G-CSF), macrophage colony-stimulating factor (M-CSF) regulate their development (6). MDSCs are composed of immature myeloid cells at different stages of myelopoiesis and are identified with certain myeloid lineage markers. As common properties of MDSCs, they have low-density (<1.077 g/mL) and express low or no expressions of HLA-DR. MDSCs are further categorized into two major groups as monocytic MDSCs (M-MDSCs) and granulocytic/polymorphonuclear MDSCs (PMN-MDSCs) (7). Early MDSCs (e-MDSCs) have also been identified in humans, recently (8). Other than their low-density and absence of HLA-DR expression, there is no distinctive phenotypical markers to discriminate MDSCs from mature neutrophils and monocytes. Therefore, functional analyses such as T cell suppression assays are critical for defining the MDSCs (9).

As a secondary lymphoid organ, the spleen is the primary site for blood filtration; and, during fetal development, it also contributes to extramedullary hematopoiesis. In tumor-bearing mice, the immature MDSCs accumulate in peripheral blood, bone marrow, tumor microenvironment, liver, and mostly spleen. Both splenic and circulating MDSCs have been well-characterized phenotypically and functionally

in mice. MDSCs support tumor generation and metastasis by interfering with anti-tumor immune responses (10, 11). However, in humans, generally peripheral blood samples have been used to study MDSCs and in several types of cancer, increased levels of MDSCs were correlated with disease severity and poor survival rates (12).

Due to the difficulties to get fresh tissue samples, there is very limited knowledge on the MDSCs in the human spleen. Hence, this study aims to determine the distribution and functions of splenic MDSCs, and their comparison with circulating MDSCs. In this manner, peripheral blood and spleen samples from treatment-naïve gastric and pancreatic cancer patients who underwent splenectomy as a part of surgical oncology were freshly obtained. After the peripheral blood and the spleen samples were layered over 1.077 g/mL gradient separation solution, PMN-MDSC ($CD11b^{+}CD14^{-}CD33^{dim}CD15^{+}CD66b^{+}HLA\text{-}DR^{-/dim}$), M-MDSC ($CD11b^{+}CD14^{+}CD33^{+}CD15^{-}CD66b^{-}HLA\text{-}DR^{-/dim}$), and e-MDSC ($CD11b^{+}CD14^{-}CD33^{+}CD15^{-}CD66b^{-}HLA\text{-}DR^{-/dim}$) phenotypes were determined as “low-density” cells by using multi-color flow cytometry. PMN-MDSCs had the highest percentages and the absolute numbers in the peripheral blood and the spleen of cancer patients compared to those from the peripheral blood samples of the healthy donors. Therefore, this thesis study further focused on the PMN-MDSCs where the spleen served as a reservoir for MDSCs. Additionally, $CD66b^{+}$ PMN cells were widely distributed in the spleen, and they were in a close contact with $CD3^{+}$ T cells. Next, PMN-MDSCs from the peripheral blood and the spleen were purified and functional assays were performed. The capacities of reactive oxygen species (ROS), nitric oxide (NO) production, and phagocytosis were evaluated. For T cell suppression assays, peripheral blood mononuclear cells (PBMCs) from healthy donors were isolated and co-cultured with PMN-MDSCs at different ratios in the presence of anti-CD3 stimulation. Both splenic and circulating PMN-MDSCs suppressed T cell proliferation and IFN-γ secretion. Furthermore, expression of several immune regulatory genes and proteins related to MDSCs were upregulated in the spleen of the cancer patients.

As non-malignant controls, the spleen specimens from the patients who underwent splenectomy due to severe abdominal trauma were included in this study. PMN-MDSCs populated the spleen in traumatic patients similar to cancer patients. Commonly, the capacity of T cell suppression, the production of ROS, NO, the

phagocytic activity, and the patterns in the expression of immune regulatory genes and proteins were comparable between the splenic PMN-MDSCs obtained from the cancer patients and the trauma patients.

Lastly, the PMN-MDSCs were associated with the clinical data. Increased percentages of PMN-MDSCs in the peripheral blood and the spleen of cancer patients were associated with poor prognosis regardless of the clinical stage. In the trauma patients, the percentages of PMN-MDSCs were positively correlated with the injury severity scores. Therefore, this thesis study sheds light on the immune biology of the spleen, under distinct pathological conditions such as cancer and trauma, and reports the impact of MDSCs on the regulation of inflammation in the human spleen.

2. LITERATURE OVERVIEW

2.1. Myelopoiesis and MDSCs

The differentiation of hematopoietic stem and progenitor cells (HSPCs) begins with the self-renewing and multipotent hematopoietic stem cells (HSCs) in the bone marrow. Differentiation of HSCs results in the formation of more mature multipotent progenitors (MPPs). MPPs can further adopt features of the myeloid or lymphoid lineages. Common myeloid precursors (CMPs) generate mature myeloid cells such as macrophages, dendritic cells, and granulocytes in healthy individuals (1). Myeloid differentiation and maturation are regulated by the colony stimulating factors (CSFs). In case of tissue damage or infections, myeloid cells activate, and migrate into the site of inflammation (2, 13). This phenomenon is called normal activation and designed to protect the organism from pathogens and microorganisms. This is a short-term process and terminated when danger signal is removed from the microenvironment. However, under chronic inflammation and stress conditions, persistent and low-level inflammatory signals (i.e., chronic inflammation) cause “pathological activation” of the myeloid cells (12, 14). Under these conditions, bone marrow becomes insufficient to meet the increased demand for myeloid cells; thus, emergency myelopoiesis is initiated upon prolonged exposure to inflammatory mediators (2, 3). Increased CSFs induce the production of myeloid cells and the egress from the bone marrow without fully maturation. In 2007, the term “myeloid derived suppressor cells (MDSCs)” was introduced to define these immature and immune suppressive myeloid cells (5). MDSCs originates from a common myeloid progenitor (CMP), and they are composed of immature myeloid cells at various stages of myelopoiesis (6) (Figure 2.1). Besides normal myelopoiesis, granulocyte-macrophage colony-stimulating factor (GM-CSF), granulocyte colony-stimulating factor (G-CSF), macrophage colony-stimulating factor (M-CSF) are also responsible for the development of MDSCs. However, MDSCs, do not represent an immature population just arising from the expansion of myeloid cells. Several years ago, to better define the differentiation of MDSCs, Dmitry Gabrilovich proposed a two-signal model (15). This model is composed of two phases. In the first phase, immature myeloid cells expand, and their differentiation is inhibited in the bone marrow through the influence of tumor-derived growth factors. The second

phase is required to convert immature myeloid cells into functional MDSCs. These processes are mediated by complex transcriptional activities and principally pro-inflammatory cytokines (15, 16). Signal transducer and activator of transcription 3 (STAT3) is one of the key transcription factors, which induces the production of growth factors and pro-inflammatory cytokines such as Interleukin (IL-6) and vascular endothelial growth factor (VEGF) and provokes differentiation of MDSCs (17). In response to growth factors, CCAAT/enhancer-binding protein beta (C/EBPβ) is another transcription factor that plays a role in the emergency myelopoiesis, differentiation and sustenance of suppressive functions of MDSCs (18). C/EBPβ is found in the downstream of JAK/STAT pathway, which is stimulated through the pro-inflammatory cytokines and growth factors (19, 20). Previous studies reported that the deletion of C/EBPβ in hematopoietic cells can inhibit the generation of MDSCs and decrease their T cell suppression capacity (21). Unlike STAT3 and C/EBPβ, another transcription factor interferon regulatory factor (IRF8) is involved as a negative regulator in the development of MDSCs (22, 23). IRF8 expression is important for myelopoiesis, and it favors the differentiation of monocytic cells over granulocytic cells (24).

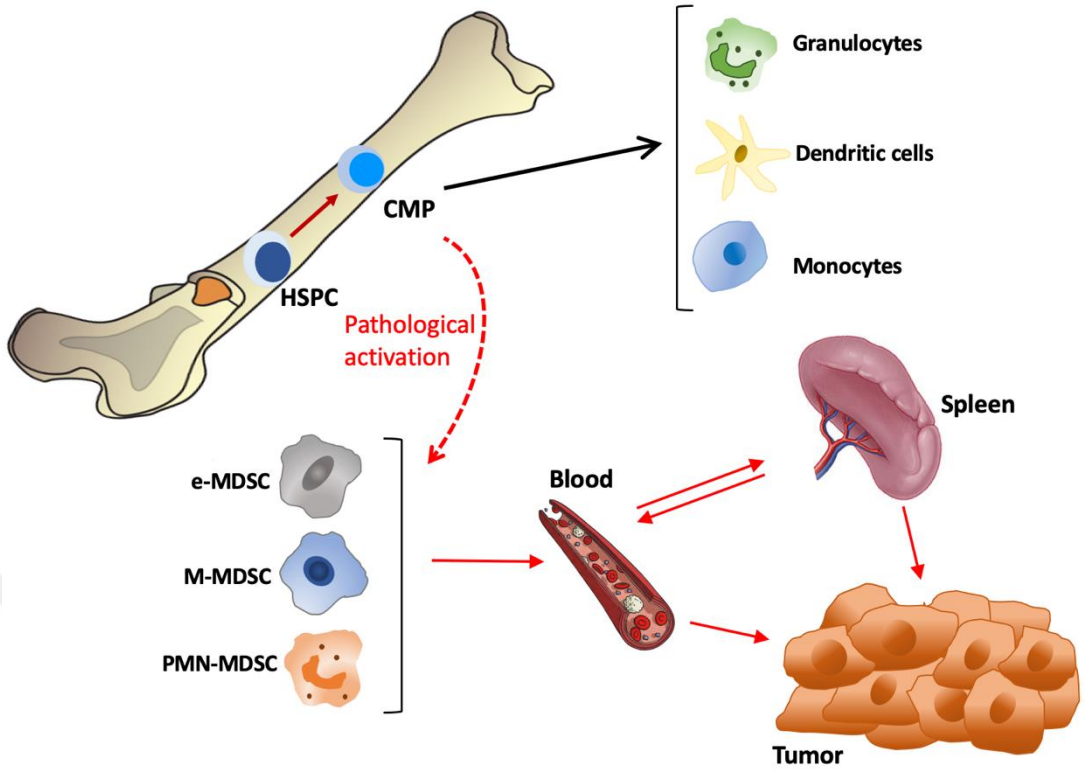

Figure 2.1. In myelopoiesis, mature granulocytes, and cells of other myeloid origins such as dendritic cells and monocytes are steadily formed under physiological conditions. Under the pathological circumstances, e-MDSC, M-MDSC and PMN-MDSCs accumulate in blood, spleen and tumor (HSPCs, hematopoietic stem and progenitor cells; CMPs, common myeloid precursors; e-MDSC, early myeloid-derived suppressor cells; M-MDSC, monocytic myeloid-derived suppressor cells; PMN-MDSCs, polymorphonuclear myeloid-derived suppressor cells).

Initially, MDSCs are categorized in two different groups based on their monocytic or granulocytic origins: monocytic MDSCs (M-MDSC) and granulocytic/polymorphonuclear MDSCs (PMN-MDSCs) both in mice and humans (8). More recently, early MDSCs (e-MDSC) which lack the lineage markers was identified in humans (8, 25). PMN-MDSCs ($CD11b^{+}CD14^{-}CD33^{dim}CD15^{+}CD66b^{+}HLA\text{-}DR^{-/dim}$) and M-MDSCs ($CD11b^{+}CD14^{+}CD33^{+}CD15^{-}CD66b^{-}HLA\text{-}DR^{-/dim}$) share common phenotypical properties with circulating neutrophils and monocytes, respectively (7, 26). On the other hand, M-MDSCs can be distinguished by the low-level or the absence of MHC class II. PMN-MDSCs accumulate in the low-density gradient (1.077 g/mL) when peripheral blood is

centrifuged. Therefore, PMN-MDSCs have lower density than that of mature neutrophils (15, 27). It has been previously shown that in monocytic myeloid-derived suppressor cells (M-MDSCs) and polymorphonuclear myeloid-derived suppressor cells (PMN-MDSCs), IRF8 expression is downregulated. In IRF8 deficient mice, myelopoiesis is impaired and myeloid cell differentiation is skewed toward MDSCs (28, 29). Additionally, a recent study has introduced lectin-type oxidized LDL receptor 1 (LOX1) as a new marker for identifying the human PMN-MDSCs (30). However, unique phenotypical markers are needed for distinguishing MDSCs, and functional analyses are essential to define them properly (9). T cell proliferation assays are commonly used methods to assess the suppressive capacity of MDSCs (31). However, functional assays on human MDSCs may give heterogeneous results which are partially lack of consensus due to the on the laboratory practices and standard operating protocols (9). To overcome these challenges, a European Cooperation in Science and Technology (COST-EU) Action BM1404 (Mye-EUNITER) was established and common methods for the isolation of MDSCs and suppression assays were reported (19). These advanced protocols include gentle and immediate processing of samples since these immature myeloid cells are susceptible to the physical stress and easily forfeit their suppressive character and prone to cell death (32). M-MDSCs and PMN-MDSCs have short lifespan. Especially, PMN-MDSCs lose viability in several days, *ex vivo* (33, 34). Because MDSCs (particularly PMN-MDSCs) are delicate and rare cells, cryopreservation is not recommended (9, 35).

2.2. Suppression Mechanisms of MDSCs and Their Recruitment

Phenotypical markers are not fully sufficient to discriminate MDSCs from other circulating myeloid cells and some distinctive properties related to their suppressive nature should be addressed (9). There are several mechanisms used by MDSCs to suppress anti-tumor immune responses. Reactive oxygen species (ROS), nitric oxide (NO) and arginase 1 (ARG1) were discovered as the primary suppression mechanisms. ARG1 can be used as a suppression mechanism by M-MDSCs and PMN-MDSCs. ROS is produced mostly by PMN-MDSCs, whereas NO is production is more common in M-MDSCs (36).

Under physiological conditions, consistent amount of cellular ROS is generated by several cell types. On the other hand, impairment in homeostasis, mitochondrial activity and metabolic processes may result in excessive ROS production that leads to oxidative stress (37-39). In order to avoid oxidative damage, ROS is tightly controlled by scavenging systems such as catalases, peroxidases, and nuclear factor erythroid 2-related factor 2 (Nrf2) which is an anti-oxidative transcription factor (19, 40). The main source of intracellular ROS is mitochondria where NADPH oxidases (NOX) that produce superoxide through transferring electrons from NADPH to oxygen. Excessive production of ROS can be observed in many cancers and during metastasis.

MDSCs release ROS to suppress T cells by damaging lipids, proteins and promoting apoptosis (41). More specifically, a study showed that ROS may also suppress antigen specific T cell responses by modifying TCR molecules and prevent them binding from MHC molecules (42). Since ROS are unstable and can be active for a very limited time, PMN-MDSCs should be in close-proximity with T cells to suppress the cell responses through ROS-mediated mechanisms (19). Increased ROS production promotes the accumulation of MDSCs in the tumor microenvironment by inducing VEGF receptors (43). In a study, MDSCs in NOX2 deficient mice could produce less amounts of ROS and were non-suppressive (44). Additionally, it has been demonstrated that when ROS production is inhibited via the catalases *in vitro*, suppressive functions of MDSCs can be impaired (45). Although excessive ROS production is toxic for many of the cell types, MDSCs are resistant to ROS through an antioxidant machinery regulated by Nrf2 (46). Under basal conditions, Nrf2 is constitutively expressed and degraded by Kelch ECH associating protein (Keap1) in the cytosol. However, in case of oxidative stress, cysteines residues of Keap1 become modified and Nrf2 is released from Keap1. Then, Nrf2 translocate into the nucleus, bind antioxidant response elements and increase to the resistance of MDSCs against ROS by producing antioxidant proteins and detoxifying enzymes. In Nrf2 deficient mice, MDSCs were found to be more apoptotic than in the wild-type mice, it can be claimed that Nrf2 can promote the survival of MDSCs (47).

Alternatively, MDSCs suppress T cell responses by the reduction of extracellular L-arginine mainly metabolizing through arginase 1 (ARG1), arginase 2

(ARG2) and inducible nitric oxide synthase (iNOS, NOS2) enzymes. ARG1 and ARG2 hydrolyze L-arginine into urea and L-ornithine whereas, iNOS hydrolyzes L-arginine into nitric oxide (NO) and L-citrulline (48). Increased ARG1 and iNOS activity in MDSCs deplete L-arginine which cause a decrease in the expression of CD3ζ chain on T cells (49, 50). The downregulation of CD3ζ chain on T cells eventually leads to the blockade of signal transduction and proliferation of the activated T cells upon antigen-specific stimulation. It has been shown that T cells are arrested in G_0/G_1 phase of the cell cycle in case of the absence of L-arginine, *ex vivo* (51). On the other hand, L-arginine replenishment can recover the expression of CD3ζ chain and T cell proliferation (52). Moreover, arginase inhibitors N(omega)-hydroxy-nor-l-arginine (nor−NOHA) and N(omega)-hydroxy-l-arginine (NOHA) can also reverse CD3ζ chain loss *in vitro.* Recently, arginase inhibitor (INCB001158) combined with chemotherapy is in phase I/II for the patients with solid tumors (53).

As a product of L-arginine catabolism, NO can suppress T cells by inhibiting janus kinase 3 (JAK3) and signal transducer and activator of transcription 5 (STAT5) in T cells, downregulating MHC-II expression on antigen presenting cells and inducing apoptosis of T cells (54, 55). iNOS produced by MDSCs can produce peroxynitrites that induce the nitration of the amino acids such as cysteine and tryptophan (56, 57). Conformational changes induced by peroxynitrites on TCR and MHC interaction cause nitration of TCR proteins on $CD8^+$ T cells. Eventually, peroxynitrites are associated with T cell unresponsiveness and apoptosis (58). Various signaling pathways such as januse kinase 2 (JAK2)/STAT3 and signal transducer and activator of transcription 6 (STAT6) involved in cell survival, differentiation and apoptosis are activated in T cells upon interaction with MDSCs. STAT3 is thought as the main transcription factor regulating expansion and the immunosuppressive capability of MDSCs (59). STAT3 signaling promotes the expression of cyclin D1, c-Myc and BCLX that prevent maturation and apoptosis, induce proliferation (60). The expression of calcium-binding pro-inflammatory proteins S100A8/S100A9 are upregulated with the activation of STAT3 (61). In case of inflammation, intracellular S100A8/S100A9 proteins are released to extracellular milieu (62). They are expressed in tumor-infiltrating cells and serve as chemoattractant for the leukocytes. S100A8/S100A9 influence the leukocytes and MDSCs by binding TLR4 and

carboxylated N-glycans receptors (36, 63). Additionally, S100A8/S100A9 heterodimers participate in the formation of NOX2 complex responsible for the ROS production and activate NF-kB pathway, which induces COX-2 and PGE_2 production. MDSCs can also synthesize S100A8/S100A9 proteins, which from an autocrine loop for migration (64). Blockade of S100A8/S100A9 binding to their receptors, reduces the number of MDSCs in the circulation of tumor-bearing mice (62).

Another pathway involves G-CSF-driven STAT3 activation resulting in increased expression of c-Myc through C/EBP-β activity (65). Therefore, STAT3 regulates C/EBP-β expression in response to G-CSF in myeloid cells (66). C/EBP-β has been reported to play role in differentiation of myeloid cells precursors into MDSCs and involved in the accumulation of the MDSCs into the spleen of tumor-bearing mice (67). STAT6 signaling promotes suppressive characteristics of the myeloid cells. Following exposure to IL-13 and IL-4 through their receptor complexes involving IL-13α and IL-4Rα (CD124) respectively, STAT6 is phosphorylated and translocated into the nucleus. STAT6 can bind to the promoter of ARG1 gene and upregulation of ARG1 activity is observed in MDSCs (28, 68). As an important regulator of STAT6 pathway, CD124 expression was identified on human and mice MDSCs (69).

The immunosuppression through MDSCs can be mediated by the checkpoint inhibitor molecules. Following the interaction with MDSCs, T cells are reported to secrete IL-10, which induces PD-L1 expression on MDSCs in a STAT3-dependent manner (70). PD-L1 binds its receptor PD-1 on T cells and induces T cell apoptosis and hyporesponsiveness. As another immunosuppression strategy, MDSCs can express Galectin-9 (Gal-9), which can bind to T cell immunoglobulin and mucin domain-containing protein 3 (TIM3) and programmed cell death protein 1 (PD-1) to restrain T cell-mediated anti-tumor immune responses. In response to Gal-9, T cells can express Fas-ligand (FasL), which binds Fas on $CD8^+$ T cells and induce apoptosis (71, 72). *In vivo* and *in vitro* studies indicated that STAT3 inhibitors may impair the suppression capacity and the accumulation of MDSCs into the tumor microenvironment and secondary lymphoid organs (73, 74).

MDSCs express indolamine 2,3-dioxygenase1 (IDO1) that converts L-tryptophan into kynurenine metabolites (75). Since L-tryptophan is a critical amino

acid for T cell proliferation, depletion of L-tryptophan suppresses T cell proliferation and promotes apoptosis via general control nonrepressed 2 (GCN2) pathways (76). Activation of GCN2 mediates downregulation of CD3ζ chain on $CD8^+$ T cells that results in the reduction of effector functions. Depletion of L-tryptophan can also trigger T cell autophagy by inhibiting the activation of protein kinase C (PKC) and mammalian target of rapamycin (mTOR) (19). When kynurenine pathway is activated through depletion of L-tryptophan, it can interact with the aryl hydrocarbon receptor (AhR) on dendritic cells and macrophages (77). This interaction drives the myeloid cells into regulatory phenotype and promotes regulatory T cells (Treg) differentiation by forkhead box p3 (FOXP3) induction of a transcription factor. The kynurenine pathway involves a downstream enzymatic reaction that produces quinolinic acid and kynurenic 3-hydroxyanthranilic acid (3-HAA). Kynurenic acid is a ligand for AhR, which leads to inhibition of interferon gamma (IFN-γ) production, $CD4^+$ T cell proliferation and cell cycle progression (78).

Another T cell suppression mechanism used by MDSCs is through ectoenzymes that hydrolyze ATP into adenosine. CD39 (ectonucleoside triphosphate phosphohydrolase 1) converts ATP into AMP; and then, CD73 (ecto-5'-nucleotidase) catalyzes the phosphorylation of AMP into adenosine. It has been shown that tumor-derived TGF-β could induce CD39 and CD73 on MDSCs. Therefore, increased amount of extracellular adenosine inhibits T cell activation by preventing phosphorylation of ERK, Akt and Zap70 (79).

As MDSCs can also secrete inhibitory cytokines transforming growth factor β (TGF-β) and IL-10. TGF-β inhibits effector T cell proliferation by impairing interleukin 2 (IL-2), granzyme B, perforin and IFN-γ production whereas, interleukin 10 (IL-10) interferes with interleukin 12 (IL-12) production involved in anti-tumor immunity. Both TGF-β and IL-10 can promote the differentiation of Treg cells (80) (Figure 2.2). Prostoglandin E_2 (PGE_2) is an inflammatory mediator generated by cancer cells and myeloid cells. It binds the receptors EP2 or EP4 on MDSCs and promotes cyclooxygenase 2 (COX-2) expression as well as ARG1, iNOS, IDO1. Endogenous PGE_2 initiates a positive feedback loop by amplifying the production of these suppressive factors (81). It eventually promotes the differentiation and accumulation of MDSCs. EP2/EP4 antagonists or COX2 inhibitors can be used to

hinder suppressive functions of MDSCs and block the endogenous production of PGE_2 (81, 82).

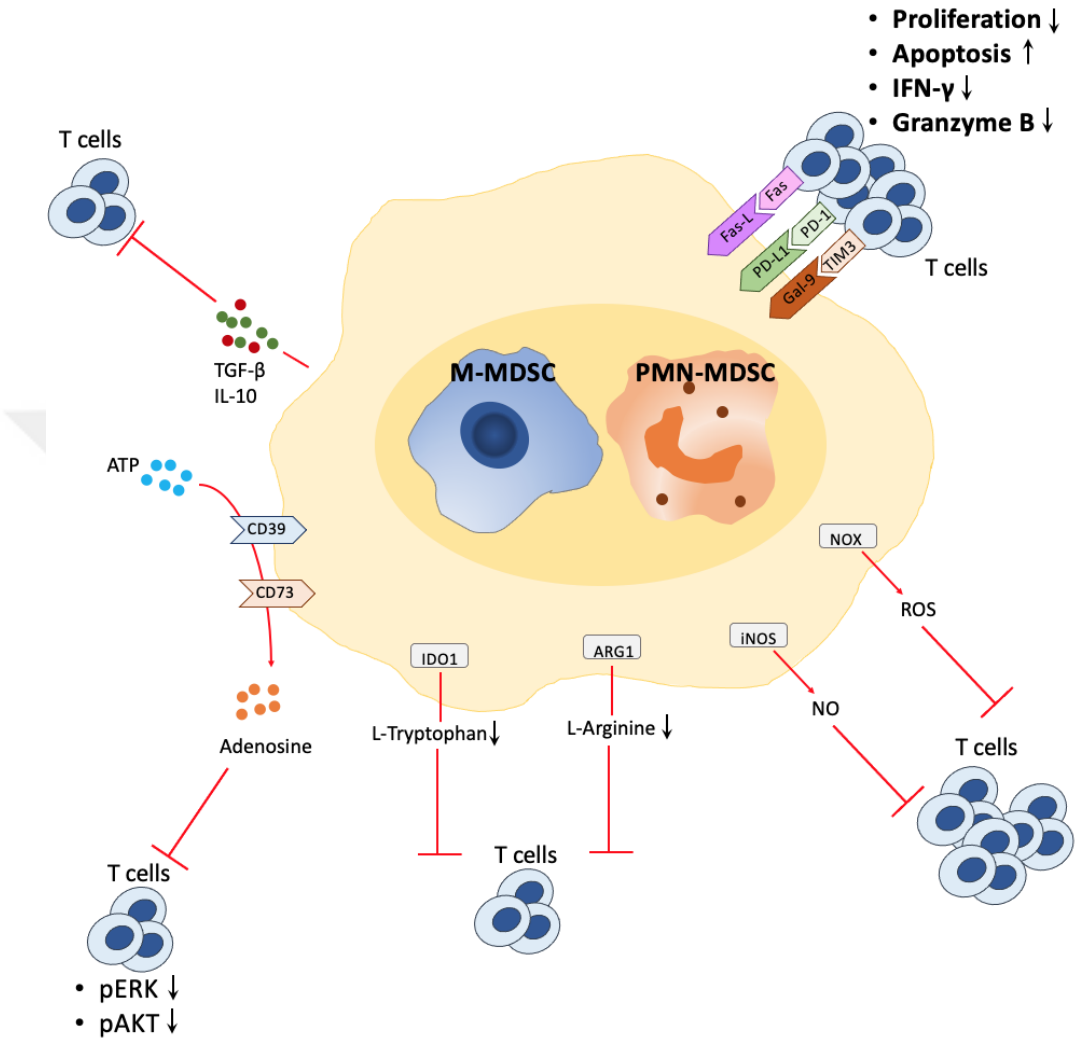

Figure 2.2. Different T cell suppression mechanisms employed by M-MDSCs and PMN-MDSCs are shown (TGF-β, transforming growth factor β; IL-10, interleukin 10; ATP, adenosine triphosphate; pERK, phosphorylated extracellular signal-regulated kinase; pAKT, phosphorylated protein kinase B; IDO1, indolamine 2,3-dioxygenase1; ARG1, arginase 1; iNOS, inducible nitric oxide synthase; NO, nitric oxide; ROS, reactive oxygen species; NOX, NADPH oxidases; TIM3, mucin domain-containing protein 3; Gal-9 Galectin-9; PD-1, programmed death protein 1; PD-L1, programmed death ligand 1; Fas-L, Fas ligand; IFN-γ, interferon gamma; M-MDSC, monocytic myeloid-derived suppressor cells; PMN-MDSC, polymorphonuclear myeloid-derived suppressor cells).

Immune suppression by MDSCs involves multiple mechanisms as given and the microenvironment shapes the characteristics of MDSCs, which have high plasticity (83). Therefore, suppressive actions may vary in the site of tumor or peripheral lymphoid organs. In several studies, MDSCs were found to be more suppressive in the tumor microenvironment than in spleen from the tumor-bearing mice. It can be claimed that tumor microenvironment can affect and change the characteristics of MDSCs. In lung and prostate cancer mice models, MDSCs isolated from tumors expressed more *Nos2* and *Arg1* genes and suppressed T cells more than splenic MDSCs (84, 85). In the tumor bearing-mice, splenic MDSCs inhibited antigen specific T cell responses via ROS whereas, tumor-infiltrating MDSCs were also capable of suppressing non-specific T cell responses via NO and Arg1 and expressed high levels of PD-L1 on their surface (86). To exert their immunosuppressive functions on T cells, MDSCs should be recruited to the tumor site or lymphoid organs to juxtapose with target cells. At this point, chemokines drive the migration of MDSCs. In mice, CCL2 and CCL5 are the major chemokines that induce the accumulation of M-MDSCs into the tumor microenvironment (87). Although main target of CCL2 is M-MDSCs, it can also attract PMN-MDSCs. In the CCL2-deficient tumor-bearing mice, the recruitment of PMN-MDSCs into the tumor microenvironment was impaired. Additionally, in colorectal cancer patients, CCL2 mRNA in tumor was found higher than in non-tumor tissue (88). CCL3, CCL4 and CCL5 can also recruit $CCR5^{+}$ M-MDSCs and Tregs into the tumor site (89). CXCL1, CXCL2, and CXCL5 primarily recruit PMN-MDSCs and accumulation of PMN-MDSCs into the tumor microenvironment was diminished in CXCR2-deficient mice (90). Other than chemokines, galectin-3 (gal3) as a β-galactoside-binding protein can also mediate recruitment of myeloid cells to the tumor site and its inhibition reduced MDSC accumulation (91). In gastric cancer patients, increased serum levels of Gal3 were correlated with the lymph node metastasis (92).

2.3. MDSC and Chronic Inflammatory Disorders

In the last decade, MDSCs were defined as one of the major regulatory cells in the context of cancer, inflammation, autoimmunity, and transplantation (93). In mice, MDSCs have been well-characterized functionally and phenotypically in tumor, spleen, bone marrow, peripheral blood, and liver (10, 11). However, due to the

challenges in obtaining fresh tissue samples, in humans MDSCs have been mostly studied in peripheral blood samples. There are few data about MDSCs in the tumor microenvironment and there is only one paper published about the MDSCs found in human spleen. In the tumor-bearing mice, the frequency of MDSCs in spleen, tumor and peripheral blood have been correlated with the tumor progression and metastasis. There has been growing evidence about using circulating MDSCs as a prognostic indicators for cancer patients (12).

The frequency of PMN-MDSCs and M-MDSCs was found higher in the peripheral blood of cervical cancer patient than in healthy donors. The levels of PMN-MDSCs were also correlated with the disease severity (94). In breast cancer patients, circulating PMN-MDSCs were found higher than in healthy donors and was directly proportional with the increased frequency of Tregs (95). In the peripheral blood of brain metastatic non-small lung cancer patients, the percentages of MDSCs and Tregs were also high. Moreover, in metastatic patients, PD-L1 expression on MDSCs was elevated (96). Similarly, in colorectal cancer, lung cancer, and renal cancer, the levels of circulating PMN-MDSCs were increased (69, 97, 98). In colorectal cancer, the frequency of circulating $Lin^{-}HLA\text{-}DR^{-}CD11b^{+}CD33^{+}$ MDSCs was increased in the patients with stage III/IV disease, and it was positively correlated with metastasis. (87). In non-small lung cancer patients, M-MDSCs were found to be increased in the peripheral blood and it was associated with unfavorable clinical outcome (99).

Markowitz et al. and Chen et al. reported association of elevated percentages of circulating MDSCs in pancreatic cancer patients and in head and neck cancer patients with the poor prognosis (100, 101). In another study, the frequency of $CD14^{+}CD11b^{+}HLA\text{-}DR^{-}$ MDSCs were elevated in the peripheral blood of pancreatic cancer patients. High GM-CSF and arginase levels were also detected in these patients and were correlated with the disease progression (102, 103). The tumor-infiltrating $Lin^{-}HLA\text{-}DR^{-}CD33^{+}CD11b^{+}CD15^{+}$ PMN-MDSCs were also accumulated in the pancreatic tumors whereas benign pancreatic cysts were bearing less numbers of MDSCs. In the same study, $Lin^{-}HLA\text{-}DR^{-}CD14^{+}$ M-MDSCs were more frequently detected in the pancreatic tumors than in the peripheral blood (104). For the first time, Jordan et al. compared the distribution and T cell suppression capacity of PMN-MDSCs and M-MDSCs in the spleen of the patients with pancreatic cancer or benign

pancreatic cysts (105). In gastric cancer patients, circulating $CD45^{+}CD33^{low}CD11b^{dim}$ MDSCs suppressed T cell responses via ARG1 production, and it was negatively correlated with the overall survival (106).

As previously mentioned, MDSCs can suppress immune responses through various mechanisms and the abundance of MDSCs are correlated with the severity of many diseases. Therefore, inhibition of MDSCs can be a promising approach especially for cancer treatment. Although there are no clinically approved therapeutic drugs targeting MDSCs, many preclinical studies and clinical trials have been conducted in the past years. Direct or indirect targeting of MDSCs can be achieved by promoting differentiation, reducing accumulation, depletion, or abrogation of the suppressive functions. Firstly, the agents may promote the differentiation of MDSCs into the mature (non-suppressive) antigen presenting cells. All-trans retinoic acid (ATRA) is one of these agents that neutralize ROS production, upregulate glutathione synthase, and induce the differentiation of MDSCs (107, 108). Vitamin D3 can also promote the maturation of MDSCs. In a phase I study, administration of vitamin D3 decreased the numbers of circulating MDSCs in the head and neck squamous carcinoma patients (109). Secondly, the recruitment of MDSCs to the tumor microenvironment can be diminished. The activation of AMP-activated protein kinase (AMPK) can inhibit the activation and expansion of MDSCs by hampering NF-kB pathway and inducing oxidative stress. An inhibitor of AMPK, sunitinib, can inhibit STAT3 activation, and reduce the frequency of MDSCs in the tumor-bearing mice and in the patients with metastatic RCC (110). Colony-stimulating factor 1 receptor (CSF1-R) is generally upregulated in many cancer types. Upon its ligation with CSF1, it promotes the expansion and accumulation of MDSCs. The inhibition of CSF1-R has a potential to inhibit the recruitment of MDSCs. A CSF1-R inhibitor, plexidartinib, has been tested in a phase II study for glioblastoma patients (111). Additionally, MDSCs can migrate into the tumor microenvironment through CCL5/CCR5 axis. In mice models, blockade of CCL5/CCR5 axis reduced the migration of MDSCs and limited their immunosuppressive activity, and metastasis (112, 113). Recently, a CCR5 antagonist, maraviroc, has been introduced in a phase I study for colorectal cancer treatment (111). Inhibition of COX-2/PGE2 signaling by a COX-2 inhibitor, celecoxib, has been shown to diminish MDSC-related suppression by decreasing

production of ROS and ARG-1, and increasing the frequency of cytotoxic T lymphocytes in mice (114). Nrf2 modulates the expression of anti-oxidant enzymes and provides cellular protection. Anti-inflammatory triterpenoids such as CCDO-Im and CCDO-Me have been shown to reduce ROS production by MDSCs through upregulation of Nrf2. In a phase I study, the efficacy of CCDO-Me on pancreatic cancer patients were shown to decrease the amount of circulating MDSCs (115). Nitroasprin was demonstrated to improve T cell responses and repress tumor growth in mice by targeting iNOS (116). STAT3 is another promising target to reduce the immunosuppressive effects of MDSCs. In a phase I study, AZD9150, a STAT3 inhibitor, has been tested for patients with B cell lymphoma and circulating PMN-MDSCs were decreased (117).

Even though MDSCs are one of the key immunosuppressive cells in the tumor microenvironment, inhibition of MDSCs may not be sufficient to promote the anti-tumor effects. In the last decade, immunotherapies, which impede tumor growth and increase the survival of the cancer patients by boosting host immune system, have revolutionized. These immunotherapeutic approaches are mainly rely on immune checkpoint blockade molecules such as CTLA-4, PD-1, and PD-L1 inhibitors (118). On the other hand, immunotherapy may not be successful in many patients. At this point, MDSCs have been demonstrated to interfere with immunotherapy responses and contribute to resistance. Accordingly, MDSCs have been proposed as prognostic markers for monitoring the response or resistance to immunotherapies (119, 120). In melanoma patients, circulating M-MDSCs were higher in non-responders to ipilimumab therapy than in the responders (121). Higher frequency of M-MDSCs hampered the efficacy of ipilimumab and caused low clinical response (122). In patients with non-small lung cancer who were treated with nivolumab, circulating PMN-MDSCs were lower in the responders than in the non-responders (123). These clinical data indicated that regardless of the cancer type, MDSCs may contribute to the resistance to immunotherapy (124). Within this context, combination immunotherapies, which also considers of MDSCs may be a promising treatment strategy. CCL2/CXCR2 axis attracts MDSCs to the tumor mass (88, 125). It was previously reported that $CXCR2^{+}$ MDSCs support tumor progression and T cell exhaustion in the tumor-bearing mice. Thus, CXCR2 can serve as a druggable receptor

to prevent the accumulation of MDSCs. In mice, a CXCR2 inhibitor, SX-682, was reported to reduce the infiltration of PMN-MDSCs into the tumor (126). However, with the combination of anti-PD-1 therapy, the effectiveness of CXCR2 inhibition may be improved (127, 128). In pancreatic cancer mice models, the survival was prolonged by CXCR2 inhibition and anti-PD-1 therapy. Recently, in melanoma patients, SX-682 combined with pembrolizumab has been tested in a phase 1 study. Other inhibitors of CXCR2, reparixin and AZ5069, are tested in a phase II study for breast cancer (111). In late-stage melanoma patients, the combination of ATRA with ipilimumab decreased the frequency of circulating MDSCs (129). In a RCC mice model, the blockade of MDSCs together with anti-PD-1 therapy resulted in increased survival compared to the anti-PD-1 therapy alone (130).

2.4. Microanatomy and Functions of the Spleen

The spleen is located in the abdomen, serves as a blood filter and is the largest secondary lymphoid organ. It is covered by a capsule made of connective tissue and because there are no afferent lymphatic vessels in the spleen, all antigens and cells reach the spleen via blood stream. The splenic arterial vessels enter the capsule and form a branched tree-like shape. Then, smaller arterial vessels end in sinuses of spleen. The spleen is mainly divided into two compartments as red pulp and white pulp, which are separated by the marginal zone. Although adaptive immune reactions take place in the white pulp, it occupies a limited area (131). Leukocytes such as dendritic cells, neutrophils, macrophages, and monocytes, which mediate the innate immunity are mostly found in the red pulp. Since red pulp has a unique venous structure, it can filter the blood, remove the aged red blood cells, dead and opsonized cells from the circulation and recycle the iron by the help of splenic macrophages. The structure of the white pulp resembles of a multiple embedded lymph node. It contains T and B cell compartments, and their localization are controlled by the chemokines to establish specific zones (132). Around the splenic arterial vessels, T cell zone also called “periarteriolar lymphoid sheath (PALS)” enables interaction with the antigen presenting cells. The ligands for CCR7, CCL19 and CCL21 are required for T cells motility towards the PALS. In the B cell zone (follicle), activated B cells clonally expand and the isotype switching of immunoglobulin takes place. Additionally, in case

of an active immune response, germinal center is formed to produce long-lived memory B cells and high affinity antibody producing plasma B cells. In the follicles, follicular dendritic cells produce CXCL13, which is a ligand for CXCR5 on the B cells. It is required for the migration of B cells toward the follicles.

The white pulp and the red pulp are not separated by a capsule but divided by multiple layers of cells form a marginal zone, mainly composed of innate immune cells (133). It is an important area for the cells to leave the bloodstream and enter the white pulp. Marginal zone macrophages, marginal zone B cells and dendritic cells uniquely designated to maintain the integrity of the structure of the marginal zone. Therefore, large antigens cannot randomly enter the white pulp, but they are carried by the cells of the marginal zone (134) (Figure 2.3). Albeit considering the location of adaptive and innate immune cells predetermined, distribution of the cells can be altered dynamically due to the magnitude of inflammation and immune responses in the spleen. Marginal zone antigen presenting cells capture the blood borne antigens and present them to T cells in the white pulp to initiate adaptive immune responses. Additionally, plasmablasts can migrate from the white pulp to the red pulp for producing the antibodies (135). Therefore, the cells of innate and adaptive immune systems can be heterogeneously found both in the red pulp and the white pulp to shape the immune responses.

The spleen may also contribute to extramedullary hematopoiesis (EMH). EMH is defined by the formation of blood cells outside of the bone marrow (136). During the fetal development, hematopoiesis takes place in the liver, spleen, and the yolk sac. Later in the embryonic stage, hematopoietic progenitor cells migrate to the bone marrow, and it becomes the predominant hematopoietic niche (137-139). As a complex process, hematopoiesis can occur in special niches containing stromal cells, megakaryocytes, adipocytes, and osteoblasts. Within the bone marrow these cells maintain the differentiation and the self-renewal of the progenitor cells (140, 141). Stromal-cell-derived factor-1 (SDF-1) or CXCL12/CXCR4 and CCL2/CCR2 axes utilize homing and retention of HSPCs (142). It has been reported that CXCL12 deficiency result in a decrease in the colonization of HSPC population and impairment in hematopoietic functions (19).

In adults, the bone marrow is the major site of the hematopoiesis but under physiological stress or inflammation such as cancer, HSPCs may migrate out of the bone marrow, home to the spleen where EMH occurs (143). In mice, spleen remains as a hematopoietic organ and HSPCs are mostly found in the red pulp. Although the spleen of mice resembles of the human spleen, since obtaining spleen samples from humans is very challenging, splenic myelopoiesis is still debatable in humans. In a study, fresh spleen samples were collected from the patients with pancreatic or colorectal cancer who underwent splenectomy. As a control group, the spleen samples from the trauma patients or benign pathological conditions were also collected. Based on CD117, CD34, CD38 and CD45RA positivity, splenic granulocyte/macrophage progenitors (GMPs)-like cells were determined. Cancer patients had higher amounts of splenic GMPs and produced more granulocyte and macrophage colonies, *ex vivo* (144). In another study, fresh spleen samples from the patients with pancreatic or gastric cancer patients and as controls from the patients with cirrhosis or benign splenic tumors were collected. CD133 was used as a marker of human HSPCs in the spleen of cancer patients, more $CD133^+$ progenitors were found compared to the controls (145). Moreover, in the spleen of myelofibrosis patients, $CD34^+$ progenitors were determined (146). In the spleen samples, which were obtained from deceased individuals because of an acute myocardial infarction, c-kit^+ progenitors were found to express Ki67 (147). These studies indicate the notion that in inflammatory disorders, the human spleen may also serve as a hematopoietic organ to support the activity of bone marrow in human.

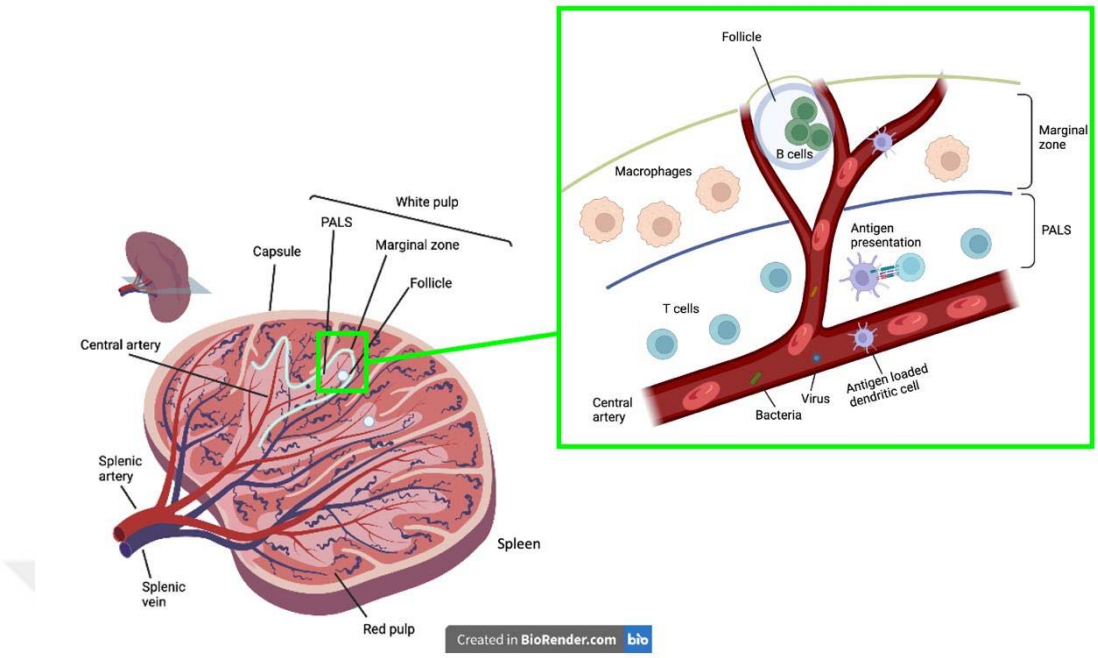

Figure 2.3. Schematic illustration of the microanatomy of spleen is given (PALS, periarteriolar lymphoid sheath; the image was created in BioRender.com.

2.5. Clinical Practices With Splenectomy

Although spleen has important immune functions, removal of the spleen (splenectomy) may be considered in certain pathological conditions. One of the most common reasons of splenectomy are ruptures due to a severe abdominal trauma. In case, the spleen cannot be repaired, the surgeon decides to perform splenectomy to prevent internal bleeding and avoid a life-threatening condition (148). Secondly, splenectomy is an effective treatment in hematological diseases and considered for the patients who cannot benefit from the medications. Idiopathic thrombocytopenic purpura (ITP) is one of the most common hematological disease, which may require splenectomy. ITP is an autoimmune disorder characterized by decreased numbers of platelets. IgG autoantibodies bind to the platelets and cause immune-mediated destruction of platelets by the phagocytes of the spleen. ITP treatment relays on immunosuppressive agents such as corticosteroids. However, in unresponsive patients, splenectomy is routinely performed to prevent uncontrolled destruction of platelets and risk of bleeding (149, 150).

Due to the anatomical proximity to a tumor, splenectomy may be performed as a part of oncological surgery for gastric and pancreatic cancers. In gastric cancer treatment, gastrectomy, and dissection of D2 lymph nodes are suggested (151). Depending on the surgeon's decision, splenectomy may be performed to dissect splenic hilar lymph nodes to prevent lymph node metastasis. However, the impact of splenectomy on survival of the patients has been still debatable. There are studies comparing gastrectomy plus splenectomy with gastrectomy alone in gastric cancer patients. In some of these studies, splenectomy was not associated with increased survival (152-155). However, since gastric cancer patients undergone splenectomy had generally larger tumors at an advanced stage, this comparison may not be always reliable. In contrast, certain studies reported that gastrectomy plus splenectomy was correlated with higher survival than gastrectomy alone (59, 156). In pancreatic ductal adenocarcinoma treatment, distal pancreatectomy is accepted as a standard procedure. Depending on the surgeon's decision, splenectomy may also be performed to clear the regional lymph nodes. In pancreatic cancer, splenectomy has also been associated either with better or worse survival (157, 158). Nevertheless, because the spleen constitutes an important immune organ, splenectomy was considered to increase the tendency of infections (159). Therefore, there is no consensus on the benefits and risks of splenectomy.

3. MATERIALS AND METHODS

This work was done in Hacettepe University Cancer Institute, Department of Basic Oncology Laboratories from January 2018 to January 2022. Human samples were obtained from Department of General Surgery, Hacettepe University and Department of General Surgery, Diskapi Yildirim Beyazit Research and Training Hospital. Immunohistochemistry experiments and morphological analyses of the cells were performed at Department of Pathology, Hacettepe University. All experiments with human samples were commenced after the approval of the Non-interventional Clinical Research Ethics Committee at Hacettepe University (Approval No.: GO 16/197).

3.1 Materials

RPMI-1640, Fetal bovine serum (FBS), Pencillin-Streptomycin (Biological Industries, Israel), Phosphate buffered saline powder (PBS) (Advansta, USA), Histopaque 1.077 g/mL, Histopaque 1.119 g/mL, anti-human CD66b microbeads, anti-human CD14 microbeads, LS column (Miltenyi Biotec, Germany), eFluor670 proliferation dye (eBioscience, USA), anti-human CD3 (clone:HIT3a), anti-human IFN-γ Legend Max pre-coated ELISA kit, Carboxyfluoresceinsuccinimidyl ester (CFSE) cell division tracker kit, 10X RBC lysis solution (Biolegend, USA), anti-human STAT3, anti-human pSTAT3 (Tyr705), anti-mouse HRP conjugated secondary antibody, anti-rabbit HRP conjugated secondary antibody (Cell Signaling Technologies, USA), anti-human CD66b (BD, USA), anti-human CD3, anti-human Ki-67, DAPI, anti-mouse Alexa 488, anti-rabbit Alexa 555, anti-mouse Alexa 647, antiray Alexa 488 secondary antibodies, mounting medium (Abcam, UK), anti-human Nrf2, anti-human pNrf2 (Ser40), Pierce BCA protein assay kit, RIPA buffer, revertAid first strand cDNA synthesis kit (Thermo Fisher Scientific, USA), TGX^{TM} FastCast^{TM} acrylamide kit 10%, TEMED, ammonium persulfate (APS), 10X Tris/Glycine SDS buffer, 10X Tris/Glycine buffer, Tween20, Clarity ECL, Clarity ECL max, XT sample buffer, dual color protein ladder, Mini Trans-Blot® filter paper, Immun-blot PVDF membrane, SSO advanced universal SYBR green supermix (Bio-Rad, USA), animal tissue RNA purification kit (Norgen Biotek, Canada), methanol (J.T. Baker, USA), OCT tissue freezing medium (Leica, Germany), skim milk powder (Serva, Germany),

Tris buffer powder (Takara, Japan), EDTA-free protease inhibitor cocktail, PhosSTOP phosphatase inhibitor (Roche, Switzerland), 5-(and-6)-carboxy- 2',7'-dichlorofluorescein diacetate (H_2-DCF-DA), 4,5-diaminofluorescein-diacetate (DAF-2DA), phorbol 12- myristate 13-acetate (PMA), PE-Texas Red labelled latex beads, NaCl, trypan blue, beta-mercaptoethanol, bovine serum albumin (BSA), May-Grünwald Giemsa, (Sigma-Aldrich, USA), DNA size marker (Thermo Fisher Scientific, USA), SeaKem® LE Agarose (Lonza, USA), 10X Tris-borate-EDTA (TBE) buffer (Thermo Fisher Scientific, USA), FACS flow, CellWash (BD, USA), cell culture plastics, 96-well plates, falcons, serological pipettes (Sarstedt, Germany; SPL, Korea).

3.2 Patients

The peripheral blood and the spleen samples from the treatment-naïve and newly diagnosed gastric and pancreatic cancer patients who underwent splenectomy as a part of oncological surgery were collected. Spleen samples from trauma patients who underwent splenectomy due to wounding such as gunshot or knife wounds, and motor vehicle accidents were collected. As controls, peripheral blood samples from age and sex-matched healthy donors who do not have any inflammatory diseases and do not take medication regularly were obtained. As another control group, peripheral blood samples from healthy individuals who have a splenectomy history at least 1 year ago due to traumatic injury were collected. The spleen samples (approximately 1 cm^3) were taken in complete RPMI-1640 by a surgeon and immediately transferred the laboratory at room temperature. The peripheral blood samples (approximately 10 mL) were collected in the blood tubes containing EDTA. All samples were freshly collected and processed within 1 hour. Informed consent was obtained from the patients by the clinicians involved in this study. Clinical data of the patients and the healthy controls enrolled in this study are given in Table 3.1. Additionally, paraffin-embedded spleen samples from patients who underwent splenectomy because of idiopathic thrombocytopenic purpura (ITP) (n=9) in the archives of Hacettepe University Department of Pathology were included in the study.

Table 3.1. Clinical data of the cancer patients, the trauma patients and the healthy controls enrolled is given.

	Healthy control	Gastric cancer	Pancreatic cancer	Trauma patients	Splenectomized healthy controls*
Number (n)	65 (PB)	26	11	25	9 (PB)
Age median (range)	42 (21-62)	65 (38-83)	64 (37-78)	36 (18-72)	32 (29-61)
Gender female/male	35/30	14/12	8/3	2/23	7/2
Clinical stage					
Stage I		3	5		
Stage II		7	1		
Stage III		13	2		
Stage IV		3	3		
ISS 1-8 (minor)					
ISS 9-15 (moderate)				4	
ISS 16-24 (serious)				9	
ISS 25-49 (severe)				11	
ISS 50-74 (critical)					
ISS 75 (maximum)				1	
SIS 1				2	
SIS 2				2	
SIS 3				9	
SIS 4				11	
SIS 5				1	

*Healthy controls with previous splenectomy history; PB, peripheral blood; ISS, Injury severity score; SIS, Splenic injury score.

3.3. Buffers and Solutions

Phosphate-buffered saline (PBS): Commercially obtained powder PBS mixture was dissolved in 500 mL distilled water to make 1X PBS. It was sterilized by autoclaving prior to use.

Fetal Bovine Serum (FBS): A bottle of heat-inactivated FBS was thawed at room temperature. It was aliquoted and stored at -20^{o}C.

Complete RPMI-1640 medium: RPMI-1640 medium was completed by adding heat-inactivated FBS (10%), 100 U/mL Penicillin, 100 µg/mL Streptomycin, and 2 mM L-glutamine. It was stored at 4^{o}C.

Anti-human CD3 monoclonal antibody (mAb): Anti-human CD3 antibody (clone, HIT3a; 1 mg/mL) was diluted with serum-free RPMI-1640 to make 2 µg/mL working solution. The working solution was stored at -20°C.

Trypan blue: Powder trypan blue (40 mg) was dissolved in 1X PBS to make %4 w/v solution. It was filtered thorough 0.22 um pore-sized filter and stored at room temperature.

MACS buffer: MACS buffer was prepared in 50 mL of 1X PBS by adding 0.5% FBS and 2 mM EDTA. It was stored at 4°C.

Cell proliferation dye: Lyophilized CFSE (5 µg) was reconstituted in 36 µL DMSO to make 5 mM solution. Lyophilized efluor670 (500 µg) was dissolved in 126 µL DMSO to make 5 mM solution. They were stored at -80°C.

Tris-Borate-EDTA buffer (TBE): TBE (10X) buffer was diluted with distilled water to make TBE (1X) solution.

Lysis buffer for protein extraction: Lysis buffer was freshly prepared by mixing 680 µL RIPA buffer, 20 µL phosphatase inhibitor and 300 µL protease inhibitor.

Running buffer: Commercially obtained 10X Tris/Glycine/SDS electrophoresis buffer (containing 25 mM Tris, 192 mM glycine and 0.1% SDS) was diluted with distilled water to make 1X running buffer. It was stored at room temperature.

Transfer buffer: Commercially obtained 100 mL 10X Tris/Glycine electrophoresis buffer (containing 25 mM Tris, 192 mM glycine), 200 mL HPLC grade methanol and 700 mL distilled water were mixed to make 1X transfer buffer.

Tris buffer: One pouch of Tris powder was dissolved in 500 mL of distilled water to make 1 M Tris buffer. It was stored at 4°C.

NaCl solution: NaCl (29.2 gram) was dissolved in 100 mL dH_2O to make 5 M NaCl solution. It was stored at room temperature.

TBST buffer: To make 1X TBST buffer, 20 mL 1M Tris buffer, 30 mL 5M NaCl, 5 mL Tween®20 (final concentration 0.1%) and 945 distilled water were mixed. It was stored at 4°C.

Primary and secondary antibodies: STAT3 and pSTAT3 antibodies in 1X TBST containing 5% BSA (1:1000 dilution), Nrf2 and pNrf2 antibodies in 1X TBST

containing 5% BSA (diluted 1:1500), beta-actin antibody in 1X TBST containing 5% skim milk (1:10000 dilution) were prepared for the western blot experiments. Anti-mouse and anti-rabbit HRP-conjugated secondary antibodies were prepared in 1X TBST containing 5% skimmed milk (1:5000 dilution). The primary antibodies used in the immunofluorescence staining (anti-CD66b, anti-CD3, anti-Ki-67, anti-pSTAT3 and anti-PD-L1) were prepared in 1X PBS containing 2% BSA (1:100 dilution), the secondary antibodies anti-mouse Alexa 488, anti-mouse Alexa 647, anti-rabbit Alexa 555, anti-rat Alexa 488 and DAPI were prepared in 1X PBS containing 2% BSA (1:200 dilution). Primary antibodies were re-used and stored at 4^{o}C for 2 weeks. Secondary antibodies were freshly prepared for each assay.

3.4. Cell isolation and Sorting

Isolation of cells by density gradient centrifugation: Spleen tissues obtained from the patients were macerated in 1X PBS by mechanical disruption. Suspension of the cells were filtered through a cell strainer (40 µm pore-sized) to eliminate aggregates and tissue debris. Peripheral blood samples were diluted with 1X PBS at 1:1 ratio. Suspension of the spleen and diluted peripheral blood samples were slowly layered over 3 mL of 1.077 g/mL and centrifuged at 400xg for 25 minutes at room temperature with no brake. After centrifugation, the cloudy layer consisting of “low-density” peripheral blood mononuclear cells (PBMCs) and PMN-MDSCs were collected. To isolate the cells with the higher densities, the samples below 1.077 g/mL gradient separation solution were resuspended and layer over 1.119 g/mL gradient separation solution. After centrifugation (400xg for 25 minutes at room temperature with no brake), the cloudy layer consisting of “normal density” PMN cells were collected. Red blood cells (RBCs) in normal density PMN cell fraction were lysed with 1X RBC lysis buffer. The buffer (3 mL) was added onto the cells and mixed by gentle pipetting for 5-10 minutes. To get rid of lysis the buffer, complete RPMI-1640 was added into the tube and centrifuged (1800 rpm, 5 min). The lysing process was repeated, when necessary. The cell pellet was then resuspended in complete RPMI-1640.

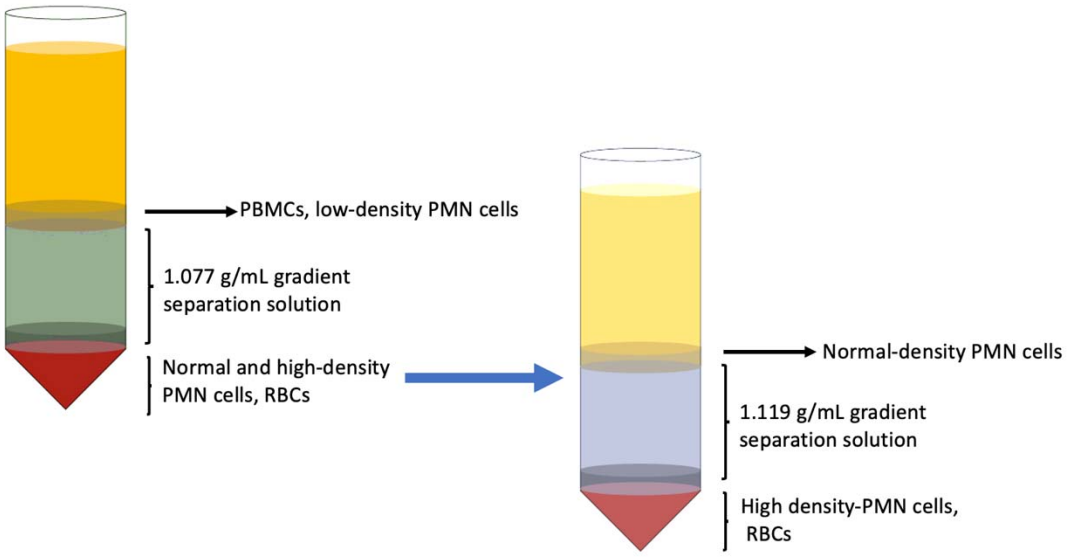

Figure 3.1. Schematic representation of the density gradient separation. PBMCs and low-density PMN cells accumulated over 1.077 g/mL gradient. The cells found at the bottom of the tube were collected and again layered over 1.119 g/mL gradient separation solution and normal-density PMN cells were recovered over 1.119 g/mL gradient.

Magnetic-activated cell sorting (MACS): According to the protocol of Miltenyi Human $CD14^+$ Positive Selection Kit, $CD14^+$ monocytes were purified from the healthy donors' PBMCs. PBMCs were counted and 10^7 cells were suspended with 100 µL MACS buffer (1X PBS containing 0.5% FBS and 2 mM EDTA) and 10 µL of CD14 microbeads were added. After 20 minutes of incubation at 4°C, the cells were washed with MACS buffer (at 1800 rpm for 5 minutes). The MACS column was placed in the magnetic MACS separator and rinsed by 2 mL of MACS buffer. Suspension of the cells were applied onto the column and the column was washed twice with MACS buffer. The cells found in the flow-through fraction were collected and called as "monocyte-depleted PBMCs". Then, the column was removed from the separator and magnetically labelled cells were flushed out into a 15 mL tube. The collected cells were resuspended in complete RPMI-1640 and an aliquot of them was labelled with anti-CD14 conjugated antibody to check the purity by the flow cytometry (Figure 3.2 A).

According to the protocol of Miltenyi Human CD66b$^+$ Positive Selection Kit, CD66b$^+$ PMN cells amongst the splenocytes and PBMCs were purified. Cells were counted and 10^7 cells suspended with 100 µL MACS buffer and 10 µL CD66b microbeads were added. After for 20 minutes of incubation at 4^{o}C, the cells were washed with MACS buffer (at 1800 rpm for 5 minutes). The MACS column was placed in the magnetic MACS separator and rinsed by 2 mL of MACS buffer. Suspension of the cells were applied onto the column and the column was washed twice with MACS buffer. Then, the column was removed from the separator and magnetically labelled cells were flushed out into a 15 mL tube. The collected cells were then resuspended in complete RPMI-1640 and an aliquot of them was labelled with fluorescent-labelled anti-CD66b conjugated antibody to check the purity through the flow cytometer (Figure 3.2 B).

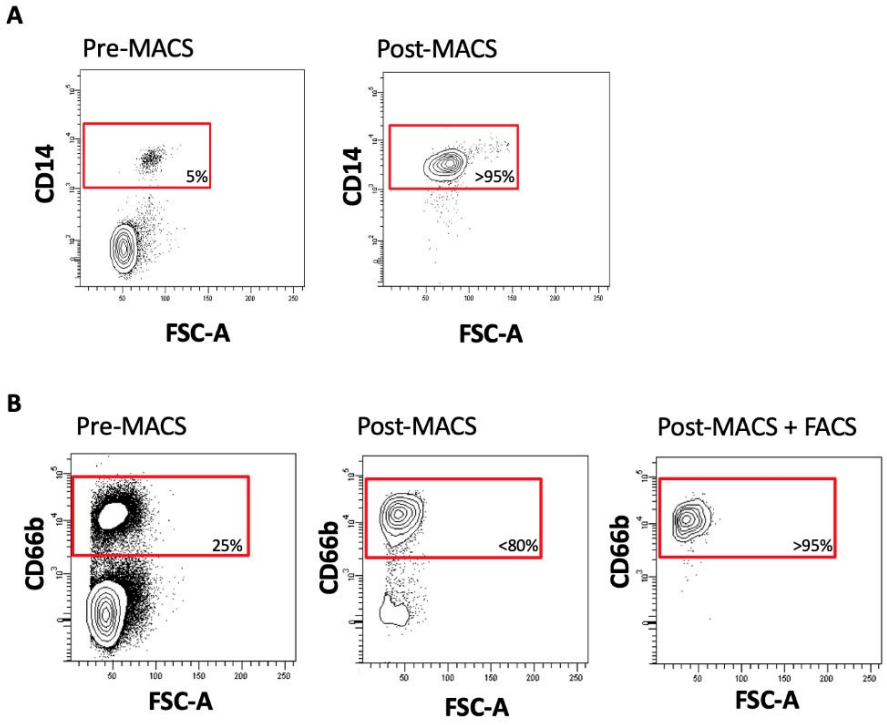

Figure 3.2. **A)** Confirmation of the purity of CD14$^+$ monocytes isolated by MACS. The cells before and after MACS were labelled with anti-CD14-FITC monoclonal antibody and analyzed on a flow cytometer. **B)** Confirmation of the purity of CD66b$^+$cells isolated by MACS and FACS. The purity of the cells before MACS, after MACS and after MACS/FACS were assessed by labelling with anti-CD66b-FITC monoclonal antibody and immunophenotyping.

Fluorescence-activated cell sorting (FACS): Followed $CD66b^+$ positive selection by MACS, in case of the cell purity is less than %90, $CD66b^+$ cells were enriched through FACS (FACSAria II, BD, USA) and FACS Diva V8.0.1 (BD, USA). To isolate a pure cell population, the sorter must be initially set according to the manufacturer's recommendations by stabilizing the stream. Accudrop beads (BD, USA) were then used to adjust the appropriate drop delay value and frequency to test the sort module of FACS. After the MACS $CD66b^+$ positive selection, the cells were resuspended in 1 mL serum-free RPMI-1640 and labelled with anti-human CD66b-FITC. Followed by an incubation for 25 minutes at room temperature, complete RPMI-1640 was added onto the labelled cells and the cell suspension were filtered through 40 µm pore-sized cell strainers to remove clumps. The cell suspension was run on FACS, and gating strategy was applied. After singlet cells were chosen and further gated depending on their size and granularity, $CD66b^+$ positive cells were sorted. The collected cells with a purity of ≥95%, were centrifuged at 1800 rpm for 5 minutes and resuspended in complete RPMI-1640 for further experiments.

3.4.1. Cell Counting

To count cells, 10 µL 0.4% trypan blue and 10 µL cell suspension were mixed and transferred in a Fuchs-Rosenthal Counting Chamber (Hausser Scientific, USA) and under a coverslip through capillary action. The size of the chamber is 0.1 mm x 0.1 mm (Figure 3.3) and the side of each sixteen square is 1 mm. The distance between the chamber and the coverslip is 0.1 mm. Under a light microscope, the cells on four of sixteen squares were counted and the cell concentration was calculated according to the formula given below (Formula 3.1).

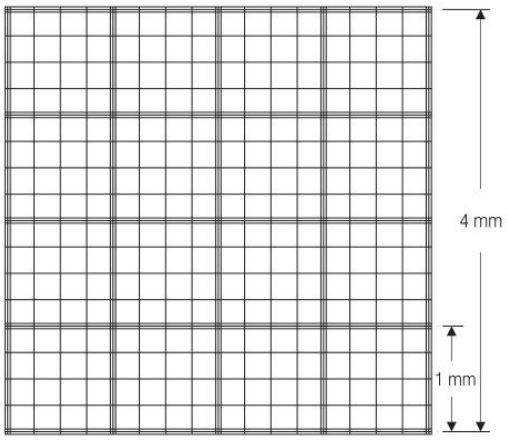

Figure 3.3. Illustration of Fuchs-Rosenthal Counting Chamber.

$$\text{Area} = 1\ \text{mm} \times 1\ \text{mm} = 1\ \text{mm}^2$$

$$\text{Volume} = 1\ \text{mm}^2 \times 0.1\ \text{mm} = 0.1\ \text{mm}^3$$

$$\text{Cell concentration} = \frac{\text{Total cell count} \times 10^4}{\text{Number of counted squares}} \times \text{Dilution factor} \qquad (3.1)$$

3.4.2. Establishing co-Cultures

Purified low-density PMN-MDSCs or normal density PMN cells were co-cultured with healthy donors' (eFluor670-labelled) monocyte-depleted PBMCs (10^5 cells/well) at different ratios (PMN: monocyte-depleted PBMCs ratio; 0:1, 0.125:1, 0.25:1, 0.5:1 and 1:1) in round bottom 96 well plates. To provide a constant stimulation, anti-CD3 monoclonal antibody (25 ng/mL) and constant number of monocytes (12.5×10^3/well) were added to each well. T cell proliferation was analyzed on a flow cytometer after 72 hours of incubation. Supernatants were collected from the co-cultures without touching the cells and stored at -80^{o}C for further experiments.

3.5. Immunological Techniques

3.5.1. Flow Cytometry

Surface staining: For immunophenotyping, the cells were resuspended in 100 µL CellWash solution in 5 mL tubes and 100 ng of the listed antibodies (Table 3.2) were added. The tubes were gently vortexed and incubated in dark at 4ºC for 40 minutes or at room temperature for 25 minutes. After incubation, 1-2 mL CellWash solution was added into the tubes and centrifuged at 1800 rpm for 5 minutes. After supernatants were discarded, the cells were resuspended in 100 µL CellWash and analyzed on the flow cytometer (FACSAria II, BD, USA). According to the isotype-matched antibodies, the percentage of positive cells and the median fluorescent intensity (MFI) values were analyzed with FlowJo software (FlowJo v10, BD, USA).

Table 3.2. Information on the antibodies used for flow cytometry is given.

Antibody	Clone	Fluorochrome	Manufacturer
CD3	UCHT1	FITC	BioLegend, USA
CD10	HI10a	FITC	BioLegend, USA
CD11b	ICRF44	APC/Cy7, APC	BioLegend, USA
CD14	M5E2	PE/Cy7, APC/Cy7, PE	BioLegend, USA
CD15	H198	APC	BioLegend, USA
CD16	3G8	PE	BioLegend, USA
CD19	SJ25C1	FITC	BioLegend, USA
CD20	2H7	FITC	BioLegend, USA
CD33	WM53	PE/ Dazzle^{TM}594, PE/Cy7	BioLegend, USA
CD45	2D1	PerCP, PE/Dazzle^{TM}594	BioLegend, USA
CD56	MEM-188	FITC	BioLegend, USA
CD66b	G10F5	APC, FITC	BioLegend, USA
CD124	G077F6	PE	BioLegend, USA
CD125	A14	PE	BD, USA
CD274 (PD-L1)	29E.2A3	PE	BD, USA
HLA-DR	L243	PerCP	BioLegend, USA
LOX-1	15C4	PE	BioLegend, USA
VEGFR-1	H-225	FITC	Santa Cruz, USA

Assessment of T cell proliferation: Monocyte-depleted PBMCs were centrifuged at 1800 rpm for 5 minutes. Then the supernatants were discarded, $5x10^6$ cells were resuspended in 1 mL serum-free RPMI 1640 and incubated with CFSE or eFluor670 dyes at 5 uM final concentration. Cells were incubated at room temperature in dark for 10 minutes and the tubes were filled with complete RPMI-1640. Then, the tubes were placed on ice for 5 minutes and were centrifuged at 1800 rpm for 5 minutes. After the supernatants were discarded, cells were resuspended with complete RPMI-1640 and stimulated with anti-CD3 (25 ng/mL) for co-cultures and proliferation assays. The CFSE or eFluor670 labelled cells were gated, and percentages of proliferated cells were determined by the flow cytometry depending on the dilution of the proliferation dye.

Assessment of ROS and NO production: Total leukocytes from the low-density and the normal density fraction (10^5 cells in 100 µL) were resuspended in serum-free RPMI-1640 in 5 mL tubes. The cells were labelled with conjugated anti-human CD66b mAb and either with 1 uM ROS indicator (5-(and-6)-carboxy- 2',7'-dichlorofluorescein diacetate, H2-DCF-DA) and 2 uM NO indicator (4,5-diaminofluorescein-diacetate, DAF-2DA). To determine maximum ROS and NO production capacities, the cells were stimulated with phorbol 12-myristate 13- acetate (PMA, 0.8 uM) at the same time of labeling with anti-CD66b and ROS or NO indicators. The tubes were gently vortexed and incubated for 25 minutes at room temperature. At the end of the incubation period, 1-2 mL CellWash was added into the tubes and immediately placed on ice. After centrifuging (1800 rpm for 5 minutes), the cells were resuspended in 100 µL CellWash and median fluorescence intensities (MFI) of $CD66b^+$ cells were analyzed on the flow cytometery. ROS and NO production index as calculated with a formula given (Formula 3.2).

$$MFI_{PMA\text{-}stimulated\ cells}/MFI_{Unstimulated\ cells} \quad (3.2)$$

Analysis of phagocytosis: Total leukocytes from the low-density and the normal-density fraction were incubated with the PE-Texas Red labelled-latex beads in RPMI-1640 supplemented with 5% FBS (1 µL latex beads were added onto 10^5 cells resuspended in 100 µL RPMI-1640) for 4 hours at 37°C. At the end of the incubation,

1-2 mL CellWash solution was added into the tubes and centrifuged at 1800 rpm for 5 minutes. Then, the cells were resuspended in 100 µL CellWash and labelled with fluorescent-conjugated anti-human CD66b mAb. After 25 minutes of incubation at room temperature, the cells were washed with 1-2 mL CellWash and centrifuged at 1800 rpm for 5 minutes. Lastly, $CD66b^+$ cells were gated, and percentages of the cells engulfed the latex beads were determined through flow cytometery.

3.5.2. ELISA

All reagents of the anti-human IFN-γ pre-coated Legend Max ELISA kit were brought to room temperature and the supernatants, which were collected from the co-cultures and stored at -80°C, were thawed on ice. Wash buffer (20X) was diluted to 1X wash buffer with deionized water. The lyophilized human IFN-γ standard was reconstituted with the assay buffer provided in the kit to make 20 ng/mL standard solution. Standards were prepared as 1000 pg/mL, 500 pg/mL, 250 pg/mL, 125 pg/mL, 62.5 pg/mL, 31.3 pg/mL and 15.6 pg/mL, by serial dilution. The assay buffer was used as 0 pg/mL standard. The pre-coated 96 well plate was washed for four times with 300 µL wash buffer prior to use. Firstly, 50 µL assay buffer and 50 µL standards or 50 µL supernatants were added into the wells and plate was incubated for 2 hours at room temperature while shaking. Then, contents of the plate were discarded and washed for four times with the wash buffer. Secondly, 100 µL human IFN-γ detection antibody was added into the wells and the plate was incubated for 1 hour at room temperature while shaking. Then, the contents of the plate were discarded and washed for four times with the wash buffer. Thirdly, 100 µL avidin-HRP solution was added into the wells and the plate was incubated for 30 minutes at room temperature while shaking. Then, contents of the plate were discarded and washed for five times with the wash buffer. Before the last step, 100 µL substrate solution was added into the wells and the plate was incubated for 15 minutes in the dark. Depending on the IFN-γ concentration, the solution turned blue in color. Lastly, the reaction was stopped by the addition of 100 µL stop solution into the wells. The color was converted from blue to yellow. The plate was measured by the plate reader at 570 nm absorbance subtracted from 450 nm. The standard curve was drawn, and concentration of the IFN-γ was calculated, accordingly.

3.5.3. May-Grünwald Giemsa Staining

Purified low-density PMN-MDSCs and normal density PMN cells were gently pipetted in 1X PBS. Slides, filter card and cytofunnel were placed into the slide holder, then the cell suspension was added into the cytofunnel. After the slides were centrifuged at 50xg for 3 minutes (Hettich Universal 320, Germany), supernatants were discarded and the cytofunnel was removed. To dry the slides, they were centrifuged at 150xg for 1 minute. Giemsa stain was diluted with dH_2O (1:9; v/v) and May-Grünwald stain applied as ready-to-use solution. Firstly, the samples were stained with May-Grünwald for 5 minutes. Then, the samples were washed with dH_2O twice. Secondly, the samples were stained with the diluted Giemsa for 5 minutes. After Giemsa staining, the samples were washed with dH_2O twice and let them dry. Air-dried samples were covered with non-aqueous media (entellan) and a cover slip. The images were captured under a light microscopy (Zeiss, Germany) at Hacettepe University Faculty of Medicine, the Department of Pathology and analyzed by the help of a pathologist.

3.5.4. Immunohistochemistry

Paraffin-embedded spleen tissues were evaluated for CD15 expression by immunohistochemistry. The experiments were performed at Hacettepe University Faculty of Medicine, the Department of Pathology. The archived spleen paraffin-embedded spleen tissues were cut as 4 μm thick sections. Briefly, deparaffination, rehydration, inactivation of peroxidases and blocking steps were performed. The slides were labelled with the anti-CD15 (C3D-1) (Diagnostic Biosystems, USA) primary antibody by using a Leica Bond-Max autostainer (Vision Biosystems, Australia). After a washing step, the slides were incubated with secondary antibodies and streptavidin biotin complex. Then, horseradish peroxidase and 3,3′-Diaminobenzidine complexes were added onto the slides and hematoxylin counterstaining was performed. Lastly, the slides were covered with mounting medium and the cover slips. The images were captured under a light microscope (Zeiss, Germany) at Hacettepe University Faculty of Medicine, the Department of Pathology and analyzed by a pathologist.

3.5.5. Immunofluorescence Staining

The spleen specimens were embedded into tissue mold containing optimal cutting temperature (OCT) tissue freezing medium. After OCT was solidified at -20^{o}C, the frozen spleen tissue sections were cut 5 µm thick in the cryostat (Leica Microsystems, Germany). The sections were then transferred onto the slides coated with poly-L-lysine. Frozen sections of the spleen were fixed with 4% paraformaldehyde for 30 minutes at room temperature. Then, the slides were washed for three times with 1X PBS for 5 minutes and blocked with %10 BSA for 1 hour. After blocking, the slides were washed for three times with 1X PBS for 5 minutes, incubated with the primary antibodies (anti-CD66b, anti-CD3, anti-Ki-67, anti-pSTAT3 and anti-PD-L1) at dilutions indicated in the buffers' sections (3.3) with different combinations prepared in 1X PBS containing 2% BSA for 2 hours. At the end of the primary antibody incubation, the slides were washed for three times with 1X PBS for 5 minutes and they were incubated with the secondary antibodies (anti-mouse Alexa 488, anti-mouse Alexa 647, anti-rabbit Alexa 555, anti-rat Alexa 488) at dilutions indicated in the buffers' sections (3.3). and DAPI prepared in 1X PBS containing 2% BSA for 1.5 hour at room temperature. Lastly, the slides were washed for three times with 1X PBS for 5 minutes and covered with mounting media and a cover glass. The images were captured with fluorescence microscopy (Olympus, USA) or confocal microscopy (Zeiss, Germany). Images were analyzed by using ImageJ software (NIH image, USA).

3.6. Molecular Techniques

3.6.1. RNA isolation

RNA isolation was performed with Animal Tissue RNA Purification Kit (Norgen Biotek, Canada). Screw-cap tubes were filled with the 1 mm zirconium beads and 300 µL buffer RL supplemented with 1% beta-mercaptoethanol. Approximately 20 mg of the spleen tissues were chopped and put into the tubes, and they were homogenized for 30 seconds by using mini bead-beater 8 (Biospect, USA) and rested on the ice for 30 seconds. The homogenization and the resting steps were repeated for three times. After the cell lysate was transferred into 1.5 mL tubes,

centrifuged for 1 minute. The supernatants were collected into clean tubes and 450 µL 96% ethanol was added and vortexed. Then, 650 µL of the mixture was applied onto the column provided by the kit and centrifuged at 6000xg for 1 minute. Afterwards, 400 µL wash solution A was applied into the column and centrifuged at 14000xg for 2 minutes. Enzyme incubation buffer A (100 uL) and DNAse I (15 uL) was added onto the filter in columns and incubated for 15 minutes at room temperature. After the columns were centrifuged at 14000xg for 1 minute, the flowthrough was discarded, wash solution A (400 uL) was added into the column and centrifuged for 14000xg for 1 minute. Elution solution A (50 uL) was added and centrifuged at 200xg for 2 minutes. The purity and concentration of RNA was measured at 230 nm, 260 nm and 280 nm by UV spectrophotometry (NanoDrop ND-1000, USA). RNA samples were stored at -80^{o}C.

3.6.2. cDNA Synthesis

Complementary DNA (cDNA) synthesis was performed with RevertAid First Strand cDNA Synthesis kit (Thermo Fisher Scientific, USA). RNA samples (1 µg) and Oligo $(dT)_{18}$ primers (1 µL) were mixed thoroughly, and nuclease-free water was added onto 12 µL final volume. Then, 4 µL 5X reaction buffer, 1 µL Ribolock RNAse inhibitor, 2 µL 10 mM dNTP mix and 1 µL RevertAid reverse transcriptase were added. Followed by an incubation at 42^{o}C for 1 hour, the reaction was terminated at 70^{o}C for 5 minutes in a thermal cycler (Arktik Thermal Cycler, Thermo Fisher Scientific, USA). cDNA products were stored at -20^{o}C.

3.6.3. Polymerase Chain Reaction (PCR)

PCR reagents were thawed, and experiments were performed on ice. A master mix containing Taq Buffer, dNTP mix, $MgCl_2$, forward primers, reverse primers, nuclease-free water and Taq DNA polymerase (Thermo Fisher Scientific, USA) was prepared and distributed equally into the PCR tubes. Then, cDNA was added, and the tubes were placed into the thermal cycler and gradient PCR program was run to determine the appropriate annealing temperatures for specification of target gene sequences. The components and the thermal cycler PCR program are given in Table

3.3 and Table 3.4, respectively. Forward and reverse primer oligonucleotide sequences designed for specific amplification of the genes of interest are listed in Table 3.5.

Table 3.3. PCR components.

Components	Volume	Final Concentration
Taq Buffer (10X)	2.5 µL	1X
dNTP mix (2 mM)	2.5 µL	0.2 mM
$MgCl_2$ (25 mM)	2.5 µL	2.5 mM
Forward Primer	1 µL	0.2 mM
Reverse Primer	1 µL	0.2 mM
Nuclease-free water	14.25 µL	
Taq DNA Polymerase (5U/ µL)	0.25 µL	0.05 U/ µL
cDNA	1 µL	
Total volume	25 µL	

Table 3.4. Gradient thermal cycler program.

Step	Temperature	Time
Initial denaturation	95°C	3 min
Denaturation	95°C	30 sec
Annealing	57-65°C	30 sec
Extension	72°C	30 sec
Final extension	72°C	5 min

40 cycles

Table 3.5. Nucleotide sequences of the primers used for RT-PCR.

Gene	Forward (5′-3′)	Reverse (5′-3′)	Product size (bp)	NCBI accession no.
ACTB	CTGGAACGGTGAAGGTGACA	AAGGGACTTCCTGTAACAATGCA	140	NM_001101.5
NOS2	GGAACCTACCAACTGACGGG	GTCGATGCACAGCTGAGTGA	348	NM_000625.4
FLT1	TCGCCGGAAGTTGTATGGTTA	GAGAAGCTTGTAGGTGGCAA	509	NM_001159920.2
IL-10	AGGACTTAAAGGGTTACCTGG	TCACATGCGCCTTGATGT	114	NM_000572.3
COX2	CCCTTGGGTGTCAAAGGTAAA	TCCATCCTTGAAAAGGCGCA	267	YP_002124305.1
IDO1	GGGACACTTTGCTAAAGGCG	TGCCTTTCCAGCCAGACAA	141	NM_002164.6
ARG1	GGAGTCATCTGGGTGGATGC	GGCACATCGGGAATCTTTCCT	125	NM_001244438.2
GAL3	GCCAACGAGCGGAAAATGG	GTTATTATCCAGCTTTGTATTGC	555	NM_002306.4
CCL2	TCGCCTCCAGCATGAAAGTC	TCTTGAAGATCACAGCTTCTTTGG	213	NM_002982.4
S100A9	CTCCTCGGCTTTGACAGAGTG	TCACCCTCGTGCATCTTCTC	321	NM_002965.4
S100A8	TCAGTATATCAGGAAAAAGGGTGC	AACTCAGCTACTCTTTGTGGC	161	NM_001319197.1
TGF-β	CTATTGCTTCAGCTCCACGG	ATGACACAGAGATCCGCAGT	482	NM_000660.7
PD-L1	CAAGGCCGAAGTCATCTGGA	GAGGTAGTTCTGGGATGACCAA	209	NM_001267706.1

3.6.4. Agarose Gel Electrophoresis

Agarose gel (1% m/v) was prepared in 1X TBE buffer. The mixture was melted in microwave oven, after cooling ethidium bromide (final concentration 250 µg/mL) was added. Next, the agarose solution was poured onto a tray equipped with a comb. After the gel was solidified, the comb was removed. The gel was placed into an electrophoresis tank, and it was filled with 1X TBE. The samples (10-15 µL) were mixed with DNA loading dye and loaded into the wells. Additionally, 0.5 µg DNA size marker (50 bp; Thermo Fisher Scientific, USA) was loaded. The electrophoresis was run for 1 hour at 120V. Lastly, product bands were visualized under UV light by Kodak gel Logic 1500 digital imaging system (Figure 3.6; Carestream Health, USA).

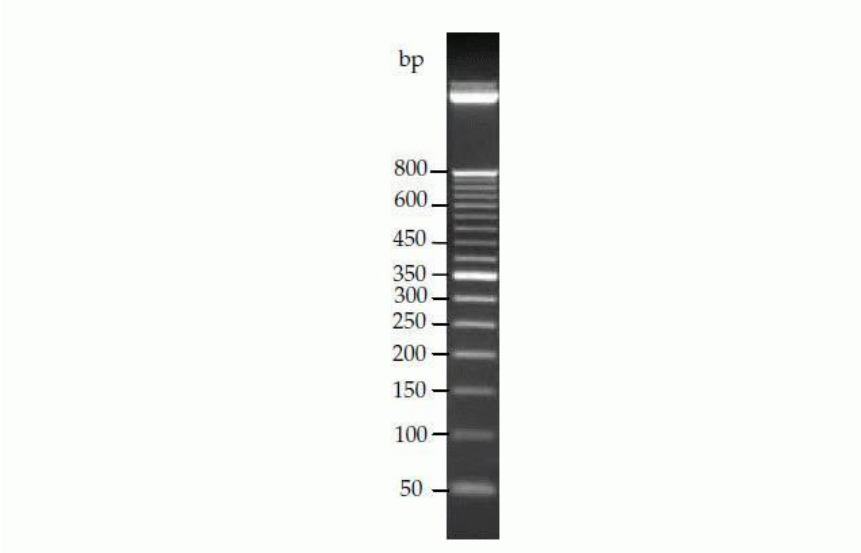

Figure 3.4. 50 bp DNA ladder (Thermo Fisher Scientific).

3.6.5. Real-time PCR (RT-PCR)

After determining the optimal annealing temperatures for each primer set, real-time PCR was performed by using SSO Advanced Universal SYBR green Supermix (Bio-Rad, USA) on CFX Connect™ Real-Time PCR Detection System (Bio-Rad, USA). The components of RT-PCR were thawed on the ice and a master mix was prepared (Table 3.6). The master mix was distributed and lastly cDNA was added into the PCR tubes. According to the previously determined annealing temperatures, the thermal cycling programs were set (Table 3.7). Relative gene expression was analyzed according to the Formula 3.3. The target gene expression in the spleen of the cancer patients was normalized to the total leukocytes obtained from the peripheral blood of the cancer patients and healthy donors. Alternatively, the target gene expression in the spleen of the trauma patients was normalized to the total leukocytes in the circulation of the healthy donors.

Table 3.6. Real-time PCR Components.

Reagent	Volume (µl)	
SsoAdvanced Universal SYBR Green Supermix (10X)	5	1X
Forward primer	1	0.5 µM
Reverse primer	1	0.5 µM
dH_2O	2	
cDNA	1	
Total volume	10	

Table 3.7. Thermal cycling program for RT-PCR.

Step	Temperature	Time	
Initial denaturation	95°C	3 min	
Denaturation	95°C	20 sec	40 cycles
Annealing	57-65°C	30 sec	
Extension	72°C	30 sec	
Melt-curve analysis	55-95°C	5 sec/step	
	0.5°C increment		

$$- \Delta\Delta Ct = -[(Ct_{\text{target gene}} - Ct_{\text{reference gene}}) - (Ct_{\text{target gene normalizer}} - Ct_{\text{reference gene}})] \quad (3.3)$$

3.6.6. Preparation of protein lysates

Screw cap tubes were filled with the 1 mm zirconium and 500 µL ice-cold lysis buffer containing 680 µL RIPA buffer, 20 µL phosphatase inhibitor and 300 µL protease inhibitor. Previously archived frozen spleen tissues were cut in small pieces and approximately 20 mg tissue was placed into the screw cap tubes. They were homogenized for 30 seconds by using mini bead-beater 8 (Biospect, USA) and rested on the ice for 30 seconds. The homogenization and resting steps were repeated for three times. After the tissue lysates were transferred into pre-cooled 1.5 mL tubes, they were centrifuged at 4°C for 10 minutes at 14000 rpm. Supernatants (protein lysates) were collected into the pre-cooled clean 1.5 mL tubes and stored at -80°C.

3.6.7. Assessment of Protein Concentration and Denaturation

Protein lysates were thawed on the ice and protein concentration were measured by bicinchoninic acid (BCA) kit (Thermo Fisher Scientific, USA). The working reagent was prepared by mixing BCA reagent A and reagent B (50:1, reagent A: reagent B). An ampule of 2 mg/mL albumin standard was serially diluted with the working reagent to prepare a set of protein standards (2 mg/mL, 1.5 mg/mL, 1 mg/mL, 0.75 mg/mL, 0.5 mg/mL, 0.25 mg/mL, 0.125 mg/mL ve 0.025 mg/mL). The working reagent (200 µL) was added into the each well of a flat bottom 96-well plate. Protein standards (10 µL) and the lysates (10 µL) were mixed, and then added into the wells containing working reagents. The plate was mixed thoroughly and incubated at 37°C for 30 minutes. Lastly, the optical densities were read on an optical microplate reader (SpectraMax Plus, Molecular Devices, USA) at 562 nm. A standard curve was drawn, and protein concentration was determined accordingly.

Beta-mercaptoethanol (5%) and 4x XT sample buffer (Bio-Rad, USA) were mixed and freshly prepared for each assay. Then, the protein lysates were mixed with beta-mercaptoethanol added 4x XT sample buffer (protein lysates:4x XT sample buffer; 3:1, v/v) and denaturated at 100°C on a heat block for 5 minutes. Lastly, the samples were placed into the ice for 5 minutes and then stored at -20°C.

3.6.8. Polyacrylamide Gel Electrophoresis

TGX™ FastCast™ acrylamide kit 10% (Bio-Rad, USA) was used to prepare hand casting gels for SDS-PAGE. Handcast glass plates were placed into the casting stand and stabilized. Ammonium persulfate (APS) was freshly dissolved in dH_2O to prepare 10% (w/v) solution. Resolving gel was prepared by mixing 6 mL Resolver A solution and 6 mL Resolver B solution. To initiate polymerization, 60 µL APS (10%), to accelerate polymerization 6 µL Tetramethyl ethylenediamine (TEMED) were added into the Resolver A and B mixture. Resolving gel solution was mixed well and dispensed into the handcast glass plates. Immediately, a stacking gel was prepared by mixing 2 mL Stacker A solution and 2 mL Stacker B solution. To initiate polymerization, 20 µL APS (10%), and to accelerate polymerization 2 µL tetramethyl ethylenediamine (TEMED) were added into the Stacker A and B mixture. Stacking gel solution was mixed well, dispensed slowly onto the resolving gel and a comb was

inserted. Gels were allowed to become polymerized for 40 minutes at room temperature before electrophoresis. Then, the plates were placed in the running module and the electrophoresis buffer tank. The tank was filled with freshly prepared 1X running buffer (1X Tris/Glycine/SDS buffer). The protein ladder (Figure 3.5, 7 µL) and the lysates containing equal amounts of protein (20 µg) were loaded into the wells. The gel was run at 75V for approximately 3 hours.

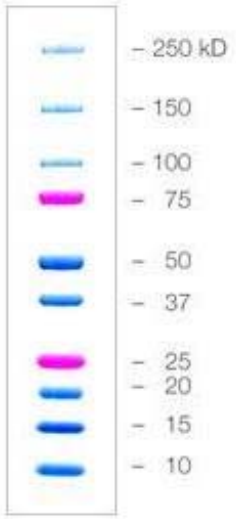

Figure 3.5. Protein ladder (dual color protein ladder, Bio-Rad, USA).

3.6.9. Protein Transfer Procedure

After SDS-PAGE was completed, the gels were removed carefully from the tank and placed into the 1X transfer buffer. PVDF membranes were hydrated with 100% methanol for 3 minutes while shaking to provide an effective transfer and protein binding. Then, PVDF membranes, filter papers and sponges were soaked in freshly prepared cold 1X transfer buffer. Transfer sandwich was prepared in a cassette as schematically demonstrated in Figure 3.6. Two filter papers were placed on two sponges, and the gel and the membrane were placed in between the filter papers. The membrane should be close to the anode (+) to allow the movement of negatively charged proteins towards the anode. Air bubbles were removed gently by a roller and the cassette was placed into the transfer tank. In the presence of a stirring magnet, proteins were transferred at 75V for 90 minutes in the cold room (+4-8^{o}C).

Figure 3.6. Schematic illustration of the western blot wet transfer cassette.

3.6.10. Primary and secondary antibody incubation

After the transfer was completed, the membranes were blocked with 1X TBST containing 5% skimmed milk while shaking (100 rpm) at room temperature. Then, the membranes were washed with 1X TBST for 10 minutes while shaking. Diluted primary antibodies (listed in Table 3.8) prepared in 1X TBST containing 5% BSA or skimmed milk were added onto the membranes and incubated while shaking at 100 rpm in the cold room, overnight. Next day, primary antibody was removed, and the membranes were washed for three times with 1X TBST while shaking (100 rpm) at room temperature. Then, dilutions of secondary antibodies (listed in Table 3.9) prepared in 1X TBST containing 5% skimmed milk were added on the membranes and incubated while shaking (100 rpm) at room temperature. The membranes were washed for three times with 1X TBST while shaking (100 rpm) at room temperature.

Table 3.8. Primary antibodies used in Western Blot experiments.

Antibody	Species	Dilution	Manufacturer
Beta-actin	Mouse	1:10000	Santa Cruz, USA
STAT3	Rabbit	1:1000	Cell Signaling Technologies, USA
p-STAT3 (Tyr 705)	Rabbit	1:1000	Cell Signaling Technologies, USA
Nrf2	Rabbit	1:1500	Thermo Fisher Scientific, USA
p-Nrf2	Rabbit	1:1500	Thermo Fisher Scientific, USA

Table 3.9. Secondary antibodies used in Western Blot experiments.

Antibody	Species	Dilution	Manufacturer
Anti-mouse IgG HRP	Horse	1:5000	Cell Signaling Technologies, USA
Anti-rabbit IgG HRP	Goat	1:5000	Cell Signaling Technologies, USA

3.6.11. Chemiluminescence Detection

Two components of Clarity ECL or Clarity ECL max kits (Bio-Rad, USA) were mixed equally and added onto the membranes. After 3 minutes of incubation in dark, the membranes were visualized on a chemiluminescence detection system (Newton 7.0, Vilber, France). The protein quantification was done by using ImageJ software (NIH image, USA).

3.7. Statistical Analysis

Data presented were obtained from at least three independent experiments. For the statistical analyses, Student's paired or unpaired t-test or analysis of variance (ANOVA) and Chi-square where appropriate were used. P values < 0.05 were evaluated as statiscally significant. The data are represented as median ± standard error of the mean (SEM) or mean ± SEM. For the survival analysis, cut-offs of PMN-MDSCs' percentages were determined according to the median values.

4. RESULTS

4.1. Characterization of MDSCs in the Peripheral blood and Spleen of Cancer Patients

To analyze myeloid cells, freshly obtained spleen and peripheral blood samples of the patients were layered over 1.077 g/mL gradient. According to the previously published work (8), immunophenotyping strategy was applied to determine the subtypes of low-density MDSCs. Initially, for a stringent gating strategy (Figure 4.1), doublets were discriminated by forward scatter area (FSC-A) versus forward scatter height (FSC-H) plot. Then, the cells were distributed based on their size and granularity by forward scatter area (FSC-A) versus side scatter area plot (SSC-A). To analyze all leukocytes, $CD45^+$ cells were gated, and lymphocytes, eosinophils and basophils were excluded by selecting Lin $(CD3\text{-}19\text{-}20\text{-}56)^-CD125^-$ cells. Depending on their HLA-DR, CD33, CD11b and CD66b expressions, $CD11b^+HLA\text{-}DR^-CD33^{mo}CD66b^+$ (PMN-MDSC) and $CD11b^+HLA\text{-}DR^{-/lo}CD33^{hi}CD66b^-CD14^+$(M-MDSC), $CD11b^+HLA\text{-}DR^{-/l}CD33^{mo}CD66b^-CD14^-$ (e-MDSC) were identified (Figure 4.1).

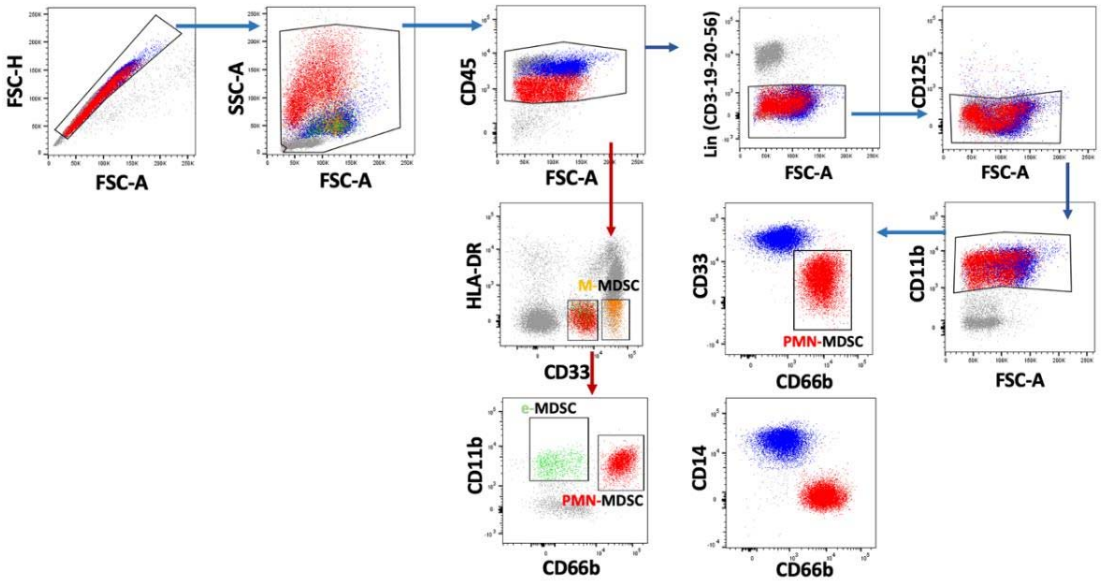

Figure 4.1. Multi-color flow cytometry immunophenotyping and gating strategy to determine PMN-MDSC, e-MDSC, M-MDSC are given. Red arrows show the gating strategy followed for e-MDSC and M-MDSC. Blue arrows show an alternative confirmatory gating strategy followed for PMN-MDSC, which can also be achieved by red arrows.

Based on the gating strategy, the percentages of PMN-MDSCs, M-MDSCs, and e-MDSCs amongst splenocytes and PBMCs of the gastric cancer patients were compared to those of in the peripheral blood of the healthy donors. The percentages of PMN-MDSCs were significantly increased both in peripheral blood and spleen of the patients compared to the healthy donors. Particularly, PMN-MDSCs were accumulated in the spleen. The percentage of myeloid cells with M-MDSC phenotype was also increased both in the peripheral blood and spleen of gastric cancer patients whereas, there was no statistical significance for e-MDSC percentages (Figure 4.2 A). In addition, the absolute number of MDSCs were also calculated in peripheral blood and spleen. PMN-MDSCs were determined at the highest numbers (Figure 4.2 B and C). The representative of flow cytometry plots showing the PMN-MDSC population was shown in Figure 4.2 D. To determine the distribution of total PMN cells, which highly comprise of PMN-MDSCs, in the spleen of patients, frozen sections of the spleens were labelled with a common PMN cell marker CD66b. $CD66b^{+}$ cells were widely distributed across the spleen (Figure 4.2 E).

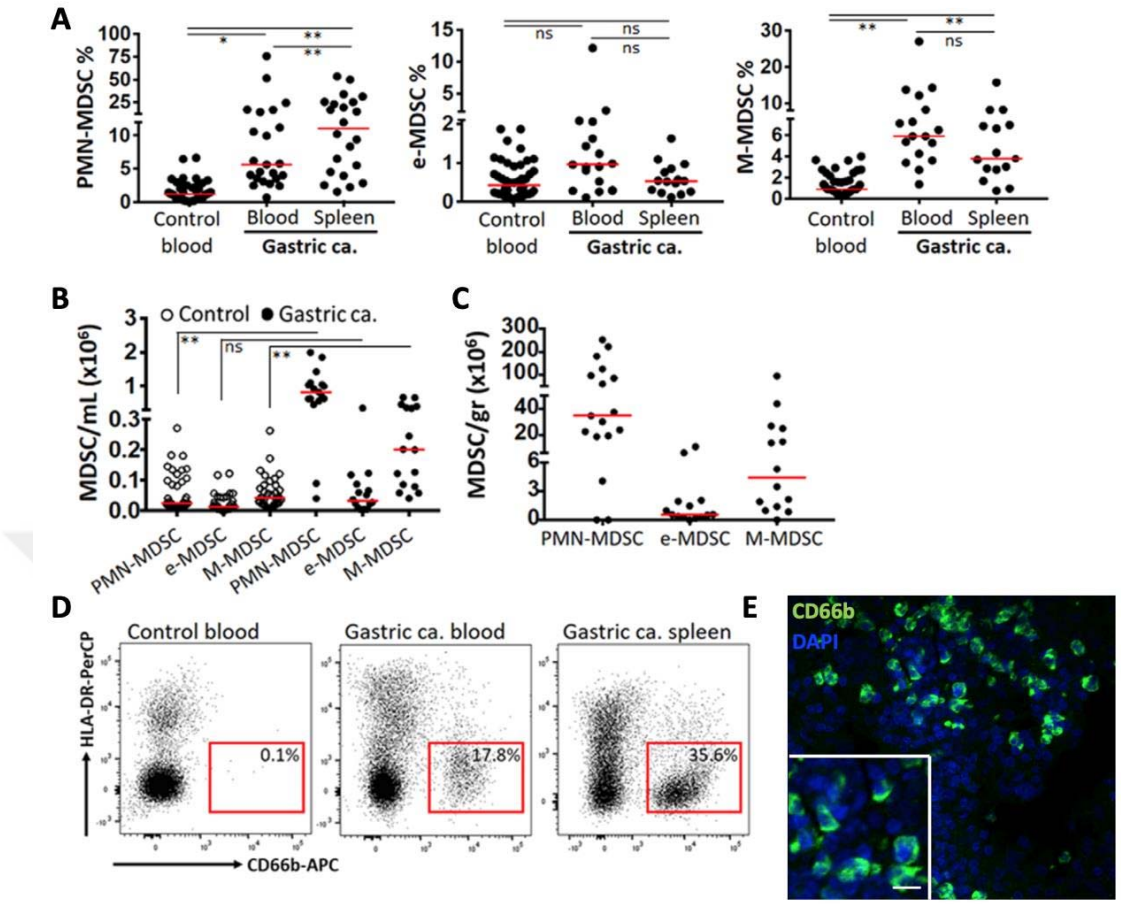

Figure 4.2. The subpopulations of MDSCs from the peripheral blood and the spleen of gastric cancer patients and their comparison with healthy donors. A) The percentages of PMN-MDSCs, e-MDSCs and M-MDSCs-related phenotypes were determined by the flow cytometry (peripheral blood, healthy donors n=41, gastric cancer patients n=23; spleen, gastric cancer patients n=22). B) Absolute numbers of MDSCs in the peripheral blood were calculated (peripheral blood, healthy donors n=38, gastric cancer patients n=16). C) Absolute numbers of MDSCs in the spleen were calculated (spleen, gastric cancer patients n=17). D) Representative flow cytometry graphs showing HLA-DR and CD66b expressions were given to indicate the distribution of PMN-MDSCs-related phenotypes. E) CD66b immunofluorescence and DAPI staining was performed on frozen sections of the spleen samples (scale bar, 10 μm). Red line shows the median value (ns, not significant; *p<0.05, **p<0.01).

The percentages and absolute numbers of MDSCs were evaluated in the peripheral blood and spleen of pancreatic cancer patients as well. Both the percentages and numbers of PMN-MDSCs were significantly increased in the peripheral blood and spleen of pancreatic cancer patients. The results obtained from the pancreatic cancer

patients were found consistent with those from the gastric cancer patients and there was no statistical difference between two cancer types in terms of MDSC levels (PMN-MDSCs% in the blood, healthy 1.52 ± 0.21%; gastric cancer 12.35 ± 3.65%; pancreatic cancer 14.31 ± 3.93%; spleen, gastric cancer 16.51 ± 3.19%; pancreatic cancer 13.12 ± 2.55%) (Figure 4.3 A and B).

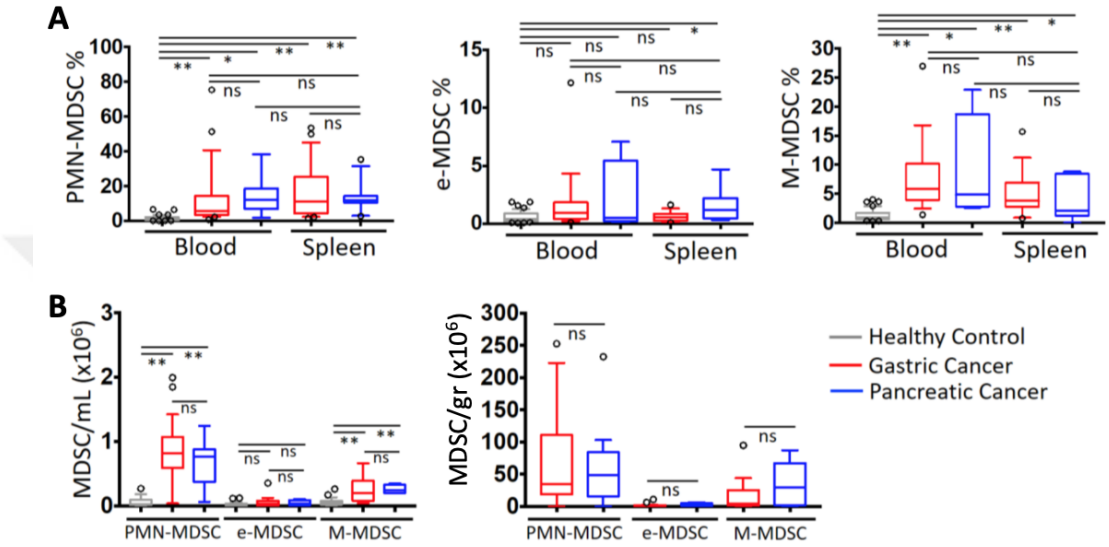

Figure 4.3. The subpopulations of MDSCs from the peripheral blood and the spleen of gastric cancer and pancreatic cancer patients and their comparison with healthy donors. A) The percentages of PMN-MDSCs, e-MDSCs and M-MDSCs-related phenotypes were determined by the flow cytometry (peripheral blood, healthy donors n=41, gastric cancer patients n=23, pancreatic cancer patients n=9; spleen, gastric cancer patients n=22, pancreatic cancer patients n=9). B) Absolute numbers of MDSCs in the peripheral blood and the spleen were calculated (peripheral blood, healthy donors n=38, gastric cancer patients n=16, pancreatic cancer patients n=9; spleen, gastric cancer patients n=17, pancreatic cancer patients n=9; ns, not significant; *p<0.05, **p<0.01).

According to the previous studies, elevated numbers, and percentages of PMN cells in peripheral blood were observed in cancer patients (12). Similarly, increased numbers and percentages of PMN cells were observed in complete blood counts, while there was no statistical significance found related with the monocytes (Figure 4.4 A and B).

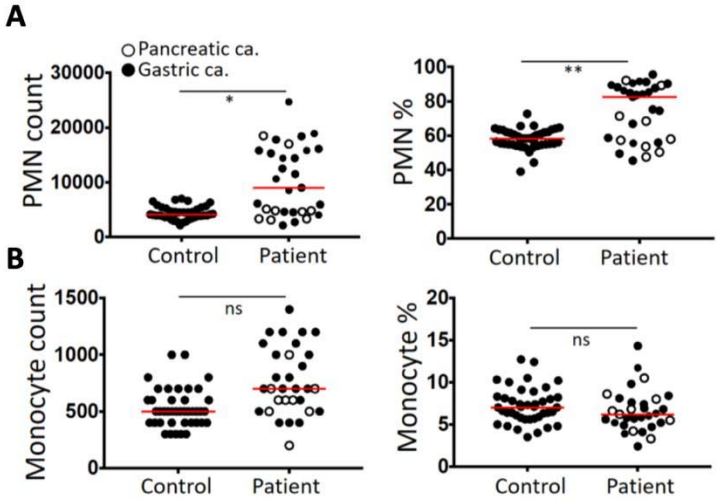

Figure 4.4. The counts and percentages of PMN cells and monocytes. A) The counts per deciliter (dL) and percentages of PMN cells of the patients and the healthy donors were given according to the total blood counts. B) The counts per deciliter (dL) and percentages of monocytes of the patients and healthy donors were given according to the total blood counts (healthy donors, n=41, gastric cancer patient n=22, pancreatic cancer patients n=9; ns, not significant; *p<0.05, **p<0.01).

In the spleen and the peripheral blood samples, the ratio of PMN cells collected from the normal-density (< 1.119 g/mL and > 1.077 g/mL gradient) and the low-density (< 1.077 g/mL gradient) fractions was determined. In the spleen, approximately 30% of the PMN cells were at low-density whereas, in peripheral blood, only 5% of the PMN cells were in the low-density fraction (Figure 4.5 A). To examine low-density PMN cells cytologically, May-Grünwald Giemsa staining was performed, and the cells were morphologically classified as band cells, metamyelocytes, myelocytes, and promyelocytes. Both in the spleen and the peripheral blood, the band cells were detected as the most frequent immature cell type. Myelocytes were found to be higher in the peripheral blood, whereas the distribution of myelocytes and metamyelocytes were comparable (Figure 4.5 B and C).

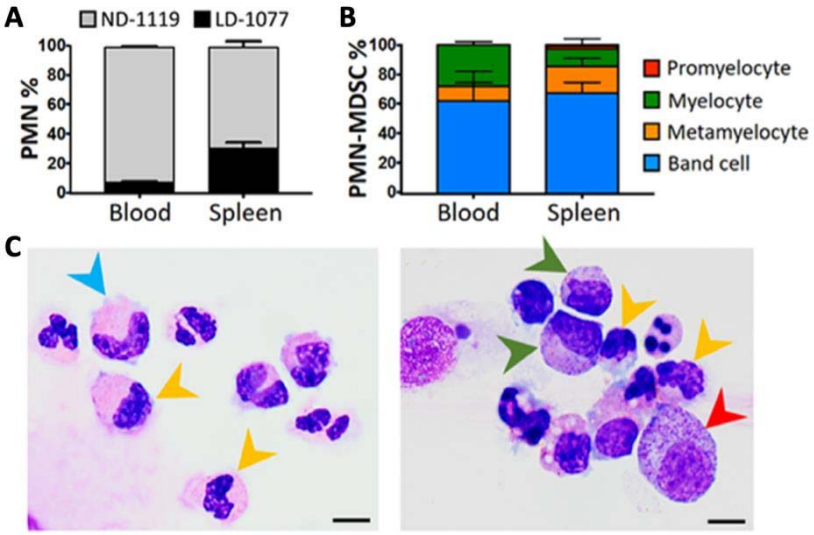

Figure 4.5. Characterization of PMN cells in the peripheral blood and the spleen of gastric cancer patients. A) The proportion of normal-density PMN cells (ND-1119) and low-density PMN cells (LD-1077) were determined in total PMN cells by the flow cytometry. B) The distribution of cytologically different stages among non-segmented cells was given. C) Representatives of PMN-MDSCs stained with May-Grünwald Giemsa were shown (scale bar, 10 μm, n=12).

To determine the differences between PMN-MDSCs isolated from the peripheral blood and the spleen in more detail, the expression of additional surface markers related to the myeloid maturation or suppressive characteristics of myeloid cells (CD11b, CD33, CD66b, HLA-DR, CD10, LOX-1, IL-4Rα, CD16, VEGFR1, PD-L1) were investigated. Median fluorescence intensities (MFI) of these markers were assessed. The expression of CD16 and CD10 were found higher on PMN-MDSCs isolated from the spleen than those found in the circulation (Table 4.1 and Figure 4.6).

Table 4.1. MFI levels of CD11b, CD33, CD66b, HLA-DR, CD10, LOX-1, IL-4Rα, CD16, VEGFR1, PD-L1 on the peripheral blood-and the spleen-derived PMN-MDSCs were given (average ± SEM).

	Blood PMN-MDSC	Spleen PMN-MDSC
CD11b	10794.7 ± 1820	10766.5 ± 1808.2
CD33	1299.2 ± 230.9	1367.2 ± 321.6
CD66b	15153.6 ± 4116.7	12110.2 ± 3828.5
HLA-DR	2554.6 ± 1645.7	951.2 ± 235.9
CD10	971.4 ± 196.9	1566.4 ± 287.8**
IL-4Rα	952.5 ± 443.8	951.2 ± 235.9
LOX-1	877.8 ± 166.2	774 ± 164.4
CD16	20555.9 ± 8329.8	50620.8 ± 14321.8*
VEGFR1	378.3 ± 45.8	348.8 ± 31.7
PD-L1	5167 ± 1780.8	3511.7 ± 1452.6

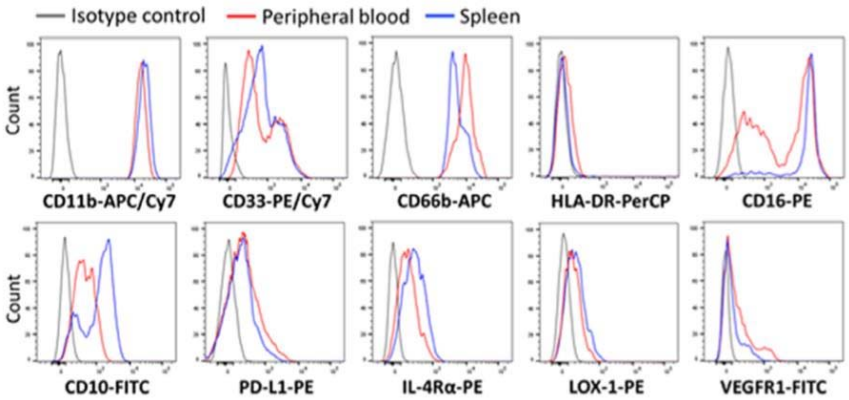

Figure 4.6. Representative flow cytometry histograms were given to demonstrate the expressions of CD11b, CD33, CD66b, HLA-DR, CD10, LOX-1, IL-4Rα, CD16, VEGFR1, PD-L1 on the peripheral blood-and the spleen-derived PMN-MDSCs.

In the frozen sections of the spleen tissue, the expression of phosphorylated-STAT3 (pSTAT3) as a transcription factor relevant to the immaturity and immune-suppressive functions of MDSCs were evaluated on the $CD66b^+$ splenocytes. The expression of pSTAT3 was frequently detected in the $CD66b^+$ splenocytes (Figure 4.7 A). As a marker of immunosuppression, the expression of PD-L1 was also evaluated on $CD66b^+$ splenocytes and PD-L1 expression were not only restricted to $CD66b^+$ cells in the gastric cancer patients' spleen (Figure 4.7 B).

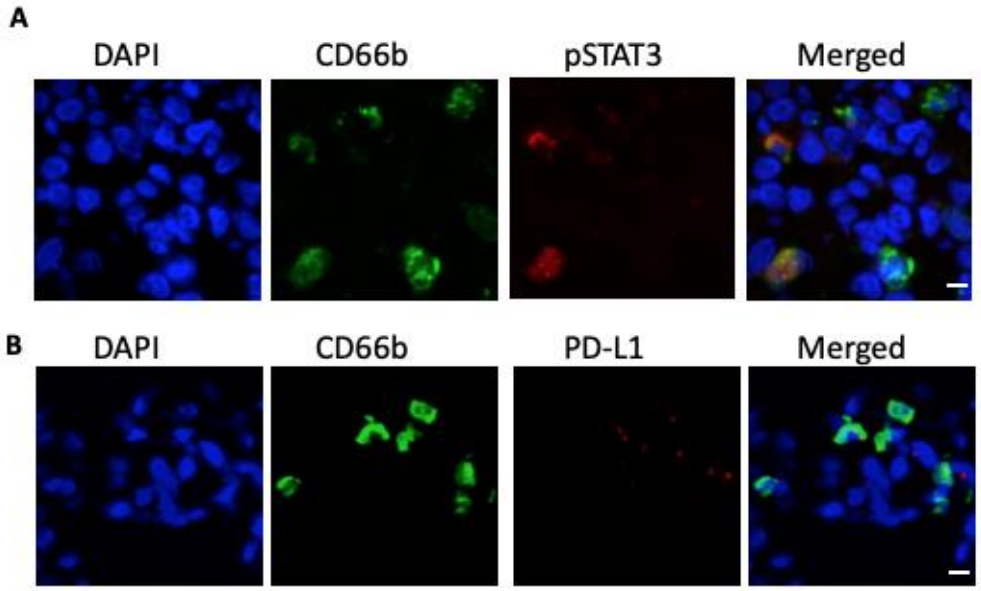

Figure 4.7. Representative images from immunofluorescence analysis on the spleen specimens for CD66b, pSTAT3 and PD-L1. A) CD66b, pSTAT3 and DAPI staining was performed on the frozen sections of the spleen (scale bar, 10 μm). B) CD66b, PD-L1 immunofluorescence staining was performed on frozen sections of the gastric cancer patients' spleen. The representatives of out of 3 patients were given.

In addition to phenotypical properties, the low-density PMN-MDSCs isolated from the peripheral blood and the spleen were compared functionally. In this manner, the ROS and NO production capacities were examined. Compared to those from the peripheral blood, the low-density PMN-MDSCs isolated from the spleen produced higher amounts of ROS, significantly (Figure 4.8 A). However, there was no significant difference detected on NO production capacity of these PMN-MDSCs (Figure 4.8 B). As another functional analysis, the phagocytosis capacities of PMN-MDSCs were tested and there was no statistical difference observed between the PMN cells obtained from the different compartments (Figure 4.8 C).

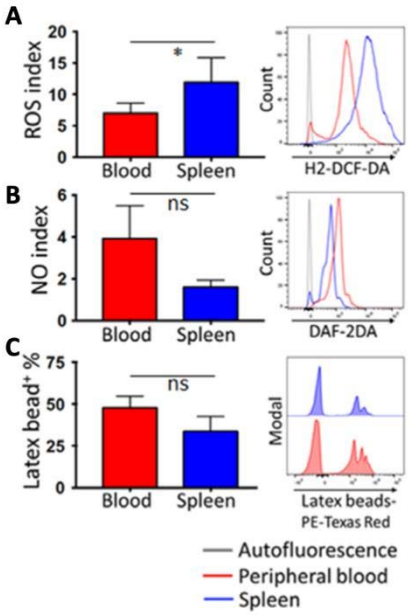

Figure 4.8. Functional characterization of the peripheral blood-and the spleen-derived PMN-MDSCs. A) Production capacity of reactive oxygen species (ROS), (B) nitric oxide (NO) and (C) phagocytosis capacity against the latex beads was compared between the peripheral blood-(n=5) and spleen-derived PMN-MDSCs (n=9). The representative flow cytometry histograms were given in the right side of the graphs. The data was presented as average ± SEM (ns, not significant; *p<0.05).

In addition to the PMN-MDSCs, the normal-density PMN cells isolated from the peripheral blood and the spleen were analyzed in terms of their morphology and functions. There was no significant difference determined related with ROS and NO production, phagocytosis capacity and morphological properties (Figure 4.9).

To sum up, spleen of the cancer patients was highly populated with the low-density PMN cells which have almost similar characteristics with the circulating PMN-MDSCs.

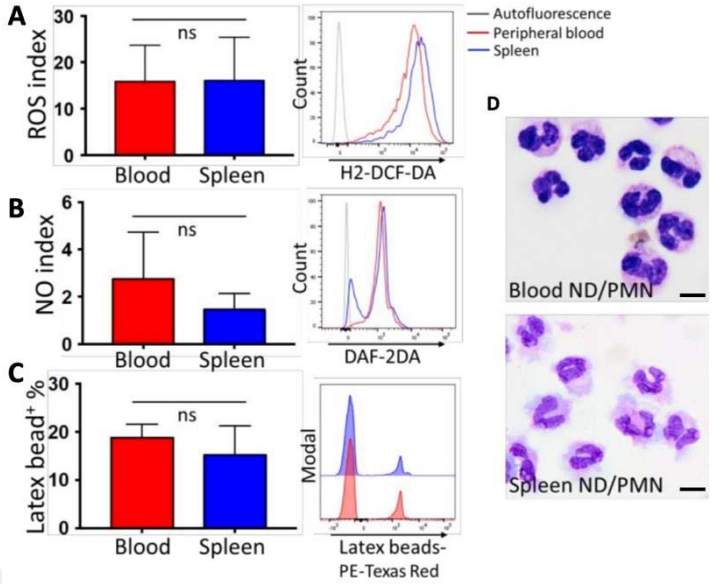

Figure 4.9. Functional and morphological characterization of the peripheral blood- and the spleen-derived normal-density PMN (ND/PMN) cells. A) Production capacity of reactive oxygen species (ROS), (B) nitric oxide (NO) and (C) phagocytosis capacity against the latex beads was compared between the peripheral blood- (n=5) and the spleen-derived ND/PMN cells (n=9). D) Representatives of the peripheral blood- and the spleen-derived ND/PMN cells stained with May-Grunwald Giemsa were shown. The representative flow cytometry histograms were given in the right side of the graphs. The data was presented as average ± SEM (ns, not significant).

Inhibition of T cells is an integral part of the suppressive nature of MDSCs (15). Especially PMN-MDSCs need to be in close proximity and cell-to-cell contact must be maintained to suppress T cell responses (57). Therefore, co-localization of the splenic PMN-MDSCs and T cells, and consequences of their interaction were analyzed. Initially, distribution of PMN cells in the spleen tissue was determined by CD15 immunohistochemistry on paraffin-embedded spleen tissue sections from the cancer patients. The spleen samples collected from the trauma patients were used as non-malignant controls. The spleen specimens obtained from the gastric cancer patients displayed higher amount of cells positive for CD15, which is another common PMN marker. Particularly, PMN cells were found primarily located in the red pulp and amassed around periarteriolar lymphoid sheaths (PALS). Quantification of $CD15^+$ cells was also given (Figure 4.10 A).

In the frozen sections of the spleen tissues obtained from the gastric cancer patients, co-localization of $CD3^+$ T cells and $CD66b^+$ PMN cells was evaluated. It was found that $CD3^+$ T cells and $CD66b^+$ PMN cells were in close contact (Figure 4.10 B). Next, the impact of PMN-MDSCs on T cell proliferation and IFN-γ secretion were determined as a functional measure of MDSCs' suppressive actions. Low-density PMN-MDSCs from the spleen and the peripheral blood of the patients were purified and co-cultured with eFluor670-labelled monocyte-depleted PBMCs at different ratios (PMN: monocyte-depleted PBMCs ratio; 0:1, 0.125:1, 0.25:1, 0.5:1 and 1:1) and a constant number of monocytes under 25 ng/mL anti-CD3 stimulation for 72 hours. At the end of the 72 hours of incubation, the percentages of proliferated T cells were determined by flow cytometry and IFN-γ secretion were analyzed through ELISA. T cell proliferation and IFN-γ secretion were suppressed by increasing amounts of the low-density PMN-MDSCs isolated from the spleen or peripheral blood samples of gastric cancer patients, while normal-density PMN cells isolated from healthy donors did not interfere with T cell proliferation. Especially at 1:1 ratio, T cell proliferation was significantly suppressed by the peripheral blood- and the spleen-derived PMN-MDSCs (The peripheral blood-derived PMN-MDSC:PBMC, 56.1±8.5%; the spleen-derived PMN-MDSC:PBMC, 67.4±19.6%) (Figure 4.10 C). Moreover, IFN-γ secretion from T cells was also hindered both by the spleen-derived and the peripheral blood-derived PMN-MDSCs (Figure 4.10 D). In addition to PMN-MDSCs, the impact of normal-density PMN cells isolated from the spleen and the peripheral blood of the patients on T cell proliferation and IFN-γ secretion were evaluated. The spleen-derived normal-density PMN cells also suppressed T cell proliferation and IFN-γ production similar to the spleen-derived low-density PMN-MDSCs, whereas the peripheral blood-derived normal-density PMN cells were not suppressive. The spleen-derived normal-density PMN cells suppressed T cell proliferation significantly at 0.5:1 and 1:1 ratios (The spleen-derived ND/PMN:PBMC, 0.5:1, 71.8±13.9%; 1:1, 35.2±12.1%) (Figure 4.10 E and F).

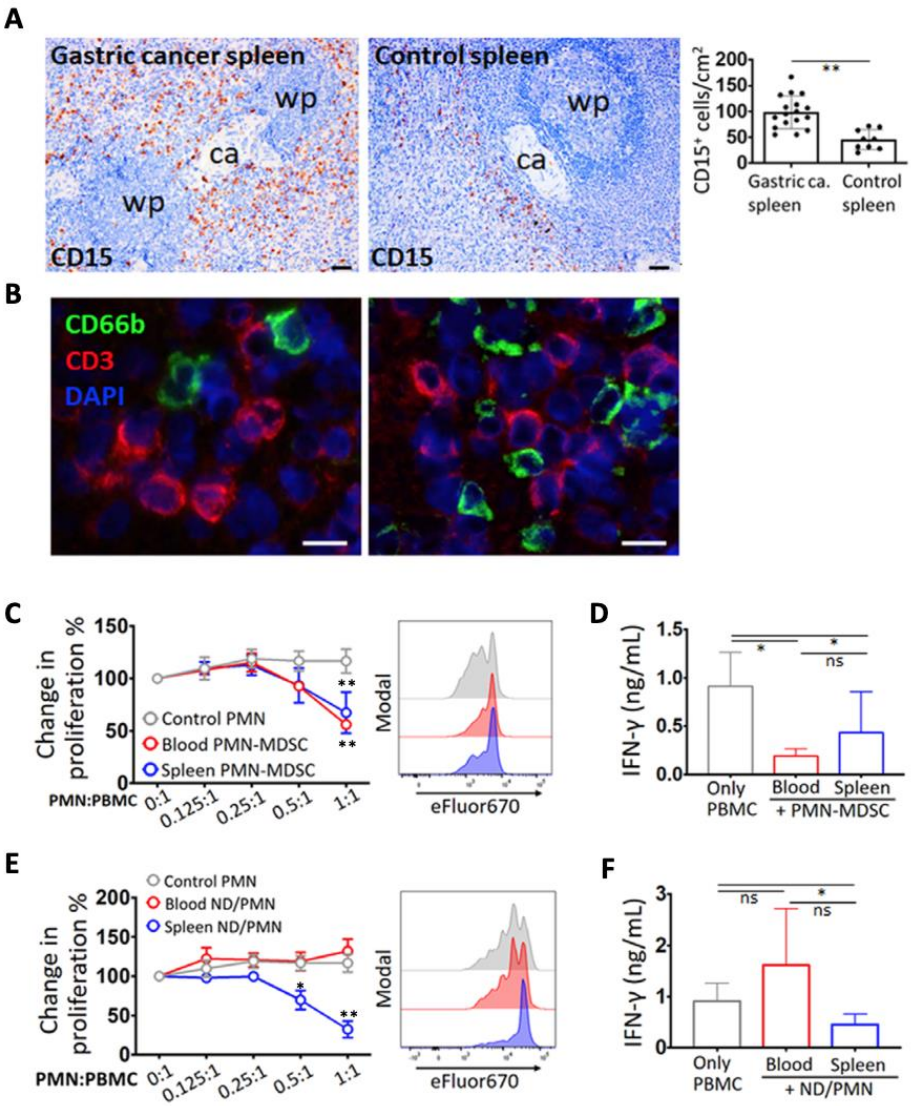

Figure 4.10. Distribution of PMN cells in the spleen and their interaction with T cells were analyzed. A) Distribution of splenic PMN cells in the gastric cancer patients (n=17) and the trauma patients (n=9, control spleen) were determined by CD15 immunohistochemistry (ca, central arteriole; wp, white pulp; scale bar, 100 µm). Quantification of $CD15^+$ cells were given. B) CD66b, CD3 and DAPI immunofluorescence staining was performed on the frozen sections of gastric cancer patients' spleen (scale bar, 20 µm). C and E) Purified peripheral blood-derived and spleen-derived PMN-MDSCs and normal-density PMN cells (n=6) were co-cultured with eFluor670-labelled monocyte-depleted PBMCs from the healthy donors (n=6) and constant numbers of monocytes isolated from healthy donors during 72 hours under anti-CD3 stimulation (25 ng/mL). D and F) At the end of the co-cultures, the amount of IFN-γ was measured by ELISA (at 0.5:1 PMN cell:PBMC ratio). The data was presented as average ± SEM (ns, not significant; *p<0.05, **p<0.01).

To better determine the immune modulation through the spleen in cancer, expression of the immune regulatory genes mainly associated with MDSCs was examined in the spleen tissues of the gastric cancer patients and the pancreatic cancer patients by RT-PCR. Especially calcium binding proteins (S100A8 and S100A9), IDO1, ARG1, COX2, and GAL3 which are related with immunosuppressive activities of MDSCs were found higher in the spleen of cancer patients than in their peripheral blood. COX2 was heterogeneously distributed among the patients, whereas NOS2, TGF-β, PD-L1, IL-10, CCL2, and VEGFR1 were in decreasing trend. Overall, there was no significant difference observed between the gastric cancer patients and the pancreatic cancer patients in terms of the expression of immune regulatory genes (Figure 4.11).

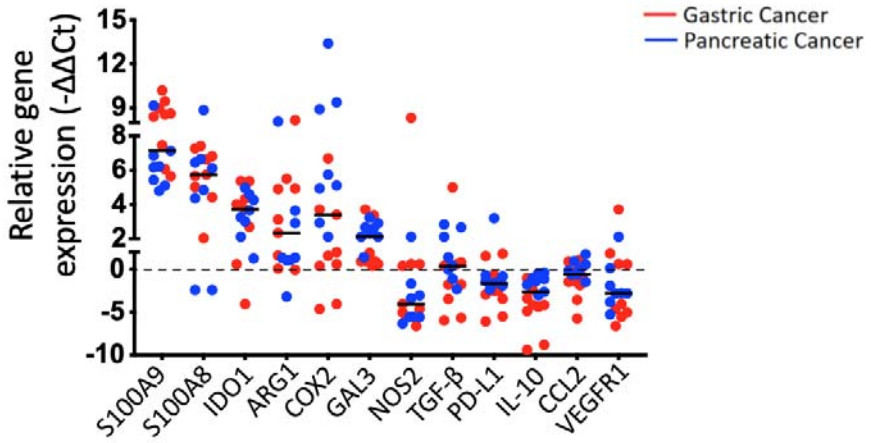

Figure 4.11. Expression of immune regulatory genes such as S100A9, S100A8, IDO1, ARG1, COX2, GAL3, NOS2, TGF-β, PD-L1, IL-10, CCL2, and VEGFR1 were examined on spleen tissues by quantitative RT-PCR. Gene expression data obtained from the spleen samples of cancer patients were normalized to the pooled peripheral blood total leukocytes from the gastric and the pancreatic cancer patients, separately. Black line represents the median value (gastric cancer patients n=9, pancreatic cancer patients n=8).

Moreover, the expression of immune regulatory transcription factors such as Nrf2 and STAT3 and their phosphorylated forms associated with the suppressive nature of MDSCs were analyzed on the spleen tissues of the gastric cancer patients and the pancreatic cancer patients by Western Blot. The activity of Nrf2 and STAT3

levels were heterogeneous among the patients. In gastric cancer, pNrf2 was found upregulated in a patient, whereas in pancreatic cancer, pNrf2 was found upregulated in 2 patients out of 8 patients studied as representatives of the cancer group. In pancreatic cancer, pSTAT3 was upregulated and found significantly higher than in gastric cancer patients (4.12 A and B).

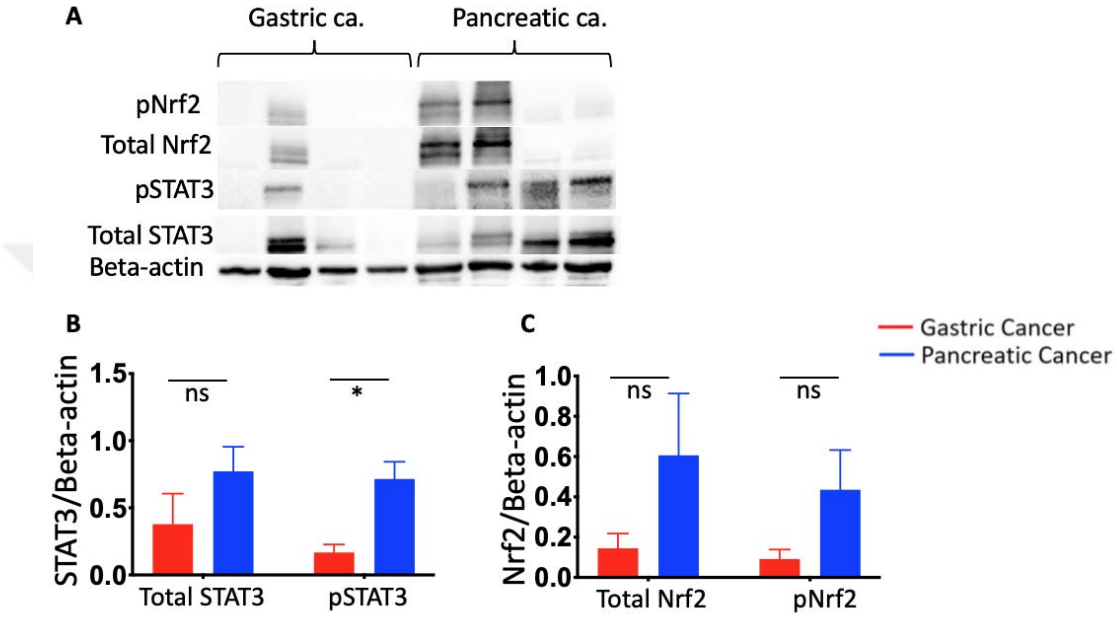

Figure 4.12. Analysis of immunoregulatory proteins on the spleen samples of cancer patients. A) The Western Blot images showing the levels of pNrf2, total Nrf2, pSTAT3, total STAT3, and beta-actin on the spleen tissues of gastric cancer patients (n=4) and pancreatic cancer patients (n=4) were represented. B) STAT3/Beta-actin and C) Nrf2/Beta-actin ratio was given (ns, not significant; *p<0.05).

4.2. Comparison of MDSCs From Cancer and Trauma Patients

The malignant disease cancer has been well-acknowledged to induce MDSCs, especially the spleen is a major organ that harbors these myeloid regulatory cells in mouse tumor models (10). Nevertheless, in humans, the status of spleen remains elusive in non-malignant diseases. Thus, the spleen samples from the patients who underwent splenectomy due to traumatic injury were used as non-malignant disorder. Based on the gating strategy (Figure 4.1), the percentages of PMN-MDSCs, M-MDSCs, and e-MDSCs amongst the splenocytes of the trauma patients were compared

with those from the gastric cancer patients and the pancreatic cancer patients as well as the peripheral blood from the healthy donors. Similar to the cancer patients, particularly PMN-MDSCs were accumulated in the spleen of trauma patients (PMN-MDSCs% in the blood, healthy 1.52 ± 0.21%; spleen, gastric cancer 16.51 ± 3.19%; pancreatic cancer 13.12 ± 2.55%; trauma patient 21.93 ± 4.4%). Although PMN-MDSCs were the most frequent subtype of MDSCs found in the traumatic spleen, the cells with e-MDSCs and M-MDSCs phenotypes were also found to be increased (e-MDSCs% in the blood, healthy donors 0.43 ± 0.07%; spleen, gastric cancer patients 0.53 ± 0.1%; pancreatic cancer patients 1.2 ± 0.65%; trauma patients 0.63 ± 0.34%; M-MDSCs% in the blood, healthy donors 0.92 ± 0.15%; spleen, gastric cancer patients 3.78 ± 0.99%; pancreatic cancer patients 2.07 ± 1.6%; trauma patients 3.26 ± 1.1%) (Figure 4.13 A). The absolute numbers of MDSCs were also compared and PMN-MDSCs were found the highest. Although M-MDSCs in the pancreatic cancer patients exhibited an increasing trend compared to the trauma patients, there was no statistical difference found in terms of the absolute numbers of the MDSCs among different patient groups (Figure 4.13 B). The presence of PMN cells across the traumatic spleen samples, frozen sections of the samples were labelled with CD66b and DAPI. $CD66b^{+}$ cells were largely distributed in the spleen as also observed in the spleen tissues of the cancer patients (Figure 4.13 C). Please refer to Figure 4.2 E for the immununofluorescence staining of the gastric cancer patients' spleen.

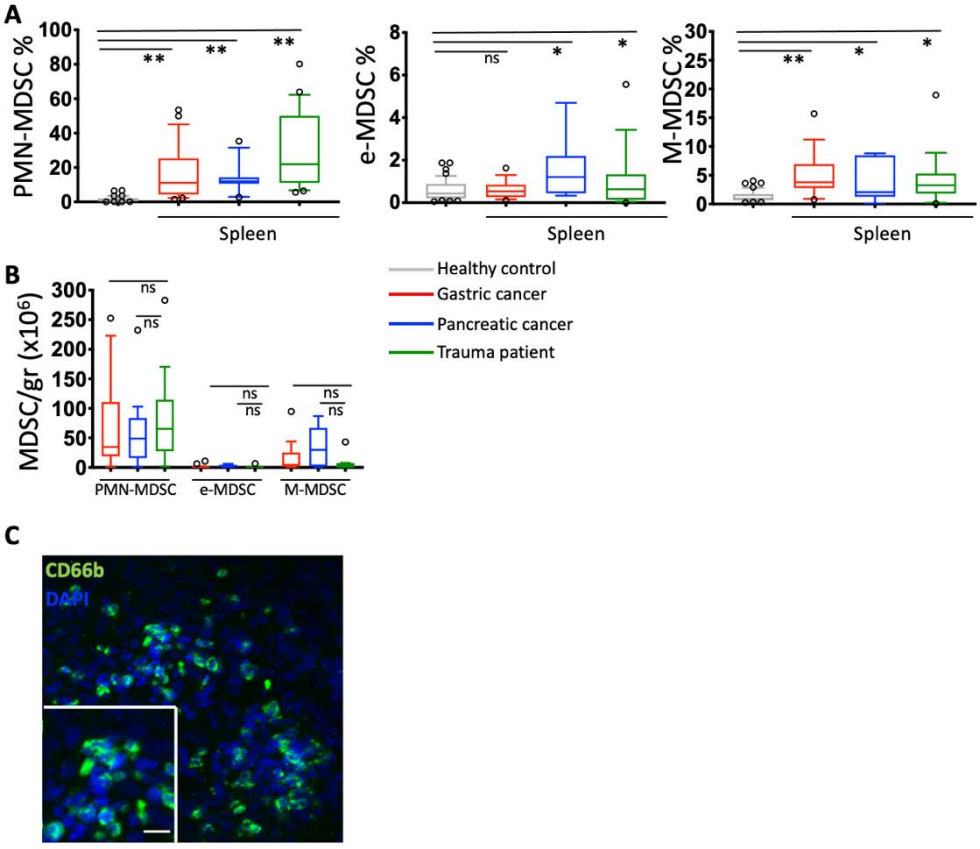

Figure 4.13. The subpopulations of MDSCs from the spleen of trauma patients and their comparison with gastric cancer and pancreatic cancer patients and the peripheral blood of healthy donors. A) The percentages of PMN-MDSCs, e-MDSCs and M-MDSCs-related phenotypes were determined by flow cytometry (peripheral blood, healthy donors n=41; spleen, gastric cancer patients n=23, pancreatic cancer patients n=9, trauma patients n=19). B) Absolute numbers of MDSCs per gram of the spleen were calculated (spleen, gastric cancer patients n=17, pancreatic cancer patients n=9, trauma patients n=19). C) CD66b and DAPI immunofluorescence staining was performed on frozen sections of the spleen samples (scale bar, 10 µm) (ns, not significant; *p<0.05, **p<0.01).

As another healthy donor group, the individuals who had a previous splenectomy history due to traumatic injury at least 1 year ago were also included. The percentages of the cells with PMN-MDSCs, e-MDSCs, and M-MDSCs phenotype were compared with those of healthy donors. Compared to the healthy individuals, the percentage and absolute number of the PMN-MDSCs were significantly increased in circulation of the blood donors without a spleen (Circulating PMN-MDSCs%, healthy donors 0.44 ± 0.13%; individuals with previous splenectomy history 2.7 ± 0.58%).

Additionally, the absence of spleen had no significant impact on neither the percentages nor absolute numbers of e-MDSCs and M-MDSCs in the peripheral blood (Figure 4.14).

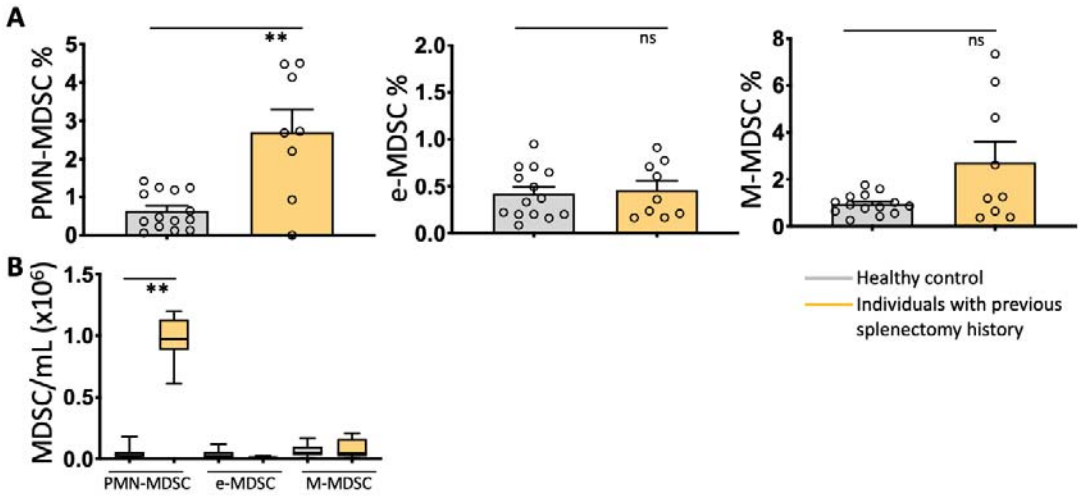

Figure 4.14. The subpopulations of MDSCs from the peripheral blood of the individuals (n=9) with previous splenectomy history due to traumatic injury at least 1 year ago and their comparison with healthy donors (n=14). A) The percentages of PMN-MDSCs, e-MDSCs and M-MDSCs-related phenotypes were determined by the flow cytometry. B) Absolute numbers of MDSCs per milliliter of the peripheral blood were calculated (ns, not significant; $**p<0.01$).

Next, the ratio of PMN cells collected from the normal-density and the low-density fractions of the cell suspension prepared from the traumatic spleen tissues was determined. Approximately, 33% and 30% of the PMN cells were at the low-density fraction in the trauma patients and the gastric cancer patients, respectively (Figure 4.15 A). PMN-MDSCs from traumatic spleen were examined cytologically by May-Grunwald Giemsa staining. Compared with the spleen of gastric cancer patients, metamyelocytes and promyelocytes were observed more frequently, whereas myelocytes were less in the spleen of trauma patients. (Figure 4.15 B). Representative images of May-Grünwald Giemsa staining of the splenic-PMN-MDSCs in the trauma patients were given in Figure 4.15 C. Please refer to Figure 4.5 C for representative

images of May-Grünwald Giemsa staining of the splenic-PMN-MDSCs in the gastric cancer patients.

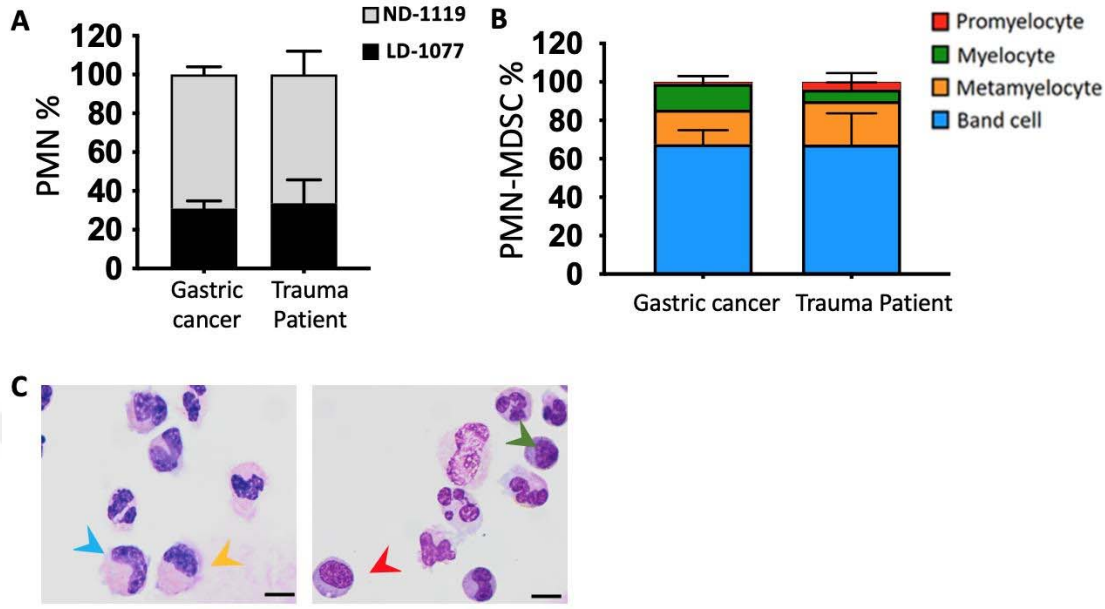

Figure 4.15. Characterization of the PMN cells in the spleen of the trauma patients (n=6) and their comparison with the gastric cancer patients (n=12). A) The proportion of normal-density PMN cells (ND-1119) and low-density PMN cells (LD-1077) were determined in total PMN cells by flow cytometry. B) The distribution of cytologically different stages among non-segmented cells was given. C) Representatives of PMN-MDSCs isolated from the spleen of the trauma patients stained with May-Grünwald Giemsa were shown (scale bar, 10 µm).

In the frozen sections of the injured spleen tissues, the expression of pSTAT3 and PD-L1 were evaluated on $CD66b^{+}$ splenocytes. As the indicators of immunosuppression, both pSTAT3 and PD-L1 were detected not only on $CD66b^{+}$ splenocytes but also other splenocytes in trauma patients. pSTAT3 was more frequent and localized in the nuclei (Figure 4.16 A and B).

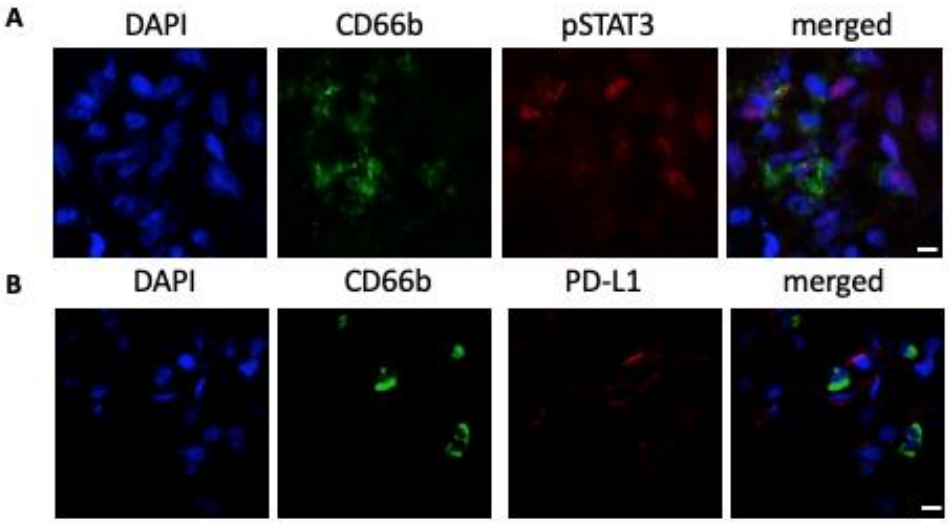

Figure 4.16. Representative images from immunofluorescence analysis for CD66b, pSTAT3 and PD-L1. A) CD66b, pSTAT3 and DAPI immunofluorescence staining was performed on frozen sections of gastric cancer and trauma patients. B) CD66b, PD-L1 immunofluorescence and DAPI staining was performed on the frozen spleen sections of the trauma patients (scale bar, 10 μm). The representatives of out of 3 patients were given.

Moreover, the functional properties of the low-density PMN-MDSCs isolated from the spleen of the gastric cancer patients and the trauma patients were compared. The production capacities of ROS, NO, and phagocytosis capacity of PMN-MDSCs were determined. Splenic PMN-MDSCs from trauma patients and gastric patients produced high amounts of ROS and NO. However, there was no statistical significance found for ROS, NO production and phagocytosis capacities (Figure 4.17 A, B, and C).

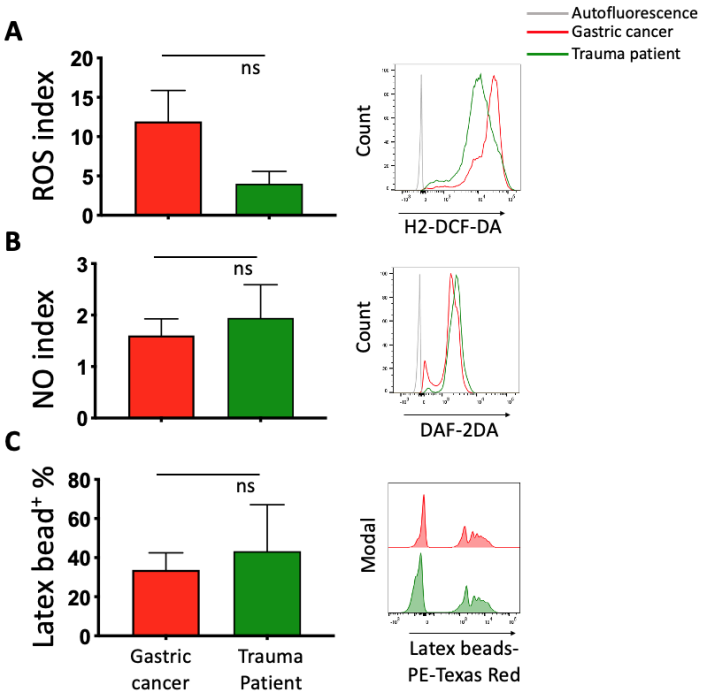

Figure 4.17. Functional characterization and comparison of the low-density PMN-MDSCs isolated from the spleen of the gastric cancer patients (n=9) and the trauma patients (n=3). A) and (B) ROS and NO production capacity and (C) Latex bead phagocytosis capacity of the cells compared. The representative flow cytometry histograms were given in the right side of the graphs. The data was presented as average ± SEM (ns, not significant).

In addition to PMN-MDSCs, the normal-density PMN cells isolated from the spleen of the gastric cancer patients and the trauma patients were analyzed and compared. Likewise, PMN-MDSCs, there was no statistically significant difference determined in terms of ROS, NO production and phagocytosis capacity of the normal-density PMN cells of these two different patient groups (Figure 4.18 A, B, and C).

In conclusion, the spleen of trauma patients was also populated with low-density PMN cells, which have almost similar morphological, phenotypical, and functional properties with low-density PMN cells in the spleen of cancer patients. Moreover, splenic PMN-MDSCs and the normal-density PMN cells had almost similar ROS and NO production capacities in the trauma patients, whereas PMN-MDSCs had higher phagocytosis capacity than the normal-density PMN cells.

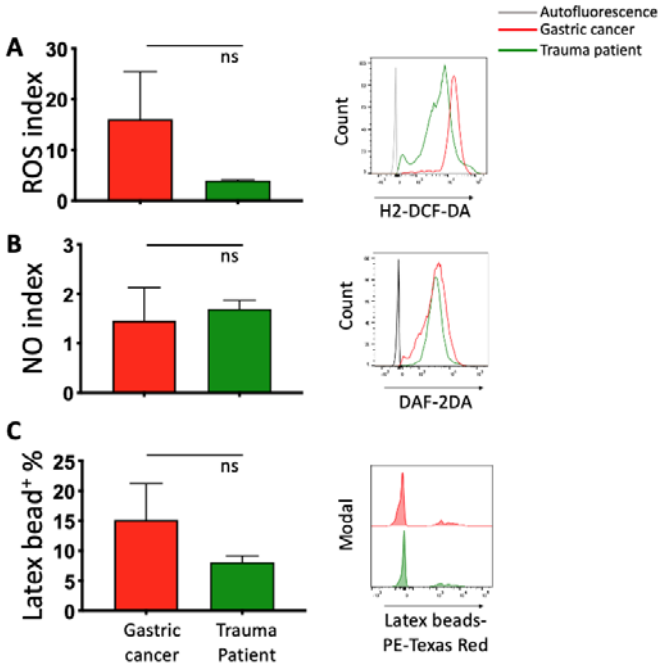

Figure 4.18. Functional characterization and the comparison of normal-density PMN (ND/PMN) cells isolated from the spleen of the gastric cancer patients (n=9) and the trauma patients (n=3). A) and (B) ROS and NO production capacity and (C) Latex bead phagocytosis capacity of the cells compared. The representative flow cytometry histograms were given in the right side of the graphs. The data was presented as average ± SEM (ns, not significant).

Next, distribution of the PMN cells was determined by CD15 immunohistochemistry on the paraffin-embedded spleen tissue sections. The spleen of the gastric cancer patients, the trauma patients, and the idiopathic thrombocytopenic purpura (ITP) patients were compared. The infiltration of $CD15^+$ cells were found significantly higher in the spleen of the gastric cancer patients compared with the trauma patients and the ITP patients (Figure 4.19 A and B). More specifically, to determine the co-localization and proliferation of $CD3^+$ T cells and $CD66b^+$ PMN cells, CD66b, CD3, Ki67, and DAPI were stained on the tissues. $CD66b^+$ PMN cells were placed in close proximity with $CD3^+$ T cells, which have low Ki-67 activity either in the spleen of the gastric cancer patients and trauma patients (Figure 4.20).

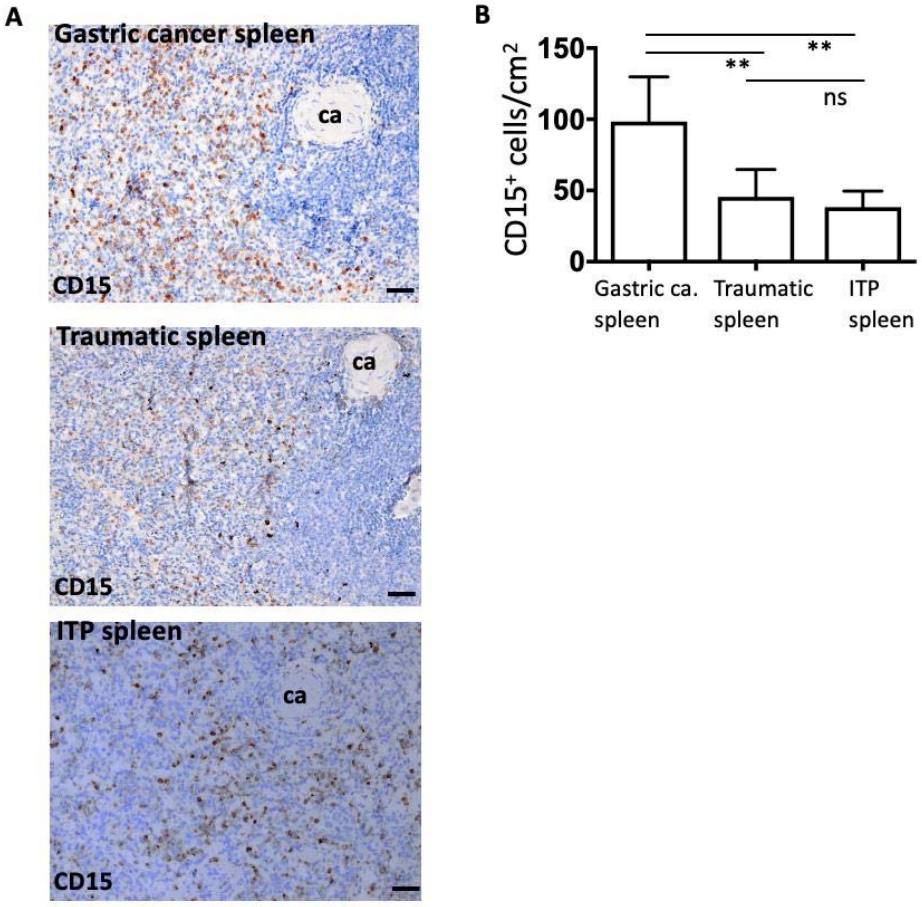

Figure 4.19. Distribution of PMN cells in the spleen and their interaction with T cells were analyzed. A) Distribution of PMN cells in the spleen of gastric cancer patients (n=17), trauma patients (n=9) and patients who had splenectomy due to idiopathic thrombocytopenic purpura (ITP) (n=9) were determined by CD15 immunohistochemistry (ca, central arteriole; scale bar, 100 μm). B) Quantification of $CD15^+$ cells were given.

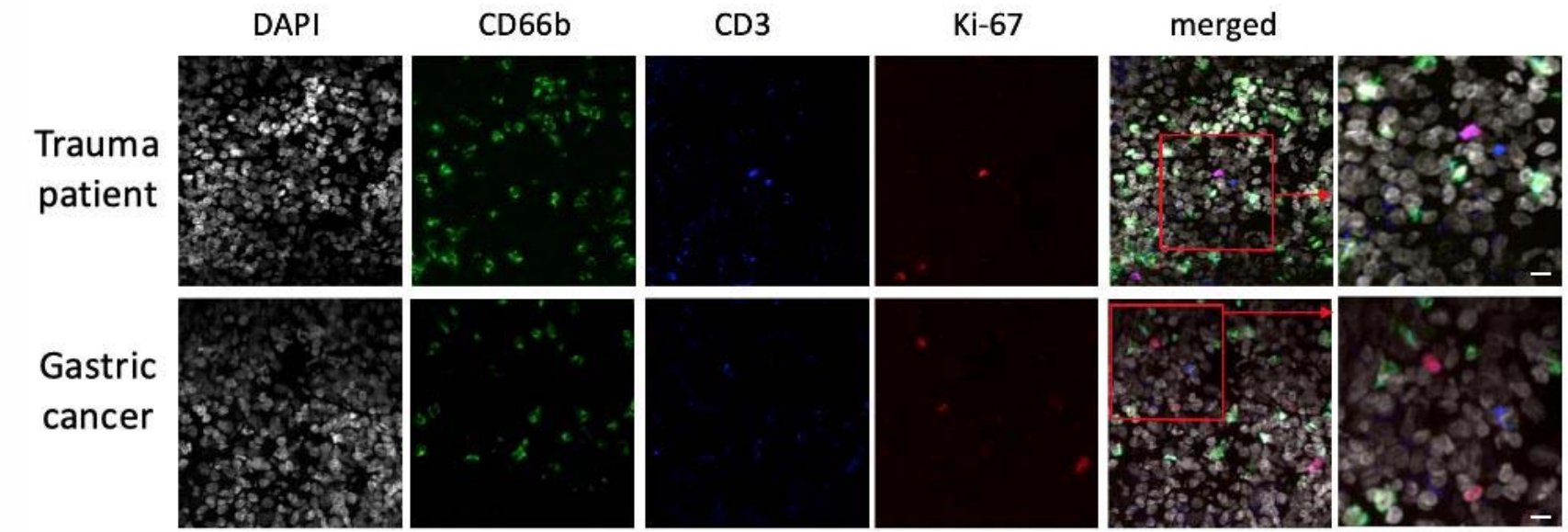

Figure 4.20. CD66b, CD3, Ki-67 and DAPI staining was performed on the frozen sections of the gastric cancer patients' and the trauma patients' spleen. Images were taken by confocal microscopy. The representatives of out of 3 patients were given (DAPI, white; CD66b, green; CD3, blue; Ki-67, red; scale bar, 10 μm).

The proximity of PMN cells with T cells in the spleen were validated. Moreover, the influence of PMN-MDSCs isolated from the traumatic spleen on T cell proliferation IFN-γ secretion was determined. For this purpose, the low-density PMN-MDSCs from the spleen were purified and co-cultured with eFluor670-labelled monocyte-depleted PBMCs at different ratios (PMN:monocyte-depleted PBMCs ratio; 0:1, 0.125:1, 0.25:1, 0.5:1 and 1:1) and a constant number of monocytes under 25 ng/mL anti-CD3 stimulation for 72 hours. At the end of the incubation period, the percentage of proliferated T cells and IFN-γ levels were determined. PMN-MDSCs isolated either from the spleen of the gastric cancer and the trauma patients significantly suppressed T cell proliferation at 1:1 ratio and IFN-γ production (Spleen, gastric cancer patients, PMN-MDSC:PBMC, 67.4±19.6%, trauma patients, PMN-MDSC:PBMC, 37.7±10.6%) (Figure 4.21 A and B). Furthermore, the impact of the normal-density PMN cells (ND/PMN) isolated from the spleen on T cell proliferation and IFN-γ secretion were evaluated. The spleen-derived ND/PMN cells from the gastric cancer patients were found more suppressive in terms of T cell proliferation and IFN-γ secretion than that of the trauma patients (Spleen, gastric cancer patients, ND/PMN:PBMC, 0.5:1, 71.8±13.9%; 1:1, 35.2±12.1%, trauma patients ND/PMN:PBMC, 0.5:1, 123±20.7%; 1:1, 76.8±17.2%) (Figure 4.21 C and D). However, spleen-derived PMN-MDSCs from the gastric cancer and the trauma patients had a similar magnitude of suppression.

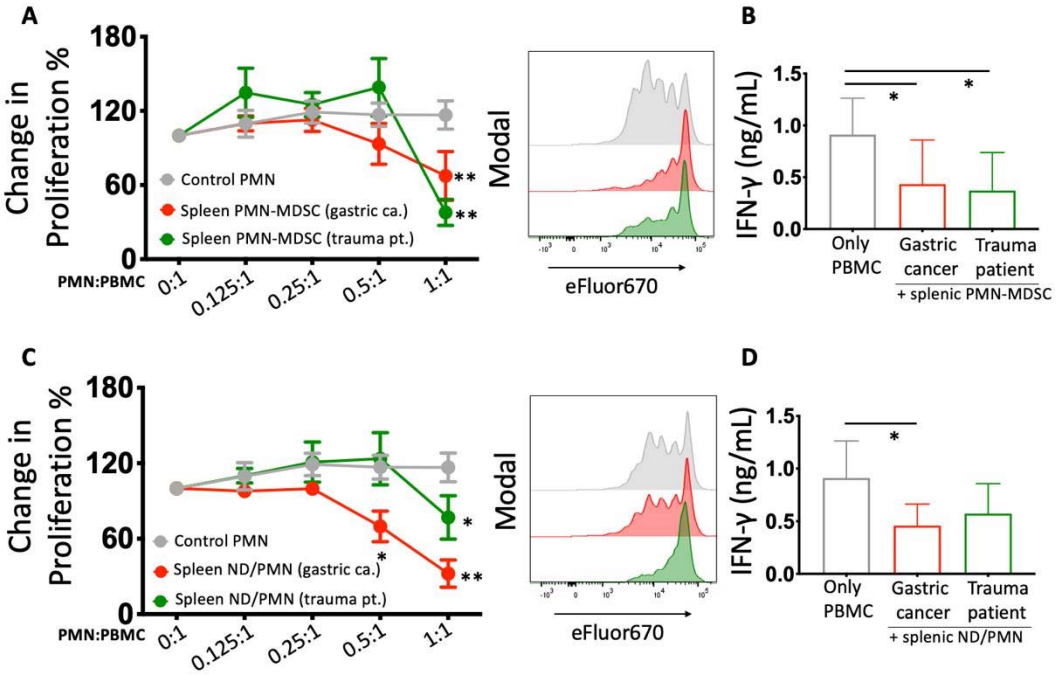

Figure 4.21. The functional effect of PMN-MDSCs from gastric cancer or trauma patients on T cell responses. A) and (C) Purified PMN-MDSCs and normal-density PMN cells from the spleen of the gastric cancer patients (n=6) and the trauma patients (n=6) and control normal-density PMN cells were co-cultured with eFluor670-labelled monocyte-depleted PBMCs from the healthy donors and constant numbers of monocytes isolated from healthy donors during 72 hours under anti-CD3 stimulation (25 ng/mL). B) and (D) At the end of the co-cultures, the amount of IFN-γ was measured by ELISA (at 0.5:1 PMN cell:PBMC ratio). The data was presented as average ± SEM (ns, not significant; *p<0.05, **p<0.01).

To evaluate the immune regulatory functions of the spleen upon trauma and compare with cancer, expression of immune regulatory genes mainly associated with MDSCs were examined on the spleen tissues of the gastric cancer patients and the pancreatic cancer patients as well as the trauma patients. The data obtained from all patient groups were normalized to pooled peripheral blood leukocytes obtained from the healthy donors. The expression of S100A9, ARG1, NOS2, TGF-β, IL-10, and VEGFR1 were increased in trauma patients compared to those obtained from the cancer patients, whereas the expression of S100A8, IDO1, COX2, GAL3, PD-L1, and CCL2 did not change among the groups (Figure 4.22 A). Other than the gene expression, expression of the immune regulatory proteins such as Nrf2 and STAT3

and their phosphorylated forms associated with the suppressive nature of MDSCs were analyzed. The expression of Nrf2 and STAT3 was found heterogenous among the patients (Figure 4.22 B and C). In trauma, pNrf2 and pSTAT3 was found upregulated only in 2 patients (Figure 4.22 D). Please refer to Figure 4.12 A for the representative Western Blot images of the gastric cancer patients' and the pancreatic cancer patients' spleen.

To sum up, immune regulatory proteins showed similar patterns both in trauma and cancer patients, and there was no statistical difference observed between them (Figure 4.22 B, C).

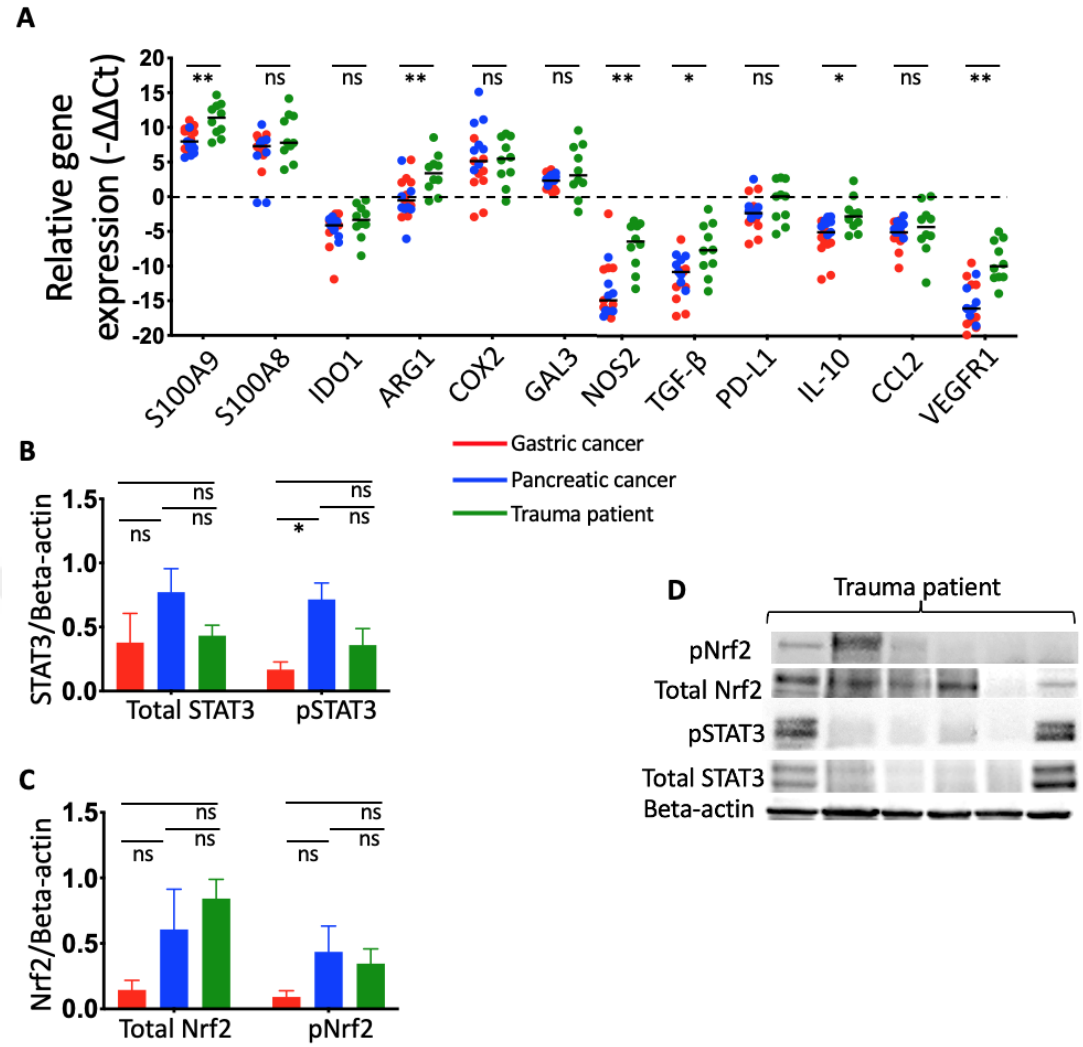

Figure 4.22. The expression of immunoregulatory genes and proteins. A) The mRNA levels of immunoregulatory genes such as S100A9, S100A8, IDO1, ARG1, COX2, GAL3, NOS2, TGF-β, PD-L1, IL-10, CCL2, and VEGFR1 were examined in the spleen tissues of the gastric cancer patients (n=9), the pancreatic cancer patients (n=8), and the trauma patients (n=10) by quantitative RT-PCR. The data obtained from all spleen samples were normalized to those from the pooled peripheral blood total leukocytes obtained from the healthy donors (n=5). Black line represents the median value. B) and (C) STAT3/Beta-actin and Nrf2/Beta-actin ratio was given. D) The Western Blot images showing the expressions of pNrf2, total Nrf2, pSTAT3, total STAT3, and beta-actin on the spleen tissues of the trauma patients (n=6) were given (ns, not significant; *p<0.05, **p<0.01).

4.3 Association of Clinical Data With PMN-MDSCs

The spleen of both the cancer patients and the trauma patients and the peripheral blood of the cancer patients harbored suppressive MDSCs, particularly PMN-MDSCs. In the last part of this thesis, clinical association with PMN-MDSC levels were investigated. The gastric cancer patients were categorized in two groups as stage I-II (n=10) and stage III-IV (n=11). In the peripheral blood and the spleen of the gastric cancer patients, the percentages of PMN-MDSCs were found to be independent of the clinical stage. However, in stage I-II PMN-MDSCs were mostly accumulated in the spleen (Figure 4.23 A). Next, to evaluate the overall survival of the gastric cancer patients, the patients with stage I-II and stage III-IV were divided into 2 groups depending on the percentages of PMN-MDSCs. In this manner, cut-offs were determined according to PMN-MDSC levels for the peripheral blood as >15% median of total $CD11b^+$ myeloid cells and for the spleen as >35% median of total $CD11b^+$ myeloid cells. Significantly, both stage I-II and stage III-IV the patients with high levels of PMN-MDSCs had shorter overall survival rates (Figure 4.23 B).

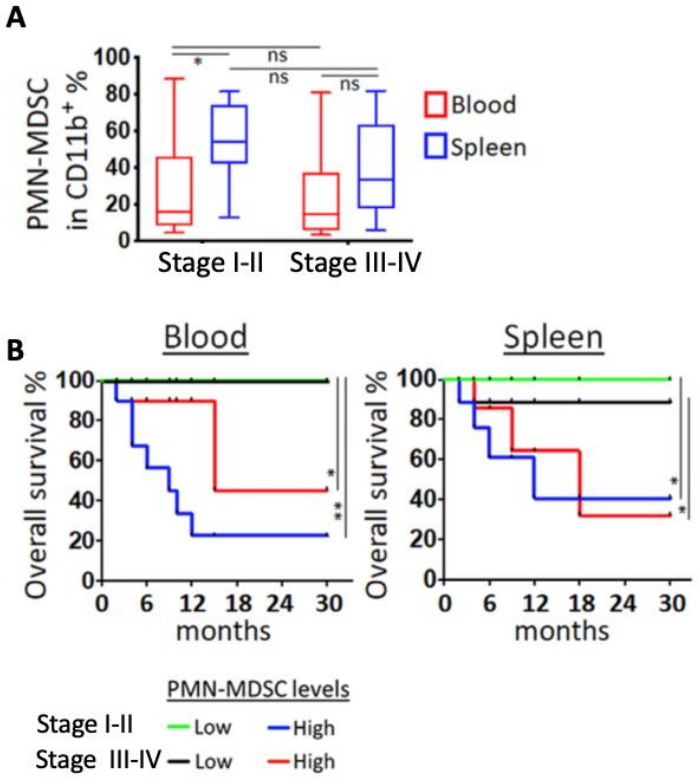

Figure 4.23. Clinical association of the levels of PMN-MDSCs in the peripheral blood and the spleen of gastric cancer patients. A) The percentages of PMN-MDSCs in $CD11b^+$ myeloid cells demonstrated according to clinical stages (Stage I-II n=10, stage III-IV n=11). The data was given as median and min-max values. B) Overall survival of the patients at thirty months were plotted. To determine low and high levels of PMN-MDSCs, cut-offs were established (for the blood >15% median of total $CD11b^+$ myeloid cells and for the spleen >35% median of total $CD11b^+$ myeloid cells), (ns, not significant; *$p<0.05$, **$p<0.01$).

Lastly, in the trauma patients, patients were categorized according to the spleen injury scores (SIS) and the injury severity scores (ISS). As the severity of the injury was increased, the percentages of PMN-MDSCs accumulated into the spleen was also found to be enhanced. Therefore, there was a positive correlation found between SIS or ISS and the percentages of PMN-MDSCs (correlation with SIS, p=0.0182, r=0.4776; for ISS, p=0.0226, r=0.4947) (Figure 4.24 A and B).

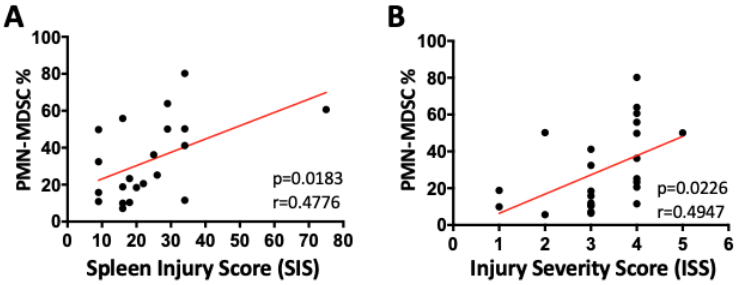

Figure 4.24. Clinical association injury scores with PMN-MDSC levels in the trauma patients. The trauma patients were distributed according to (A) spleen injury scores (SIS) and (B) injury severity scores (ISS) and correlated with the percentages of PMN-MDSC.

5. DISCUSSION

As a secondary lymphoid organ, the spleen has a unique microanatomy, which can filter whole blood and enable interactions for residing adaptive immune system components such as T and B cells and circulating leukocytes and blood-borne antigens (131). In this way, the spleen plays role in adaptive and humoral immune responses. Other than its central role in immune responses, iron recycling, and filtering blood, the spleen may also contribute to extramedullary hematopoiesis (EMH) (136). During fetal development, hematopoiesis takes places in the spleen and liver. Later in embryonic development, hematopoietic stem, and progenitor cells (HSPCs) migrate to the bone marrow where it becomes the major site for hematopoiesis. In mice, the spleen remains as a hematopoietic site throughout their lives, whereas in humans, HSPCs may migrate from the bone marrow and locate in the spleen for EMH in case of physiological stress or inflammation such as cancer (137, 138). In previous studies, progenitor cells were detected in the spleen of cancer patients to support bone marrow as a hematopoietic organ (144, 146). Since bone marrow becomes insufficient to meet the increased demand for myeloid cells, they egress from bone marrow without full maturation. The term “myeloid-derived suppressor cells (MDSCs)” was introduced to define these immature and suppressive myeloid cells. In mice, MDSCs accumulate in bone marrow, peripheral blood, liver, tumor microenvironment, and spleen.

In tumor-bearing mice, due to the accumulation of immature MDSCs, the spleen can become enlarged, and splenomegaly is observed (160). However, in cancer patients, the splenic volume may vary and there is no agreement about splenomegaly (161). Although the spleens of mice and humans may seem similar at first sight, the human spleen is much more complex, and many splenic cells are not completely characterized (133). This study has the feature of one of the exceptional studies conducted with freshly collected splenocytes from cancer patients and trauma patients to analyze PMN-MDSCs and PMN cells. In this study, it was demonstrated that the spleen is a reservoir for PMN cells in cancer patients and trauma patients. It allows PMN cells to communicate with T cells and eventually enables them to regulate T cell responses.

In physiological conditions, the spleen is recognized as a major pooling for circulating leukocytes, which are dynamically exchanged between circulation and the

spleen. Red blood cells and lymphocytes have the shortest intrasplenic transit times, whereas granulocytes have longer transit times (162). Splenomegaly causes abnormal pooling of leukocytes and more specifically, this abnormal pooling causes neutropenia in many patients suffering splenomegaly (163). It may be hypothesized that granulocytes retain longer in the spleen thus, they are more prone to be influenced by splenic microenvironment and inflammatory stimulus. In acute or chronic inflammation, production and egress of myeloid cells are increased due to emergency myelopoiesis (3). It increases circulating PMN-MDSCs and due to trafficking between circulation and spleen, it may serve as a supply for the reservoir of PMN-MDSCs in the spleen. Thus, in cancer patients, PMN-MDSCs mostly accumulated in the spleen compared to peripheral blood even in the patients with early stages.

To mediate immune suppression, MDSCs should be in close proximity with target immune cells, which are particularly T cells (25). Therefore, to regulate immune responses, MDSCs need to be present in the tumor microenvironment or at the site of inflammation. The microenvironment can shape the suppressive functions of MDSCs (164). In mice models, tumor infiltrating MDSCs were more suppressive than MDSCs in lymphoid tissues and circulation. However, there was no drastic difference reported in suppressive capacities of MDSCs from different tissues and circulation (84, 85). In humans, peripheral blood has been commonly used to evaluate MDSCs due to challenges in obtaining fresh tissue samples. In this study, both splenic and circulating PMN-MDSCs from gastric and pancreatic cancer patients suppressed T cells to a similar extent. The suppressive functions of circulating low-density PMN-MDSCs have been demonstrated in many of the studies, whereas circulating normal-density PMN cells are not suppressive. In contrast, splenic normal-density PMN cells were almost as suppressive as splenic low-density PMN-MDSCs in cancer patients and trauma patients. It may be interpreted that normal-density PMN cells adopt regulatory functions because of exposure to the inflammatory microenvironment in the spleen.

Even though the low-density PMN cells co-purified with mononuclear cells are increased in several pathological conditions, low-density fraction not only includes PMN-MDSCs but also activated normal-density PMN cells. In response to several inflammatory mediators and physical forces, normal-density PMN cells may become activated, and their density may be altered dynamically. Therefore, the low-density of

PMN cells is not always correlated with immaturity (165). To date, since there is no discrete phenotypical marker to distinguish normal-density PMN cells and low-density PMN-MDSCs, functional assays are mandatory to discern between them. Although T cell suppression assays are the most common way to analyze MDSCs, numerous approaches for T cell suppression assays have been introduced and different results have been reported in the literature (9). To overcome these variations, a European Cooperation in Science and Technology (COST-EU) Action BM1404 (Mye-EUNITER) was established (35). Different working groups attended this consortium to develop standardized functional protocols to identify MDSCs. Because PMN-MDSCs are very sensitive and susceptible to physical stress, these advanced protocols were carefully performed in this study.

PMN-MDSCs consist of heterogeneous groups of PMN cells, which have different phenotypes, morphology, maturation stages, and activation status (8). CD10, CD16, and CD11b are well-known markers to determine the differentiation status of MDSCs and these molecules upregulate during granulocytic differentiation. Based on previously published data, differential expressions of CD10, CD16, and CD11b were used to propose different subtypes of PMN-MDSCs. The high expressions of CD10, CD16, and CD11b indicated the most suppressive phenotype of PMN-MDSCs (165, 166). Accordingly, in our study, splenic and circulating PMN-MDSCs were highly expressing these markers in cancer patients.

Compared to the peripheral blood samples of healthy donors, high levels of S100A8 and S100A9 as a chemoattractant for PMN-MDSCs were observed in the spleen of cancer patients and trauma patients. Furthermore, the expressions of anti-inflammatory genes ARG1 and COX2 were also upregulated in cancer patients' and trauma patients' spleen. Therefore, the spleen may adopt an anti-inflammatory character in cancer and trauma. As PMN cells are exposed to this regulatory microenvironment, they adopt immune suppressive and regulatory phenotypes. As previously mentioned, functional assays were performed to analyze PMN-MDSCs in detail. Splenic and circulating PMN-MDSCs were purified and co-cultured with PBMCs isolated from healthy donors under anti-CD3 stimulation for 72 hours. Splenic and circulating PMN-MDSCs suppressed T cell proliferation IFN-γ secretion. Because peripheral blood samples could not be collected from trauma patients, only splenic

PMN-MDSCs were evaluated, and they were also suppressive. As additional functional analyses, the production of ROS, NO, and the capacity of phagocytosis were analyzed. In cancer patients, splenic PMN-MDSCs had a higher capacity for ROS production than circulating PMN-MDSCs and it may be hypothesized that they may be more influential on T cell suppression. Although splenic PMN-MDSCs from trauma patients tended to produce less ROS than splenic PMN-MDSCs from cancer patients, there was no statistical difference observed.

As a weakness of this study, immune suppressive mechanisms of normal-density PMN cells were not specifically analyzed. Furthermore, the functions and recruitment of other immune cells such as dendritic cells, NK cells, B cells, macrophages, and Tregs were not investigated. The interactions of these immune cells with splenic PMN-MDSCs may have been analyzed.

In the literature, there is only one paper published about the presence of PMN-MDSCs and M-MDSCs in the spleen of patients with pancreatic tumors and benign cysts (105). However, due to difficulties having spleen tissue samples, the main problem of these studies is the modest sample size. In the context of trauma, although MDSCs have been mostly associated with chronic inflammation due to prolonged and low-strength inflammatory stimulus, under acute inflammatory conditions such as traumatic injury MDSCs are expanded in mice studies (167). However, there is still lacking knowledge about the functionality and clinical significance of MDSCs in traumatic injury (168). Recently, a study reported the presence of suppressive PMN-MDSCs in the peripheral blood of trauma patients and, the percentages of PMN-MDSCs were positively correlated with injury severity scores. Additionally, high levels of PMN-MDSCs were associated with low levels of IFN-γ and TGF-β in the serum of these patients (169). In our study, spleen samples of trauma patients were analyzed for the first time in terms of the presence and functionality of MDSCs. Immune suppressive PMN-MDSCs accumulated in the traumatic spleen and their frequencies were positively correlated with injury severity and spleen severity scores. In contrast to cancer patients, the presence of PMN-MDSCs in traumatic injury is beneficial in terms of tissue repair and wound healing.

All in all, in this study, which mainly focused on gastric cancer, pancreatic cancer, and trauma patients, comprehensive phenotypical and functional analyses of

PMN-MDSCs were performed. The human spleen becomes a reservoir for suppressive PMN cells, which interact with T cells and immune regulatory organ in cancer and trauma.

6. RESULTS AND RECOMMENDATION

- After the peripheral blood and the spleen samples of the treatment-naïve the gastric cancer patients and the pancreatic cancer patients were layered over 1.077 g/mL gradient separation solution, PMN-MDSC ($CD11b^{+}CD14^{-}CD33^{dim}CD15^{+}CD66b^{+}HLA\text{-}DR^{-/dim}$), M-MDSC ($CD11b^{+}CD14^{+}CD33^{+}CD15^{-}CD66b^{-}HLA\text{-}DR^{-/dim}$), and e-MDSC ($CD11b^{+}CD14^{-}CD33^{+}CD15^{-}CD66b^{-}HLA\text{-}DR^{-/dim}$) phenotypes were determined as “low-density”.
- PMN-MDSCs had the highest percentages and the absolute numbers in the peripheral blood and the spleen of cancer patients compared to those from the peripheral blood samples of the healthy donors.
- $CD66b^{+}$ PMN cells were widely distributed in the spleen, and they were in a close contact with $CD3^{+}$ T cells.
- Peripheral blood mononuclear cells (PBMCs) from healthy donors were isolated and co-cultured with PMN-MDSCs at different ratios in the presence of anti-CD3 stimulation. Both splenic and circulating PMN-MDSCs suppressed T cell proliferation and IFN-γ secretion.
- Expression of several immune regulatory genes and proteins related to MDSCs were upregulated in the spleen of the cancer patients.
- As non-malignant controls, the spleen specimens from the patients who underwent splenectomy due to severe abdominal trauma were included and PMN-MDSCs populated the spleen in traumatic patients similar to cancer patients.
- The capacity of T cell suppression, the production of ROS, NO, the phagocytic activity, and the patterns in the expression of immune regulatory genes and proteins were comparable between the splenic PMN-MDSCs obtained from the cancer patients and the trauma patients.
- Increased percentages of PMN-MDSCs in the peripheral blood and the spleen of cancer patients were associated with poor prognosis regardless of the clinical stage.
- In the trauma patients, the percentages of PMN-MDSCs were positively correlated with the injury severity scores.

- In conclusion, our results demonstrated the immune modulatory function of the human spleen through MDSCs in inflammatory disorders such as cancer and trauma.
- In this study, the specific immune suppression mechanisms of PMN-MDSCs were not covered. In the co-cultures, by using specific inhibitors such as for ROS, NO, and ARG1, specific T cell suppression mechanisms of PMN-MDSCs may be investigated.
- In case of trauma, the role of spleen through MDSCs needs to be better elucidated. In this manner, mice models of trauma may be used to mimic human trauma. This experiment may enable to compare the healthy spleen and the traumatic spleen.
- Lastly, after this thesis, the cancer patients will be followed to determine 5-year overall survival.

7. REFERENCES

1. Iwasaki H, Akashi K. Myeloid lineage commitment from the hematopoietic stem cell. Immunity. 2007;26(6):726-40.
2. Sica A, Guarneri V, Gennari A. Myelopoiesis, metabolism and therapy: a crucial crossroads in cancer progression. Cell Stress. 2019;3(9):284-94.
3. Millrud CR, Bergenfelz C, Leandersson K. On the origin of myeloid-derived suppressor cells. Oncotarget. 2017;8(2):3649-65.
4. Kumar V, Patel S, Tcyganov E, Gabrilovich DI. The Nature of Myeloid-Derived Suppressor Cells in the Tumor Microenvironment. Trends Immunol. 2016;37(3):208-20.
5. Gabrilovich DI, Bronte V, Chen SH, Colombo MP, Ochoa A, Ostrand-Rosenberg S, et al. The terminology issue for myeloid-derived suppressor cells. Cancer Res. 2007;67(1):425; author reply 6.
6. Parker KH, Beury DW, Ostrand-Rosenberg S. Myeloid-Derived Suppressor Cells: Critical Cells Driving Immune Suppression in the Tumor Microenvironment. Adv Cancer Res. 2015;128:95-139.
7. Bergenfelz C, Leandersson K. The Generation and Identity of Human Myeloid-Derived Suppressor Cells. Front Oncol. 2020;10:109.
8. Bronte V, Brandau S, Chen SH, Colombo MP, Frey AB, Greten TF, et al. Recommendations for myeloid-derived suppressor cell nomenclature and characterization standards. Nat Commun. 2016;7:12150.
9. Bruger AM, Dorhoi A, Esendagli G, Barczyk-Kahlert K, van der Bruggen P, Lipoldova M, et al. How to measure the immunosuppressive activity of MDSC: assays, problems and potential solutions. Cancer Immunol Immunother. 2019;68(4):631-44.
10. Youn JI, Nagaraj S, Collazo M, Gabrilovich DI. Subsets of myeloid-derived suppressor cells in tumor-bearing mice. J Immunol. 2008;181(8):5791-802.
11. Vanhaver C, van der Bruggen P, Bruger AM. MDSC in Mice and Men: Mechanisms of Immunosuppression in Cancer. J Clin Med. 2021;10(13).
12. Ge Y, Cheng D, Jia Q, Xiong H, Zhang J. Mechanisms Underlying the Role of Myeloid-Derived Suppressor Cells in Clinical Diseases: Good or Bad. Immune Netw. 2021;21(3):e21.
13. Schultze JL, Mass E, Schlitzer A. Emerging Principles in Myelopoiesis at Homeostasis and during Infection and Inflammation. Immunity. 2019;50(2):288-301.
14. Dai J, El Gazzar M, Li GY, Moorman JP, Yao ZQ. Myeloid-derived suppressor cells: paradoxical roles in infection and immunity. J Innate Immun. 2015;7(2):116-26.
15. Veglia F, Sanseviero E, Gabrilovich DI. Myeloid-derived suppressor cells in the era of increasing myeloid cell diversity. Nat Rev Immunol. 2021;21(8):485-98.

16. Karin N. The Development and Homing of Myeloid-Derived Suppressor Cells: From a Two-Stage Model to a Multistep Narrative. Front Immunol. 2020;11:557586.

17. Johnson DE, O'Keefe RA, Grandis JR. Targeting the IL-6/JAK/STAT3 signalling axis in cancer. Nat Rev Clin Oncol. 2018;15(4):234-48.

18. Fultang N, Li X, Li T, Chen YH. Myeloid-Derived Suppressor Cell Differentiation in Cancer: Transcriptional Regulators and Enhanceosome-Mediated Mechanisms. Front Immunol. 2020;11:619253.

19. Ara T, Tokoyoda K, Sugiyama T, Egawa T, Kawabata K, Nagasawa T. Long-term hematopoietic stem cells require stromal cell-derived factor-1 for colonizing bone marrow during ontogeny. Immunity. 2003;19(2):257-67.

20. Wang W, Xia X, Mao L, Wang S. The CCAAT/Enhancer-Binding Protein Family: Its Roles in MDSC Expansion and Function. Front Immunol. 2019;10:1804.

21. Marigo I, Bosio E, Solito S, Mesa C, Fernandez A, Dolcetti L, et al. Tumor-induced tolerance and immune suppression depend on the C/EBPbeta transcription factor. Immunity. 2010;32(6):790-802.

22. Valanparambil RM, Tam M, Gros PP, Auger JP, Segura M, Gros P, et al. IRF-8 regulates expansion of myeloid-derived suppressor cells and Foxp3+ regulatory T cells and modulates Th2 immune responses to gastrointestinal nematode infection. PLoS Pathog. 2017;13(10):e1006647.

23. Waight JD, Netherby C, Hensen ML, Miller A, Hu Q, Liu S, et al. Myeloid-derived suppressor cell development is regulated by a STAT/IRF-8 axis. J Clin Invest. 2013;123(10):4464-78.

24. Netherby CS, Messmer MN, Burkard-Mandel L, Colligan S, Miller A, Cortes Gomez E, et al. The Granulocyte Progenitor Stage Is a Key Target of IRF8-Mediated Regulation of Myeloid-Derived Suppressor Cell Production. J Immunol. 2017;198(10):4129-39.

25. Gabrilovich DI. Myeloid-Derived Suppressor Cells. Cancer Immunol Res. 2017;5(1):3-8.

26. Hegde S, Leader AM, Merad M. MDSC: Markers, development, states, and unaddressed complexity. Immunity. 2021;54(5):875-84.

27. Zhou J, Nefedova Y, Lei A, Gabrilovich D. Neutrophils and PMN-MDSC: Their biological role and interaction with stromal cells. Semin Immunol. 2018;35:19-28.

28. Condamine T, Mastio J, Gabrilovich DI. Transcriptional regulation of myeloid-derived suppressor cells. J Leukoc Biol. 2015;98(6):913-22.

29. Kramer ED, Abrams SI. Granulocytic Myeloid-Derived Suppressor Cells as Negative Regulators of Anticancer Immunity. Front Immunol. 2020;11:1963.

30. Condamine T, Dominguez GA, Youn JI, Kossenkov AV, Mony S, Alicea-Torres K, et al. Lectin-type oxidized LDL receptor-1 distinguishes population of human

polymorphonuclear myeloid-derived suppressor cells in cancer patients. Sci Immunol. 2016;1(2).

31. Haile LA, Greten TF, Korangy F. Immune suppression: the hallmark of myeloid derived suppressor cells. Immunol Invest. 2012;41(6-7):581-94.
32. Damuzzo V, Pinton L, Desantis G, Solito S, Marigo I, Bronte V, et al. Complexity and challenges in defining myeloid-derived suppressor cells. Cytometry B Clin Cytom. 2015;88(2):77-91.
33. Marvel D, Gabrilovich DI. Myeloid-derived suppressor cells in the tumor microenvironment: expect the unexpected. J Clin Invest. 2015;125(9):3356-64.
34. De Veirman K, Van Valckenborgh E, Lahmar Q, Geeraerts X, De Bruyne E, Menu E, et al. Myeloid-derived suppressor cells as therapeutic target in hematological malignancies. Front Oncol. 2014;4:349.
35. Bruger AM, Vanhaver C, Bruderek K, Amodio G, Tavukcuoglu E, Esendagli G, et al. Protocol to assess the suppression of T-cell proliferation by human MDSC. Methods Enzymol. 2020;632:155-92.
36. Gabrilovich DI, Nagaraj S. Myeloid-derived suppressor cells as regulators of the immune system. Nat Rev Immunol. 2009;9(3):162-74.
37. Panieri E, Santoro MM. ROS homeostasis and metabolism: a dangerous liason in cancer cells. Cell Death Dis. 2016;7(6):e2253.
38. Ray PD, Huang BW, Tsuji Y. Reactive oxygen species (ROS) homeostasis and redox regulation in cellular signaling. Cell Signal. 2012;24(5):981-90.
39. Forrester SJ, Kikuchi DS, Hernandes MS, Xu Q, Griendling KK. Reactive Oxygen Species in Metabolic and Inflammatory Signaling. Circ Res. 2018;122(6):877-902.
40. Kovac S, Angelova PR, Holmstrom KM, Zhang Y, Dinkova-Kostova AT, Abramov AY. Nrf2 regulates ROS production by mitochondria and NADPH oxidase. Biochim Biophys Acta. 2015;1850(4):794-801.
41. Ohl K, Tenbrock K. Reactive Oxygen Species as Regulators of MDSC-Mediated Immune Suppression. Front Immunol. 2018;9:2499.
42. Nagaraj S, Gupta K, Pisarev V, Kinarsky L, Sherman S, Kang L, et al. Altered recognition of antigen is a mechanism of CD8+ T cell tolerance in cancer. Nat Med. 2007;13(7):828-35.
43. Kusmartsev S, Eruslanov E, Kubler H, Tseng T, Sakai Y, Su Z, et al. Oxidative stress regulates expression of VEGFR1 in myeloid cells: link to tumor-induced immune suppression in renal cell carcinoma. J Immunol. 2008;181(1):346-53.
44. Corzo CA, Cotter MJ, Cheng P, Cheng F, Kusmartsev S, Sotomayor E, et al. Mechanism regulating reactive oxygen species in tumor-induced myeloid-derived suppressor cells. J Immunol. 2009;182(9):5693-701.
45. Liu Y, Wei J, Guo G, Zhou J. Norepinephrine-induced myeloid-derived suppressor cells block T-cell responses via generation of reactive oxygen species. Immunopharmacol Immunotoxicol. 2015;37(4):359-65.

46. Ostrand-Rosenberg S, Fenselau C. Myeloid-Derived Suppressor Cells: Immune-Suppressive Cells That Impair Antitumor Immunity and Are Sculpted by Their Environment. J Immunol. 2018;200(2):422-31.

47. Beury DW, Carter KA, Nelson C, Sinha P, Hanson E, Nyandjo M, et al. Myeloid-Derived Suppressor Cell Survival and Function Are Regulated by the Transcription Factor Nrf2. J Immunol. 2016;196(8):3470-8.

48. Gabrilovich DI. The Dawn of Myeloid-Derived Suppressor Cells: Identification of Arginase I as the Mechanism of Immune Suppression. Cancer Res. 2021;81(15):3953-5.

49. Ochoa AC, Zea AH, Hernandez C, Rodriguez PC. Arginase, prostaglandins, and myeloid-derived suppressor cells in renal cell carcinoma. Clin Cancer Res. 2007;13(2 Pt 2):721s-6s.

50. Harari O, Liao JK. Inhibition of MHC II gene transcription by nitric oxide and antioxidants. Curr Pharm Des. 2004;10(8):893-8.

51. Bronte V, Zanovello P. Regulation of immune responses by L-arginine metabolism. Nat Rev Immunol. 2005;5(8):641-54.

52. Zea AH, Rodriguez PC, Culotta KS, Hernandez CP, DeSalvo J, Ochoa JB, et al. L-Arginine modulates CD3zeta expression and T cell function in activated human T lymphocytes. Cell Immunol. 2004;232(1-2):21-31.

53. Lemberg KM, Gori SS, Tsukamoto T, Rais R, Slusher BS. Clinical development of metabolic inhibitors for oncology. J Clin Invest. 2022;132(1).

54. Verdeil G, Lawrence T, Schmitt-Verhulst AM, Auphan-Anezin N. Targeting STAT3 and STAT5 in Tumor-Associated Immune Cells to Improve Immunotherapy. Cancers (Basel). 2019;11(12).

55. Bingisser RM, Tilbrook PA, Holt PG, Kees UR. Macrophage-derived nitric oxide regulates T cell activation via reversible disruption of the Jak3/STAT5 signaling pathway. J Immunol. 1998;160(12):5729-34.

56. Feng S, Cheng X, Zhang L, Lu X, Chaudhary S, Teng R, et al. Myeloid-derived suppressor cells inhibit T cell activation through nitrating LCK in mouse cancers. Proc Natl Acad Sci U S A. 2018;115(40):10094-9.

57. Monu NR, Frey AB. Myeloid-derived suppressor cells and anti-tumor T cells: a complex relationship. Immunol Invest. 2012;41(6-7):595-613.

58. Brito C, Naviliat M, Tiscornia AC, Vuillier F, Gualco G, Dighiero G, et al. Peroxynitrite inhibits T lymphocyte activation and proliferation by promoting impairment of tyrosine phosphorylation and peroxynitrite-driven apoptotic death. J Immunol. 1999;162(6):3356-66.

59. Yu W, Choi GS, Chung HY. Randomized clinical trial of splenectomy versus splenic preservation in patients with proximal gastric cancer. Br J Surg. 2006;93(5):559-63.

60. Kujawski M, Kortylewski M, Lee H, Herrmann A, Kay H, Yu H. Stat3 mediates myeloid cell-dependent tumor angiogenesis in mice. J Clin Invest. 2008;118(10):3367-77.

61. Wang S, Song R, Wang Z, Jing Z, Wang S, Ma J. S100A8/A9 in Inflammation. Front Immunol. 2018;9:1298.

62. Sinha P, Okoro C, Foell D, Freeze HH, Ostrand-Rosenberg S, Srikrishna G. Proinflammatory S100 proteins regulate the accumulation of myeloid-derived suppressor cells. J Immunol. 2008;181(7):4666-75.

63. Huang M, Wu R, Chen L, Peng Q, Li S, Zhang Y, et al. S100A9 Regulates MDSCs-Mediated Immune Suppression via the RAGE and TLR4 Signaling Pathways in Colorectal Carcinoma. Front Immunol. 2019;10:2243.

64. Gabrilovich DI, Ostrand-Rosenberg S, Bronte V. Coordinated regulation of myeloid cells by tumours. Nat Rev Immunol. 2012;12(4):253-68.

65. Shimozaki K, Nakajima K, Hirano T, Nagata S. Involvement of STAT3 in the granulocyte colony-stimulating factor-induced differentiation of myeloid cells. J Biol Chem. 1997;272(40):25184-9.

66. Huber R, Pietsch D, Panterodt T, Brand K. Regulation of C/EBPbeta and resulting functions in cells of the monocytic lineage. Cell Signal. 2012;24(6):1287-96.

67. Zhang H, Nguyen-Jackson H, Panopoulos AD, Li HS, Murray PJ, Watowich SS. STAT3 controls myeloid progenitor growth during emergency granulopoiesis. Blood. 2010;116(14):2462-71.

68. Davidov V, Jensen G, Mai S, Chen SH, Pan PY. Analyzing One Cell at a TIME: Analysis of Myeloid Cell Contributions in the Tumor Immune Microenvironment. Front Immunol. 2020;11:1842.

69. Mandruzzato S, Solito S, Falisi E, Francescato S, Chiarion-Sileni V, Mocellin S, et al. IL4Ralpha+ myeloid-derived suppressor cell expansion in cancer patients. J Immunol. 2009;182(10):6562-8.

70. Pinton L, Solito S, Damuzzo V, Francescato S, Pozzuoli A, Berizzi A, et al. Activated T cells sustain myeloid-derived suppressor cell-mediated immune suppression. Oncotarget. 2016;7(2):1168-84.

71. Sinha P, Chornoguz O, Clements VK, Artemenko KA, Zubarev RA, Ostrand-Rosenberg S. Myeloid-derived suppressor cells express the death receptor Fas and apoptose in response to T cell-expressed FasL. Blood. 2011;117(20):5381-90.

72. Rowlands M, Segal F, Hartl D. Myeloid-Derived Suppressor Cells as a Potential Biomarker and Therapeutic Target in COVID-19. Front Immunol. 2021;12:697405.

73. Bitsch R, Kurzay A, Ozbay Kurt F, De La Torre C, Lasser S, Lepper A, et al. STAT3 inhibitor Napabucasin abrogates MDSC immunosuppressive capacity and prolongs survival of melanoma-bearing mice. J Immunother Cancer. 2022;10(3).

74. Hellsten R, Lilljebjorn L, Johansson M, Leandersson K, Bjartell A. The STAT3 inhibitor galiellalactone inhibits the generation of MDSC-like monocytes by prostate cancer cells and decreases immunosuppressive and tumorigenic factors. Prostate. 2019;79(14):1611-21.

75. Peyraud F, Guegan JP, Bodet D, Cousin S, Bessede A, Italiano A. Targeting Tryptophan Catabolism in Cancer Immunotherapy Era: Challenges and Perspectives. Front Immunol. 2022;13:807271.

76. Lee GK, Park HJ, Macleod M, Chandler P, Munn DH, Mellor AL. Tryptophan deprivation sensitizes activated T cells to apoptosis prior to cell division. Immunology. 2002;107(4):452-60.

77. Hezaveh K, Shinde RS, Klotgen A, Halaby MJ, Lamorte S, Ciudad MT, et al. Tryptophan-derived microbial metabolites activate the aryl hydrocarbon receptor in tumor-associated macrophages to suppress anti-tumor immunity. Immunity. 2022;55(2):324-40 e8.

78. Krishnamoorthy M, Gerhardt L, Maleki Vareki S. Immunosuppressive Effects of Myeloid-Derived Suppressor Cells in Cancer and Immunotherapy. Cells. 2021;10(5).

79. Li J, Wang L, Chen X, Li L, Li Y, Ping Y, et al. CD39/CD73 upregulation on myeloid-derived suppressor cells via TGF-beta-mTOR-HIF-1 signaling in patients with non-small cell lung cancer. Oncoimmunology. 2017;6(6):e1320011.

80. Yaseen MM, Abuharfeil NM, Darmani H, Daoud A. Mechanisms of immune suppression by myeloid-derived suppressor cells: the role of interleukin-10 as a key immunoregulatory cytokine. Open Biol. 2020;10(9):200111.

81. Obermajer N, Muthuswamy R, Lesnock J, Edwards RP, Kalinski P. Positive feedback between PGE2 and COX2 redirects the differentiation of human dendritic cells toward stable myeloid-derived suppressor cells. Blood. 2011;118(20):5498-505.

82. Rodriguez PC, Hernandez CP, Quiceno D, Dubinett SM, Zabaleta J, Ochoa JB, et al. Arginase I in myeloid suppressor cells is induced by COX-2 in lung carcinoma. J Exp Med. 2005;202(7):931-9.

83. Tcyganov E, Mastio J, Chen E, Gabrilovich DI. Plasticity of myeloid-derived suppressor cells in cancer. Curr Opin Immunol. 2018;51:76-82.

84. Hossain F, Al-Khami AA, Wyczechowska D, Hernandez C, Zheng L, Reiss K, et al. Inhibition of Fatty Acid Oxidation Modulates Immunosuppressive Functions of Myeloid-Derived Suppressor Cells and Enhances Cancer Therapies. Cancer Immunol Res. 2015;3(11):1236-47.

85. Haverkamp JM, Crist SA, Elzey BD, Cimen C, Ratliff TL. In vivo suppressive function of myeloid-derived suppressor cells is limited to the inflammatory site. Eur J Immunol. 2011;41(3):749-59.

86. Corzo CA, Condamine T, Lu L, Cotter MJ, Youn JI, Cheng P, et al. HIF-1alpha regulates function and differentiation of myeloid-derived suppressor cells in the tumor microenvironment. J Exp Med. 2010;207(11):2439-53.

87. Zhang J, Patel L, Pienta KJ. CC chemokine ligand 2 (CCL2) promotes prostate cancer tumorigenesis and metastasis. Cytokine Growth Factor Rev. 2010;21(1):41-8.

88. Chun E, Lavoie S, Michaud M, Gallini CA, Kim J, Soucy G, et al. CCL2 Promotes Colorectal Carcinogenesis by Enhancing Polymorphonuclear Myeloid-Derived Suppressor Cell Population and Function. Cell Rep. 2015;12(2):244-57.

89. Schlecker E, Stojanovic A, Eisen C, Quack C, Falk CS, Umansky V, et al. Tumor-infiltrating monocytic myeloid-derived suppressor cells mediate CCR5-dependent recruitment of regulatory T cells favoring tumor growth. J Immunol. 2012;189(12):5602-11.

90. Srivastava MK, Sinha P, Clements VK, Rodriguez P, Ostrand-Rosenberg S. Myeloid-derived suppressor cells inhibit T-cell activation by depleting cystine and cysteine. Cancer Res. 2010;70(1):68-77.

91. Wang T, Chu Z, Lin H, Jiang J, Zhou X, Liang X. Galectin-3 contributes to cisplatin-induced myeloid derived suppressor cells (MDSCs) recruitment in Lewis lung cancer-bearing mice. Mol Biol Rep. 2014;41(6):4069-76.

92. Cheng D, Liang B, Li Y. Serum galectin-3 as a potential marker for gastric cancer. Med Sci Monit. 2015;21:755-60.

93. Cassetta L, Bruderek K, Skrzeczynska-Moncznik J, Osiecka O, Hu X, Rundgren IM, et al. Differential expansion of circulating human MDSC subsets in patients with cancer, infection and inflammation. J Immunother Cancer. 2020;8(2).

94. Liang Y, Lu B, Zhao P, Lu W. Increased circulating GrMyeloid-derived suppressor cells correlated with tumor burden and survival in locally advanced cervical cancer patient. J Cancer. 2019;10(6):1341-8.

95. Wang J, Yang J. Identification of CD4(+)CD25(+)CD127(-) regulatory T cells and CD14(+)HLA(-)DR(-)/low myeloid-derived suppressor cells and their roles in the prognosis of breast cancer. Biomed Rep. 2016;5(2):208-12.

96. Li YD, Lamano JB, Lamano JB, Quaggin-Smith J, Veliceasa D, Kaur G, et al. Tumor-induced peripheral immunosuppression promotes brain metastasis in patients with non-small cell lung cancer. Cancer Immunol Immunother. 2019;68(9):1501-13.

97. Rodriguez PC, Ernstoff MS, Hernandez C, Atkins M, Zabaleta J, Sierra R, et al. Arginase I-producing myeloid-derived suppressor cells in renal cell carcinoma are a subpopulation of activated granulocytes. Cancer Res. 2009;69(4):1553-60.

98. Liu CY, Wang YM, Wang CL, Feng PH, Ko HW, Liu YH, et al. Population alterations of L-arginase- and inducible nitric oxide synthase-expressed CD11b+/CD14(-)/CD15+/CD33+ myeloid-derived suppressor cells and CD8+ T lymphocytes in patients with advanced-stage non-small cell lung cancer. J Cancer Res Clin Oncol. 2010;136(1):35-45.

99. Vetsika EK, Koinis F, Gioulbasani M, Aggouraki D, Koutoulaki A, Skalidaki E, et al. A circulating subpopulation of monocytic myeloid-derived suppressor cells as an independent prognostic/predictive factor in untreated non-small lung cancer patients. J Immunol Res. 2014;2014:659294.

100. Markowitz J, Brooks TR, Duggan MC, Paul BK, Pan X, Wei L, et al. Patients with pancreatic adenocarcinoma exhibit elevated levels of myeloid-derived

suppressor cells upon progression of disease. Cancer Immunol Immunother. 2015;64(2):149-59.

101. Chen MF, Tsai MS, Chen WC, Chen PT. Predictive Value of the Pretreatment Neutrophil-to-Lymphocyte Ratio in Head and Neck Squamous Cell Carcinoma. J Clin Med. 2018;7(10).

102. Xu XD, Hu J, Wang M, Peng F, Tian R, Guo XJ, et al. Circulating myeloid-derived suppressor cells in patients with pancreatic cancer. Hepatobiliary Pancreat Dis Int. 2016;15(1):99-105.

103. Gabitass RF, Annels NE, Stocken DD, Pandha HA, Middleton GW. Elevated myeloid-derived suppressor cells in pancreatic, esophageal and gastric cancer are an independent prognostic factor and are associated with significant elevation of the Th2 cytokine interleukin-13. Cancer Immunol Immunother. 2011;60(10):1419-30.

104. Khaled YS, Ammori BJ, Elkord E. Increased levels of granulocytic myeloid-derived suppressor cells in peripheral blood and tumour tissue of pancreatic cancer patients. J Immunol Res. 2014;2014:879897.

105. Jordan KR, Kapoor P, Spongberg E, Tobin RP, Gao D, Borges VF, et al. Immunosuppressive myeloid-derived suppressor cells are increased in splenocytes from cancer patients. Cancer Immunol Immunother. 2017;66(4):503-13.

106. Mao FY, Zhao YL, Lv YP, Teng YS, Kong H, Liu YG, et al. CD45(+)CD33(low)CD11b(dim) myeloid-derived suppressor cells suppress CD8(+) T cell activity via the IL-6/IL-8-arginase I axis in human gastric cancer. Cell Death Dis. 2018;9(7):763.

107. Mirza N, Fishman M, Fricke I, Dunn M, Neuger AM, Frost TJ, et al. All-trans-retinoic acid improves differentiation of myeloid cells and immune response in cancer patients. Cancer Res. 2006;66(18):9299-307.

108. Iclozan C, Antonia S, Chiappori A, Chen DT, Gabrilovich D. Therapeutic regulation of myeloid-derived suppressor cells and immune response to cancer vaccine in patients with extensive stage small cell lung cancer. Cancer Immunol Immunother. 2013;62(5):909-18.

109. Lathers DM, Clark JI, Achille NJ, Young MR. Phase 1B study to improve immune responses in head and neck cancer patients using escalating doses of 25-hydroxyvitamin D3. Cancer Immunol Immunother. 2004;53(5):422-30.

110. Ko JS, Zea AH, Rini BI, Ireland JL, Elson P, Cohen P, et al. Sunitinib mediates reversal of myeloid-derived suppressor cell accumulation in renal cell carcinoma patients. Clin Cancer Res. 2009;15(6):2148-57.

111. Law AMK, Valdes-Mora F, Gallego-Ortega D. Myeloid-Derived Suppressor Cells as a Therapeutic Target for Cancer. Cells. 2020;9(3).

112. Blattner C, Fleming V, Weber R, Himmelhan B, Altevogt P, Gebhardt C, et al. CCR5(+) Myeloid-Derived Suppressor Cells Are Enriched and Activated in Melanoma Lesions. Cancer Res. 2018;78(1):157-67.

113. Velasco-Velazquez M, Jiao X, De La Fuente M, Pestell TG, Ertel A, Lisanti MP, et al. CCR5 antagonist blocks metastasis of basal breast cancer cells. Cancer Res. 2012;72(15):3839-50.

114. Veltman JD, Lambers ME, van Nimwegen M, Hendriks RW, Hoogsteden HC, Aerts JG, et al. COX-2 inhibition improves immunotherapy and is associated with decreased numbers of myeloid-derived suppressor cells in mesothelioma. Celecoxib influences MDSC function. BMC Cancer. 2010;10:464.

115. Nagaraj S, Youn JI, Weber H, Iclozan C, Lu L, Cotter MJ, et al. Anti-inflammatory triterpenoid blocks immune suppressive function of MDSCs and improves immune response in cancer. Clin Cancer Res. 2010;16(6):1812-23.

116. De Santo C, Serafini P, Marigo I, Dolcetti L, Bolla M, Del Soldato P, et al. Nitroaspirin corrects immune dysfunction in tumor-bearing hosts and promotes tumor eradication by cancer vaccination. Proc Natl Acad Sci U S A. 2005;102(11):4185-90.

117. Reilley MJ, McCoon P, Cook C, Lyne P, Kurzrock R, Kim Y, et al. STAT3 antisense oligonucleotide AZD9150 in a subset of patients with heavily pretreated lymphoma: results of a phase 1b trial. J Immunother Cancer. 2018;6(1):119.

118. Seidel JA, Otsuka A, Kabashima K. Anti-PD-1 and Anti-CTLA-4 Therapies in Cancer: Mechanisms of Action, Efficacy, and Limitations. Front Oncol. 2018;8:86.

119. Gao X, Sui H, Zhao S, Gao X, Su Y, Qu P. Immunotherapy Targeting Myeloid-Derived Suppressor Cells (MDSCs) in Tumor Microenvironment. Front Immunol. 2020;11:585214.

120. De Cicco P, Ercolano G, Ianaro A. The New Era of Cancer Immunotherapy: Targeting Myeloid-Derived Suppressor Cells to Overcome Immune Evasion. Front Immunol. 2020;11:1680.

121. Meyer C, Cagnon L, Costa-Nunes CM, Baumgaertner P, Montandon N, Leyvraz L, et al. Frequencies of circulating MDSC correlate with clinical outcome of melanoma patients treated with ipilimumab. Cancer Immunol Immunother. 2014;63(3):247-57.

122. Weide B, Martens A, Zelba H, Stutz C, Derhovanessian E, Di Giacomo AM, et al. Myeloid-derived suppressor cells predict survival of patients with advanced melanoma: comparison with regulatory T cells and NY-ESO-1- or melan-A-specific T cells. Clin Cancer Res. 2014;20(6):1601-9.

123. Passaro A, Mancuso P, Gandini S, Spitaleri G, Labanca V, Guerini-Rocco E, et al. Gr-MDSC-linked asset as a potential immune biomarker in pretreated NSCLC receiving nivolumab as second-line therapy. Clin Transl Oncol. 2020;22(4):603-11.

124. Weber R, Fleming V, Hu X, Nagibin V, Groth C, Altevogt P, et al. Myeloid-Derived Suppressor Cells Hinder the Anti-Cancer Activity of Immune Checkpoint Inhibitors. Front Immunol. 2018;9:1310.

125. Gschwandtner M, Derler R, Midwood KS. More Than Just Attractive: How CCL2 Influences Myeloid Cell Behavior Beyond Chemotaxis. Front Immunol. 2019;10:2759.

126. Sun L, Clavijo PE, Robbins Y, Patel P, Friedman J, Greene S, et al. Inhibiting myeloid-derived suppressor cell trafficking enhances T cell immunotherapy. JCI Insight. 2019;4(7).

127. Zhang H, Ye YL, Li MX, Ye SB, Huang WR, Cai TT, et al. CXCL2/MIF-CXCR2 signaling promotes the recruitment of myeloid-derived suppressor cells and is correlated with prognosis in bladder cancer. Oncogene. 2017;36(15):2095-104.

128. Steele CW, Karim SA, Leach JDG, Bailey P, Upstill-Goddard R, Rishi L, et al. CXCR2 Inhibition Profoundly Suppresses Metastases and Augments Immunotherapy in Pancreatic Ductal Adenocarcinoma. Cancer Cell. 2016;29(6):832-45.

129. Tobin RP, Jordan KR, Robinson WA, Davis D, Borges VF, Gonzalez R, et al. Targeting myeloid-derived suppressor cells using all-trans retinoic acid in melanoma patients treated with Ipilimumab. Int Immunopharmacol. 2018;63:282-91.

130. Orillion A, Hashimoto A, Damayanti N, Shen L, Adelaiye-Ogala R, Arisa S, et al. Entinostat Neutralizes Myeloid-Derived Suppressor Cells and Enhances the Antitumor Effect of PD-1 Inhibition in Murine Models of Lung and Renal Cell Carcinoma. Clin Cancer Res. 2017;23(17):5187-201.

131. Mebius RE, Kraal G. Structure and function of the spleen. Nat Rev Immunol. 2005;5(8):606-16.

132. Zhao L, Liu L, Guo B, Zhu B. Regulation of adaptive immune responses by guiding cell movements in the spleen. Front Microbiol. 2015;6:645.

133. Lewis SM, Williams A, Eisenbarth SC. Structure and function of the immune system in the spleen. Sci Immunol. 2019;4(33).

134. Bronte V, Pittet MJ. The spleen in local and systemic regulation of immunity. Immunity. 2013;39(5):806-18.

135. Lindquist RL, Niesner RA, Hauser AE. In the Right Place, at the Right Time: Spatiotemporal Conditions Determining Plasma Cell Survival and Function. Front Immunol. 2019;10:788.

136. Oda A, Tezuka T, Ueno Y, Hosoda S, Amemiya Y, Notsu C, et al. Niche-induced extramedullary hematopoiesis in the spleen is regulated by the transcription factor Tlx1. Sci Rep. 2018;8(1):8308.

137. Wildes TJ, DiVita Dean B, Flores CT. Myelopoiesis during Solid Cancers and Strategies for Immunotherapy. Cells. 2021;10(5).

138. Short C, Lim HK, Tan J, O'Neill HC. Targeting the Spleen as an Alternative Site for Hematopoiesis. Bioessays. 2019;41(5):e1800234.

139. Yamamoto K, Miwa Y, Abe-Suzuki S, Abe S, Kirimura S, Onishi I, et al. Extramedullary hematopoiesis: Elucidating the function of the hematopoietic stem cell niche (Review). Mol Med Rep. 2016;13(1):587-91.

140. Kim CH. Homeostatic and pathogenic extramedullary hematopoiesis. J Blood Med. 2010;1:13-9.

141. Fernandez-Garcia V, Gonzalez-Ramos S, Martin-Sanz P, Castrillo A, Bosca L. Contribution of Extramedullary Hematopoiesis to Atherosclerosis. The Spleen as a Neglected Hub of Inflammatory Cells. Front Immunol. 2020;11:586527.

142. Jung H, Mithal DS, Park JE, Miller RJ. Localized CCR2 Activation in the Bone Marrow Niche Mobilizes Monocytes by Desensitizing CXCR4. PLoS One. 2015;10(6):e0128387.

143. Wu C, Hua Q, Zheng L. Generation of Myeloid Cells in Cancer: The Spleen Matters. Front Immunol. 2020;11:1126.

144. Cortez-Retamozo V, Etzrodt M, Newton A, Rauch PJ, Chudnovskiy A, Berger C, et al. Origins of tumor-associated macrophages and neutrophils. Proc Natl Acad Sci U S A. 2012;109(7):2491-6.

145. Wu C, Ning H, Liu M, Lin J, Luo S, Zhu W, et al. Spleen mediates a distinct hematopoietic progenitor response supporting tumor-promoting myelopoiesis. J Clin Invest. 2018;128(8):3425-38.

146. Wang X, Prakash S, Lu M, Tripodi J, Ye F, Najfeld V, et al. Spleens of myelofibrosis patients contain malignant hematopoietic stem cells. J Clin Invest. 2012;122(11):3888-99.

147. Dutta P, Courties G, Wei Y, Leuschner F, Gorbatov R, Robbins CS, et al. Myocardial infarction accelerates atherosclerosis. Nature. 2012;487(7407):325-9.

148. Fransvea P, Costa G, Serao A, Cortese F, Balducci G, Sganga G, et al. Laparoscopic splenectomy after trauma: Who, when and how. A systematic review. J Minim Access Surg. 2021;17(2):141-6.

149. Chaturvedi S, Arnold DM, McCrae KR. Splenectomy for immune thrombocytopenia: down but not out. Blood. 2018;131(11):1172-82.

150. Zufferey A, Kapur R, Semple JW. Pathogenesis and Therapeutic Mechanisms in Immune Thrombocytopenia (ITP). J Clin Med. 2017;6(2).

151. Yang K, Zang ZY, Niu KF, Sun LF, Zhang WH, Zhang YX, et al. The Survival Benefit and Safety of Splenectomy for Gastric Cancer With Total Gastrectomy: Updated Results. Front Oncol. 2020;10:568872.

152. Ohkura Y, Haruta S, Shindoh J, Tanaka T, Ueno M, Udagawa H. Efficacy of prophylactic splenectomy for proximal advanced gastric cancer invading greater curvature. World J Surg Oncol. 2017;15(1):106.

153. Son SY, Shin DJ, Park YS, Oo AM, Jung DH, Lee CM, et al. Spleen-preserving lymphadenectomy versus splenectomy in laparoscopic total gastrectomy for advanced gastric cancer. Surg Oncol. 2017;26(2):207-11.

154. Wang Q, Dang T, Meng X, Li K, Ren W, Ma X, et al. Is concomitant splenectomy necessary in radical gastric cancer surgery? A systematic review and meta-analysis. Asia Pac J Clin Oncol. 2019;15(2):e28-e35.

155. Jeong O, Kim HG, Ryu SY, Park YK, Jung MR. Adverse prognostic impact of splenectomy on survival in gastric carcinoma patients: Regression and propensity score matching analysis of 1074 patients. PLoS One. 2018;13(9):e0203820.

156. Csendes A, Burdiles P, Rojas J, Braghetto I, Diaz JC, Maluenda F. A prospective randomized study comparing D2 total gastrectomy versus D2 total gastrectomy plus splenectomy in 187 patients with gastric carcinoma. Surgery. 2002;131(4):401-7.

157. Fernandez-Cruz L, Orduna D, Cesar-Borges G, Lopez-Boado MA. Distal pancreatectomy: en-bloc splenectomy vs spleen-preserving pancreatectomy. HPB (Oxford). 2005;7(2):93-8.

158. Cui M, Liu JK, Zheng B, Liu QF, Zhang L, Zhang L, et al. Dynamic hematological changes in patients undergoing distal pancreatectomy with or without splenectomy: a population-based cohort study. BMC Surg. 2020;20(1):265.

159. Weledji EP. Benefits and risks of splenectomy. Int J Surg. 2014;12(2):113-9.

160. DuPre SA, Hunter KW, Jr. Murine mammary carcinoma 4T1 induces a leukemoid reaction with splenomegaly: association with tumor-derived growth factors. Exp Mol Pathol. 2007;82(1):12-24.

161. Simpson AL, Leal JN, Pugalenthi A, Allen PJ, DeMatteo RP, Fong Y, et al. Chemotherapy-induced splenic volume increase is independently associated with major complications after hepatic resection for metastatic colorectal cancer. J Am Coll Surg. 2015;220(3):271-80.

162. Peters AM. Why the spleen is a very rare site for metastases from epithelial cancers. Med Hypotheses. 2012;78(1):26-8.

163. Brubaker LH, Johnson CA. Correlation of splenomegaly and abnormal neutrophil pooling (margination). J Lab Clin Med. 1978;92(4):508-15.

164. Condamine T, Gabrilovich DI. Molecular mechanisms regulating myeloid-derived suppressor cell differentiation and function. Trends Immunol. 2011;32(1):19-25.

165. Lang S, Bruderek K, Kaspar C, Hoing B, Kanaan O, Dominas N, et al. Clinical Relevance and Suppressive Capacity of Human Myeloid-Derived Suppressor Cell Subsets. Clin Cancer Res. 2018;24(19):4834-44.

166. Marini O, Costa S, Bevilacqua D, Calzetti F, Tamassia N, Spina C, et al. Mature CD10(+) and immature CD10(-) neutrophils present in G-CSF-treated donors display opposite effects on T cells. Blood. 2017;129(10):1343-56.

167. Husecken Y, Muche S, Kustermann M, Klingspor M, Palmer A, Braumuller S, et al. MDSCs are induced after experimental blunt chest trauma and subsequently alter antigen-specific T cell responses. Sci Rep. 2017;7(1):12808.

168. Sayyadioskoie SR, Schwacha MG. Myeloid-Derived Suppressor Cells (MDSCs) and the Immunoinflammatory Response to Injury (Mini Review). Shock. 2021;56(5):658-66.

169. Li X, Liu J, Xing Z, Tang J, Sun H, Zhang X, et al. Polymorphonuclear myeloid-derived suppressor cells link inflammation and damage response after trauma. J Leukoc Biol. 2021;110(6):1143-61.

8. APPENDICES

APPENDIX 1: Ethics Committee Approval

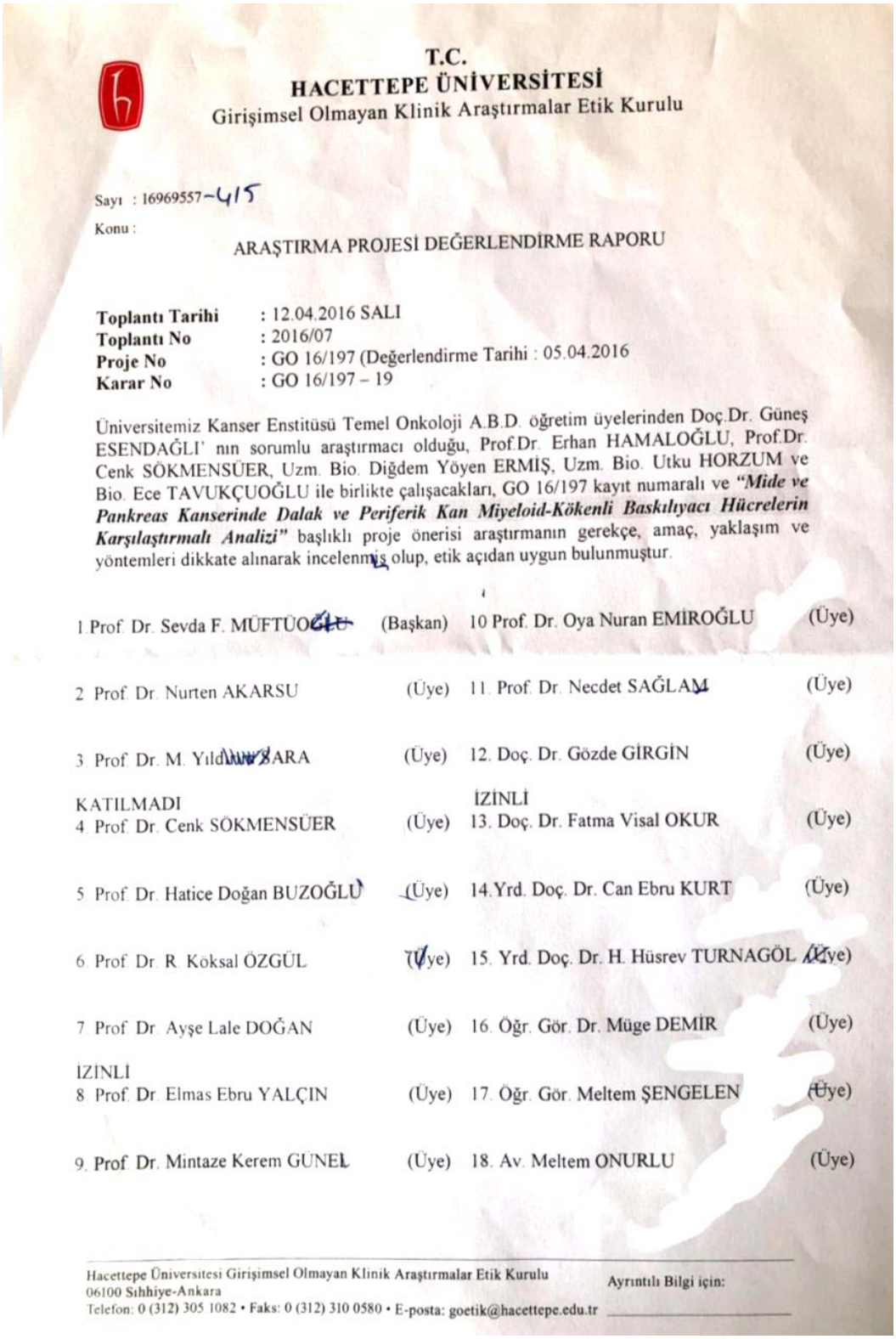

T.C.
HACETTEPE ÜNİVERSİTESİ
Girişimsel Olmayan Klinik Araştırmalar Etik Kurulu

Sayı : 16969557-415
Konu :

ARAŞTIRMA PROJESİ DEĞERLENDİRME RAPORU

Toplantı Tarihi : 12.04.2016 SALI
Toplantı No : 2016/07
Proje No : GO 16/197 (Değerlendirme Tarihi : 05.04.2016
Karar No : GO 16/197 – 19

Üniversitemiz Kanser Enstitüsü Temel Onkoloji A.B.D. öğretim üyelerinden Doç.Dr. Güneş ESENDAĞLI' nın sorumlu araştırmacı olduğu, Prof.Dr. Erhan HAMALOĞLU, Prof.Dr. Cenk SÖKMENSÜER, Uzm. Bio. Diğdem Yöyen ERMİŞ, Uzm. Bio. Utku HORZUM ve Bio. Ece TAVUKÇUOĞLU ile birlikte çalışacakları, GO 16/197 kayıt numaralı ve ***"Mide ve Pankreas Kanserinde Dalak ve Periferik Kan Miyeloid-Kökenli Baskılıyacı Hücrelerin Karşılaştırmalı Analizi"*** başlıklı proje önerisi araştırmanın gerekçe, amaç, yaklaşım ve yöntemleri dikkate alınarak incelenmiş olup, etik açıdan uygun bulunmuştur.

1 Prof. Dr. Sevda F. MÜFTÜOĞLU	(Başkan)	10 Prof. Dr. Oya Nuran EMİROĞLU	(Üye)
2 Prof. Dr. Nurten AKARSU	(Üye)	11. Prof. Dr. Necdet SAĞLAM	(Üye)
3 Prof. Dr. M. Yıldırım KARA	(Üye)	12. Doç. Dr. Gözde GİRGİN	(Üye)
KATILMADI 4 Prof. Dr. Cenk SÖKMENSÜER	(Üye)	İZİNLİ 13. Doç. Dr. Fatma Visal OKUR	(Üye)
5 Prof. Dr. Hatice Doğan BUZOĞLU	(Üye)	14.Yrd. Doç. Dr. Can Ebru KURT	(Üye)
6 Prof. Dr. R. Köksal ÖZGÜL	(Üye)	15. Yrd. Doç. Dr. H. Hüsrev TURNAGÖL	(Üye)
7 Prof. Dr. Ayşe Lale DOĞAN	(Üye)	16. Öğr. Gör. Dr. Müge DEMİR	(Üye)
İZİNLİ 8 Prof. Dr. Elmas Ebru YALÇIN	(Üye)	17. Öğr. Gör. Meltem ŞENGELEN	(Üye)
9. Prof. Dr. Mintaze Kerem GÜNEL	(Üye)	18. Av. Meltem ONURLU	(Üye)

Hacettepe Üniversitesi Girişimsel Olmayan Klinik Araştırmalar Etik Kurulu
06100 Sıhhiye-Ankara
Telefon: 0 (312) 305 1082 • Faks: 0 (312) 310 0580 • E-posta: goetik@hacettepe.edu.tr

Ayrıntılı Bilgi için:

T.C.
HACETTEPE ÜNİVERSİTESİ
Girişimsel Olmayan Klinik Araştırmalar Etik Kurulu

Sayı : 16969557 -2126
Konu : ARAŞTIRMA PROJESİ DEĞERLENDİRME RAPORU

Toplantı Tarihi : 27 KASIM 2018 SALI
Toplantı No : 2018/28
Proje No : GO 16/197 (Onay Tarihi: 12.04.2016
Karar No : GO 16/197-05

Kurulumuzun 12.04.2016 tarihli toplantısında GO 16/197 kayıt numarası ile onaylanmış olan, Üniversitemiz Kanser Enstitüsü Temel Onkoloji Anabilim Dalı öğretim üyelerinden Prof. Dr. Güneş ESENDAĞLI' nın sorumlu araştırmacı olduğu, Prof. Dr. Erhan HAMALOĞLU, Prof. Dr. Cenk SÖKMENSÜER, Uzm. Bio. Diğdem Yöyen ERMİŞ, Uzm. Mol. Bio. Utku HORZUM ve Uzm. Mol. Bio. Ece TAVUKÇUOĞLU ile birlikte çalışacakları, GO 16/197 kayıt numaralı ve ***"Mide ve Pankreas Kanserinde Dalak ve Periferik Kan Miyeloid-Kökenli Baskılayıcı Hücrelerin Karşılaştırmalı Analizi"*** başlıklı projeye 20.11.2018 tarihinde gönderilen protokol revizyonu ve süre uzatması talebi değerlendirilmiş olup araştırmaya Sağlık Bilimleri Üniversitesi Dışkapı Yıldırım Beyazıt Eğitim ve Araştırma Hastanesi Genel Cerrahi Anabilim Dalından Doç. Dr. Kerim Bora YILMAZ'ın yardımcı araştırmacı ekibine eklenmesi çalışmanın Uzm. Mol. Bio. Ece TAVUKÇUOĞLU'nun doktora tezi olarak tamamlanması ve çalışma süresinin projede yaşanan gecikmeler dikkate alınarak 01 Nisan 2020 tarihine kadar uzatılması etik açıdan uygun bulunmuştur.

İZİNLİ

1.Prof. Dr. Nurten AKARSU	(Başkan)	10 Doç. Dr. Gözde GİRGİN	(Üye)
2. Prof. Dr. Sevda F. MÜFTÜOĞLU	(Üye)	11 Doç. Dr. Fatma Visal OKUR	(Üye)
3. Prof. Dr. M. Yıldırım SARAY	(Üye)	12. Doç. Dr. Can Ebru KURT	(Üye)
4. Prof. Dr. Necdet SAĞLAM	(Üye)	13. Doç. Dr. H. Hüsrev TURNAGÖL	(Üye)
İZİNLİ 5. Prof. Dr. Hatice Doğan BUZOĞLU	(Üye)	14. Dr. Öğr. Üyesi Özay GÖKÖZ	(Üye)
İZİNLİ 6. Prof. Dr. R. Köksal ÖZGÜL	(Üye)	15. Dr. Öğr. Üyesi Müge DEMİR	(Üye)
7. Prof. Dr. Ayşe Lale DOĞAN	(Üye)	16. Öğr. Gör. Dr. Meltem ŞENGELEN	
İZİNLİ 8. Prof. Dr. Mintaze Kerem GÜNEL	(Üye)	17. Av. Meltem ONURLU	(Üye)
9. Prof. Dr. Oya Nuran EMİROĞLU	(Üye)		

Hacettepe Üniversitesi Girişimsel Olmayan Klinik Araştırmalar Etik Kurulu
06100 Sıhhiye-Ankara
Telefon: 0 (312) 305 1082 • Faks: 0 (312) 310 0580 • E-posta: goetik@hacettepe.edu.tr

Ayrıntılı Bilgi için:

T.C.
HACETTEPE ÜNİVERSİTESİ
Girişimsel Olmayan Klinik Araştırmalar Etik Kurulu

Sayı : 16969557-109
Konu : ARAŞTIRMA PROJESİ DEĞERLENDİRME RAPORU

Toplantı Tarihi : 21 OCAK 2020 SALI
Toplantı No : 2020/02
Proje No : GO 16/197 (Onay Tarihi: 12.04.2016)
Karar No : 2020/02-01

Kurulumuzun 12.04.2016 tarihli toplantısında GO 16/197 kayıt numarası ile onaylanmış olan, Üniversitemiz Kanser Enstitüsü Temel Onkoloji Anabilim Dalı öğretim üyelerinden Prof. Dr. Güneş ESENDAĞLI'nın sorumlu araştırmacı olduğu, Prof. Dr. Erhan HAMALOĞLU, Prof. Dr. Cenk SÖKMENSÜER, Doç. Dr. Kerim Bora YILMAZ, Uzm. Bio. Diğdem Yöyen ERMİŞ, Uzm. Mol. Bio. Utku HORZUM ile birlikte çalışacakları ve Uzm. Mol. Bio. Ece TAVUKÇUOĞLU'nun doktora tezi olan, GO 16/197 kayıt numaralı ve ***"Mide ve Pankreas Kanserinde Dalak ve Periferik Kan Miyeloid-Kökenli Baskılayıcı Hücrelerin Karşılaştırmalı Analizi"*** başlıklı projeniz için vermiş olduğunuz 08.01.2020 tarihli araştırmacı eklenmesi, protokol revizyonu ve süre uzatması talebi Kurulumuzun 21.01.2020 tarihli toplantısında görüşülmüş ve **uygun bulunmuştur**. Üniversitemiz Tıp Fakültesi Genel Cerrahi Anabilim Dalı öğretim üyelerinden Prof. Dr. Derya KARAKOÇ ve Tıbbi Patoloji Anabilim Dalı öğretim üyelerinden Prof. Dr. Ayşegül ÜNER yardımcı araştırmacı olarak proje ekibine dahil edilmiş ve kayıtlarımıza eklenmiştir. Projenin yeni sonlanım tarihi 01 Nisan 2021 olarak belirlenmiştir. Çalışma tamamlandığında sonuçlarını içeren bir rapor örneğinin Etik Kurulumuza gönderilmesi gerekmektedir.

1.Prof. Dr. Ayşe Lale DOĞAN	(Başkan)	9. Doç. Dr. Fatma Visal OKUR	(Üye)
2. Prof. Dr. Sevda F. MÜFTÜOĞLU	(Üye)	10. Doç. Dr. Can Ebru KURT	(Üye)
3. Prof. Dr. M. Yıldırım SAHİN	(Üye)	11. Doç. Dr. H. Hüsrev TURNAGÖL	(Üye)
4. Prof. Dr. Nevhis SAKINCI	(Üye)	12. Dr. Öğr. Üyesi Özay GÖKÖZ	(Üye)
5. Prof. Dr. Mintaze Kerem GÜNEL	(Üye)	13. Dr. Öğr. Üyesi Müge DEMİR	(Üye)
6. Prof. Dr. Oya Nuran EMİROĞLU	(Üye)	14. Öğr. Gör. Dr. Meltem ŞENGELEN	
7. Prof. Dr. M. Özgür UYANIK	(Üye)	15. Av. Meltem ONURLU	(Üye)
8. Doç. Dr. Gözde GİRGİN	(Üye)		

Hacettepe Üniversitesi Girişimsel Olmayan Klinik Araştırmalar Etik Kurulu
06100 Sıhhiye-Ankara
Telefon: 0 (312) 305 1082 • Faks: 0 (312) 310 0580 • E-posta: goetik@hacettepe.edu.tr

Ayrıntılı Bilgi için:

APPENDIX 2: Scientific meetings where the data of this thesis were presented.

Oral presentation

1. **Tavukcuoglu E.,** Horzum U., Yoyen-Ermis D., Aydin B., Yilmaz K. B., Uner A., Karakoc D., Hamaloglu E., Esendagli G. "Analysis of spleen-derived MDSCs in pancreatic and gastric cancer patients".1st European Symposium On Myeloid Regulatory Cells in Health And Disease. 2018 November 1-3, Essen, Germany, O-18.
2. **Tavukcuoglu E.,** Horzum U., Yanik H., Yoyen-Ermis D., Uner A., Aydin B., Yilmaz K. B., Karakoc D., Hamaloglu E., Esendagli. Mide ve pankreas kanseri hastalarının kan ve dalağındaki granülositik miyeloid-kökenli immün baskılayıcı hücrelerin analizi ve prognozla ilişkisi. 20-22 Kasım 2020. XXV. Ulusal İmmünoloji Kongresi.

APPENDIX 3: Thesis originality report.

Tezin tam başlığı: COMPARATIVE ANALYSIS OF MYELOID-DERIVED SUPPRESSOR CELLS FROM BLOOD AND SPLEEN IN GASTRIC AND PANCREATIC CANCER

Öğrencinin adı soyadı: Ece Tavukçuoğlu
Dosyanın toplam sayfa sayısı: 88

ORİJİNALLİK RAPORU

%22	%15	%16	%4
BENZERLİK ENDEKSİ	İNTERNET KAYNAKLARI	YAYINLAR	ÖĞRENCİ ÖDEVLERİ

BİRİNCİL KAYNAKLAR

1	acikbilim.yok.gov.tr İnternet Kaynağı	%4
2	Ece Tavukcuoglu, Utku Horzum, Hamdullah Yanik, Aysegul Uner et al. "Human splenic polymorphonuclear myeloid_derived suppressor cells (PMN_MDSC) are strategically_located immune regulatory cells in cancer", European Journal of Immunology, 2020 Yayın	%4
3	openaccess.hacettepe.edu.tr:8080 İnternet Kaynağı	%1
4	link.springer.com İnternet Kaynağı	%1
5	Ece Tavukcuoglu, Utku Horzum, Hamdullah Yanik, Aysegul Uner et al. "Human splenic polymorphonuclear myeloid_derived suppressor cells (PMN_MDSC) are strategically located immune regulatory cells in cancer", European Journal of Immunology, 2020 Yayın	<%1

APPENDIX 4: Digital Receipt

turnitin

Dijital Makbuz

Bu makbuz ödevinizin Turnitin'e ulaştığını bildirmektedir. Gönderiminize dair bilgiler şöyledir:

Gönderinizin ilk sayfası aşağıda gönderilmektedir.

Gönderen:	Ece Tavukçuoğlu
Ödev başlığı:	ece deneme
Gönderi Başlığı:	tez final
Dosya adı:	ece_tez_turnitin.docx
Dosya boyutu:	14.62M
Sayfa sayısı:	88
Kelime sayısı:	19,069
Karakter sayısı:	108,659
Gönderim Tarihi:	22-Tem-2022 12:03ÖÖ (UTC+0300)
Gönderim Numarası:	1873515973

COMPARATIVE ANALYSIS OF MYELOID-DERIVED SUPPRESSOR CELLS FROM BLOOD AND SPLEEN IN GASTRIC AND PANCREATIC CANCER

Ph.D. Ece TAVUKÇUOĞLU

ANKARA
2022

9. CURRICULUM VITAE

Personal and contact details

Name: Ece Tavukçuoğlu